

REPORT DOCUMENTATION PAGE			Form Approved OMB NO. 0704-0188		
<p>The public reporting burden for this collection of information is estimated to average 1 hour per response, including the time for reviewing instructions, searching existing data sources, gathering and maintaining the data needed, and completing and reviewing the collection of information. Send comments regarding this burden estimate or any other aspect of this collection of information, including suggestions for reducing this burden, to Washington Headquarters Services, Directorate for Information Operations and Reports, 1215 Jefferson Davis Highway, Suite 1204, Arlington VA, 22202-4302. Respondents should be aware that notwithstanding any other provision of law, no person shall be subject to any penalty for failing to comply with a collection of information if it does not display a currently valid OMB control number. PLEASE DO NOT RETURN YOUR FORM TO THE ABOVE ADDRESS.</p>					
1. REPORT DATE (DD-MM-YYYY) 24-08-2015		2. REPORT TYPE Final Report		3. DATES COVERED (From - To) 6-Apr-2011 - 14-Apr-2015	
4. TITLE AND SUBTITLE Final Report: Information-Driven Blind Doppler Shift Estimation and Compensation Methods for Underwater Wireless Sensor Networks			5a. CONTRACT NUMBER W911NF-11-1-0144		
			5b. GRANT NUMBER		
			5c. PROGRAM ELEMENT NUMBER 206022		
6. AUTHORS Dr. Paul Cotae			5d. PROJECT NUMBER		
			5e. TASK NUMBER		
			5f. WORK UNIT NUMBER		
7. PERFORMING ORGANIZATION NAMES AND ADDRESSES The University of the District of Columbia Computer Science and Informati Briana Lowe Wellman Washington, DC 20008 -1122			8. PERFORMING ORGANIZATION REPORT NUMBER		
9. SPONSORING/MONITORING AGENCY NAME(S) AND ADDRESS (ES) U.S. Army Research Office P.O. Box 12211 Research Triangle Park, NC 27709-2211			10. SPONSOR/MONITOR'S ACRONYM(S) ARO		
			11. SPONSOR/MONITOR'S REPORT NUMBER(S) 58962-NS-REP.24		
12. DISTRIBUTION AVAILABILITY STATEMENT Approved for Public Release; Distribution Unlimited					
13. SUPPLEMENTARY NOTES The views, opinions and/or findings contained in this report are those of the author(s) and should not be construed as an official Department of the Army position, policy or decision, unless so designated by other documentation.					
14. ABSTRACT We investigated different methods for blind Doppler shift estimation and compensation in underwater acoustic wireless sensor networks. Our study is based on the data collected from our underwater experiments. We analyzed the data collected by using non-data aided techniques such as Power Spectrum analysis, Autocorrelation, and Squaring Time Phase Recovery (Oerder & Meyr) to estimate Doppler shift in collaborative distributed underwater sensor networks. We also extensively investigated optimal sensor placement in a tree structured multi-hop hierarchical network. We focused on a symmetric tree-like multi-hop hierarchical routing topology, which can					
15. SUBJECT TERMS underwater communication, Doppler shift, wireless sensor networks, blind methods					
16. SECURITY CLASSIFICATION OF:		17. LIMITATION OF ABSTRACT	15. NUMBER OF PAGES	19a. NAME OF RESPONSIBLE PERSON	
a. REPORT	b. ABSTRACT			c. THIS PAGE	Paul Cotae
UU	UU	UU		19b. TELEPHONE NUMBER 202-274-6290	

Report Title

Final Report: Information-Driven Blind Doppler Shift Estimation and Compensation Methods for Underwater Wireless Sensor Networks

ABSTRACT

We investigated different methods for blind Doppler shift estimation and compensation in underwater acoustic wireless sensor networks. Our study is based on the data collected from our underwater experiments. We analyzed the data collected by using non-data aided techniques such as Power Spectrum analysis, Autocorrelation, and Squaring Time Phase Recovery (Oerder & Meyr) to estimate Doppler shift in collaborative distributed underwater sensor networks. We also extensively investigated optimal sensor placement in a tree structured multi-hop hierarchical network. We focused on a symmetric tree like multi-hop hierarchical routing topology, which can potentially cover larger areas as we go deeper in the water than flat placement of underwater sensor networks. We used information theoretic tools such as entropy, conditional entropy, probability mass function etc. of input and output data signal to analyze the mutual information, information loss, bit error rate, and channel capacity. We focused on the optimizing mutual information between transmitted data and received data for a specific sensor network in underwater channel. Specifically, we used multiple sensor nodes in a relay network to transfer the data into long distance looking for maximum mutual information. In addition, we studied the relationship of channel capacity to transmitted power, bandwidth and carrier frequency.

Enter List of papers submitted or published that acknowledge ARO support from the start of the project to the date of this printing. List the papers, including journal references, in the following categories:

(a) Papers published in peer-reviewed journals (N/A for none)

<u>Received</u>	<u>Paper</u>
08/21/2012 2.00	Ira S. MOSKOWITZ, Paul COTAE, Myong H. KANG, Pedro N. SAFIER. Capacity Approximations for a DeterministicMIMO Channel, Advances in Electrical and Computer Engineering, (11 2011): 3. doi:
TOTAL:	1

Number of Papers published in peer-reviewed journals:

(b) Papers published in non-peer-reviewed journals (N/A for none)

<u>Received</u>	<u>Paper</u>
-----------------	--------------

TOTAL:

Number of Papers published in non peer-reviewed journals:

(c) Presentations

- P.1) Raju Shrestha and Paul Cotae, "On the Mutual Information of the Moving Targets in Underwater Wireless Communication" 2013 ASEE Mid-Atlantic Conference at UDC, Oct 11-12, 2013.
- P.2) Daniel Gebremicheal and Paul Cotae "On the Probability of Error for Treshold Binary - Input Ternary – Output Discrete Memoryless Channels" 2013 ASEE Mid-Atlantic Conference at UDC, Oct 11-12, 2013.
- P.3) Birajan Singh Bista and Paul Cotae, "On the Filter Design for Underwater Communication Channel", 2013 ASEE Mid-Atlantic Conference at UDC, Oct 11-12, 2013.
- P.4) Ayele Woldemariam and Paul Cotae "Tracking the Speed of Moving Source Underwater by Using the Acoustic Wireless Sensor Networks" Xerox fellowship project presentation, School of Engineering and Applied Sciences, May 10, 2013.
- P.5) Missi Sogbohossou and Paul Cotae "Modulation Schemes for Underwater Acoustic Communications", Xerox fellowship project presentation, School of Engineering and Applied Sciences, May 10, 2013.
- P.6) Hadis Dashtestani and Paul Cotae, "On the Optimal Placement of Underwater Sensors in a Tree Shaped Multi-hop Hierarchical Network" UDC Engineering week 2013, Feb.26, 2013.
- P.7) Daniel Gebremichael and Paul Cotae, "Stochastic Resonance" UDC Engineering week 2013, Feb.26, 2013.
- P.8) Suresh Regmi and Paul Cotae "Performance Analysis of Non Data Aided Doppler Shift Estimation and Detection for Underwater Moving Targets- a Practical Approach", UDC Engineering week 2013, Feb.26, 2013.
- P.9) Paul Cotae, "On the Inverse Eigenvalue Problem by using the Kolmogorov-Sinai Entropy", Dynamics Days US 2013, Marriot City Center, Denver, Colorado, January 3-6, 2013.
- P.10) Paul Cotae "Research on Underwater Sensor Networks" Quantitative Methods in Defense and National Security, QMDNS 2012, April 30-May 1, 2012, George Mason University.
- P.11) Roland Kamdem and Paul Cotae "Threshold Based Stochastic Resonance for the Binary-Input Ternary –Output Discrete Memoryless Channels" Research Group Meeting SEAS, Jan. 31, 2012, UDC Engineering week 2012, Feb.27, 2012.
- P.12) Abayomi Dairo, Nikola Jovic and Paul Cotae "Designing a Low Cost Acoustic Modem with Data Transmission Based on FSK Modulation", Undergraduate Research Day, UDC Windows Lounge April 26, 2012
- P.13) Suresh Regmi and Paul Cotae "Analysis of Advance Method for Decisions-Making on Target Detection with Underwater Sensor Network in the Context of Blind Doppler Shift Estimation and Detection", UDC Engineering week 2012, Feb.27, 2012.
- P.14) Hadis Dashtestani and Paul Cotae "Sensor Planning and Optimum Sensor Locations Based on Information Functions for Underwater Acoustic Communications", UDC Engineering week 2012, Feb.27, 2012.
- P.15) Birajan Bista and Paul Cotae "Minimization of false alarm in wireless sensor networks using various techniques to reduce the false alarm and increase the target detection" UDC Engineering week 2012, Feb.27, 2012.
- P.16) Abayomi Dairo, Nikola Jovic and Paul Cotae "Acoustic Communication Modem", UDC Engineering week 2012, Feb.27, 2012.
- P.17) Babatunde Taiwo, John Brandon and Paul Cotae "Data Acquisition of an Underwater Communication Network", UDC Engineering week 2012, Feb.27, 2012, Undergraduate Research Day, April 26, Windows Lounge, UDC.
- P.18) Mahmoud El-Sayed and Paul Cotae "Wireless GPS Tracking system with Graphical User Interface" UDC Engineering week 2012, Feb.27, 2012.
- P.19) Paul Cotae "On the Inverse Eigenvalue Problem and the Mutual Kolmogorov-Sinai Entropy" Dynamics Days 2012 Conference organized by the University of Maryland, The Sheraton Inner Harbor Hotel, Baltimore, MD, January 4-7, 2012.

Number of Presentations: 19.00

Non Peer-Reviewed Conference Proceeding publications (other than abstracts):

Received

Paper

TOTAL:

Number of Non Peer-Reviewed Conference Proceeding publications (other than abstracts):

Peer-Reviewed Conference Proceeding publications (other than abstracts):

<u>Received</u>	<u>Paper</u>
07/24/2015 20.00	Mahmoud Elsayed, Paul Cotaе . On The Performance and Modulation Techniques of Underwater Acoustic Sensors Network: Work in Progress, Proceedings of the ASEE Gulf-Southwest Annual Conference, March 25-27, the University of Texas at San Antonio, San Antonio, Texas, USA. . 25-MAR-15, . . ,
07/24/2015 22.00	Mahmoud Elsayed, Paul Cotaе. On the Performance of Underwater Mobile Acoustic Sensor Networks: Work in Progress , ASEE'14 Conference, Swarthmore College, Swarthmore, PA, USA, 14-15 Nov, 2014.. 14-NOV-14, . . ,
08/19/2013 7.00	Hadis Dashtestani, Paul Cotaе, Ira S. Moskowitz. On the Optimal Placement of Underwater Sensors in a Tree Shaped Multi-hop Hierarchical Network, Proceedings of the IEEE 47th Annual Conference on Information Sciences and Systems - CISS 2013. 20-MAR-13, . . ,
08/19/2013 8.00	Abayomi Dairo, Nikola Jovic, Paul Cotaе. LOW COST FREQUENCY SHIFT KEYING ACOUSTIC MODEM FOR UNDERWATER WIRELESS SENSOR NETWORKS, Proceedings of the Spring 2013 Mid-Atlantic Section Conference of the American Society of Engineering Education (ASEE),. 26-APR-13, . . ,
08/19/2013 6.00	Ira S. Moskowitz, Pedro N. Safier, Paul Cotaе. ALGEBRAIC INFORMATION THEORY AND KOSKO'S FORBIDDEN INTERVAL THEOREM, Proceedings of the IASTED International Conference. 10-APR-13, . . ,
08/21/2012 1.00	Roland Kamdem, Paul Cotaе, Ira S. Moskowitz. Threshold based Stochastic Resonance for the Binary-Input Ternary-Output Discrete Memoryless Channels, Imaging and Signal Processing in Health Care and Technology. , Baltimore, USA. . . ,
08/21/2012 5.00	NIKOLA JOVIC, ABAYOMI DAIRO, ASHENAFI TESFAYE, AIME VALERE, YANNICK ROLAND KAMDEM, SASAN HAGHANI, PAUL COTAE,. Detecting Falls Among Elderly Patients in Nursing Homes by Using Wireless Sensor Networks, Proceedings of the ASEE MidAtlantic Section Fall Conference 2011. 21-OCT-11, . . ,
08/21/2012 4.00	Ira S. Moskowitz, Paul Cotaе, Pedro N. Safier. Algebraic Information Theory and Stochastic Resonance for Binary Input Binary Output Channels, Proceedings IEEE 46th Annual Conference on Information Sciences and Systems-CISS 2012, Princeton University. 21-MAR-12, . . ,
08/21/2012 3.00	Ira S. Moskowitz, Paul Cotaе, Pedro N. Safier , Daniel L. Kang. Capacity Bounds and Stochastic Resonance for Binary Input Binary Output Channels, Proceedings of the IEEE ComCompAp 2012, Hong Kong, China. 11-JAN-12, . . ,
09/02/2014 13.00	Hadis Dashtestani, Paul Cotaе, Ira S Moskowitz. Joint Optimal Placement and Energy Allocation of Underwater Sensors in a Tree Topology , IEEE CISS 2014. 20-MAR-14, . . ,
09/02/2014 14.00	Paul Cotaе, Suresh Regmi, Ira S. Moskowitz. Non-data aided doppler shift estimation for underwater acoustic communication, 2014 10th International Conference on Communications (COMM). 29-MAY-14, Bucharest, Romania. . . ,

- 09/02/2014 15.00 Raju Shrestha, Mahmoud Elsayed, Paul Cotae. On the Mutual Information of Sensor Networks in Underwater Wireless Communication: An Experimental Approach, ASEE 2014 Zone I Conference, April 3-5, 2014, University of Bridgeport, Bridgeport, CT, USA.. 03-APR-14, . . . ,
- 09/02/2014 16.00 Daniel Gebremichael, Paul Cotae. On the probability of Error of Threshold Devices , ASEE 2014 Zone I Conference, April 3-5, 2014, University of Bridgeport, Bridgeport, CT, USA.. 03-APR-14, . . . ,
- 09/02/2014 17.00 Birajan Singh Bista, Paul Cotae. On the Filter Design for Underwater Communication Channel, ASEE 2013 Midatlantic Conference . 17-OCT-13, . . . ,
- 09/02/2014 18.00 Raju Shrestha, Paul Cotae. ON THE MUTUAL INFORMATION OF THE MOVING TARGETS IN UNDERWATER WIRELSS COMMUNICATION , ASEE 2013 Midatlantic Conference at UDC. 17-OCT-13, . . . ,

TOTAL: 15

Number of Peer-Reviewed Conference Proceeding publications (other than abstracts):

(d) Manuscripts

Received Paper

- 07/24/2015 21.00 Mahmoud Elsayed, Paul Cotae, Ira S. Moskowitz. On The Performance of Underwater Acoustic Sensors Network: An Experimental Approach, " ASEE 2015 North-East Section Regional Conference, April 30 - May 2, 2015, Northeastern University, Boston, Massachusetts, USA. (05 2015)

TOTAL: 1

Number of Manuscripts:

Books

Received Book

TOTAL:

Received

Book Chapter

TOTAL:

Patents Submitted

Patents Awarded

Awards

A) IEEE Honors and Awards (last 5 years)

-
- Executive Chair Globecomm Conference 2016, Washington DC
 - Chair of Governance Committee, Board of Governors, IEEE Communication Society, 2014-2015.
 - 2013 IEEE Washington DC Section: Director 2013-2014, Nomination and Appointments Committee Chair 2013-2014.
 - 2013 IEEE Distinguished Service Award in recognition of “Outstanding Leadership of the Communication Society and receiving the GLOBECOM 2016 Executive Chair Leadership” from the IEEE Washington Section, May 25, 2013.
 - 2013 IEEE Washington Section Chair Award in recognition and appreciation for “Distinguished service and outstanding leadership as IEEE Washington Section Chair in 2012” from IEEE Washington Section, May 25, 2013.
 - 2012 IEEE Washington Section Distinguished Service Award Citation” in recognition of his outstanding service in providing Leadership as a Vice Chair to the Section”.
 - 2012 Board Member of the IEEE ComSoc North America Region (as IEEE ComSoc Region 2 representative and Student Activities Support)
 - 2011 IEEE Communication Society: North America Region Chapter Achievement Award (CAA ComSoc), Citation “For achieving excellence in chapter activities and for contributions in furthering the objectives of the society”.
 - 2011 IEEE Communication Society: Chapter of the Year Award (CoY ComSoc), Citation “For achieving the highest excellence in chapter activities and for outstanding contributions furthering the objectives of the society”.

B) Academic Honors and Awards (last 5 years)

- 2009-2015 ONR Faculty Fellow for the ONR-ASEE Summer Faculty Research Program.
- 2014-2015 ONR Faculty Fellow for the ONR-ASEE Sabbatical Faculty Research Program
- 2013 Selected in Top 25 Professors at Affordable Historically Black Colleges by Affordable College Online.
- 2013 Faculty Recognition award for “Outstanding Research and Professional Service” in the School of Engineering and Applied Sciences at the University of the District of Columbia, May 1st , 2013.
- 2013 Chair of the ASEE Mid-Atlantic Conference at UDC, October 11-12, 2013.
- Panelist for the U. S. Department of Energy's 2013 Phase I Release 1 SBIR/STTR.
- Panelist for the 2013 NASA ASP (Aeronautics Scholarship Program) and SMART (Science, Mathematics And Research for Transformation) Scholarship Program of DoD (Department of Defense) at the ASEE (American Society for Engineering Education) February 13-14, 2013.
- UDC School of Engineering and Applied Sciences, Engineering Week 2012: First and second place paper award at the Graduate student section with Roland Kamdem and Suresh Regmi, respectively; First place and third place paper award at the Undergraduate section with Nikola Jovic, Dairo Abayomi, John Brandon and Babatunde Taiwo February 27, 2012.
- UDC 4th Edition of the Undergraduate Research Day 2011: second place for oral presentation with the “Submersed Wireless Sensor Data Retrieving Network” presented by Prakash Regmi.
- UDC School of Engineering and Applied Sciences, Engineering Week 2011: First and second place paper award with Prakash Regmi and

Graduate Students

<u>NAME</u>	<u>PERCENT SUPPORTED</u>	Discipline
Suresh Regmi	1.00	
Hadis Dashestani	1.00	
Birajan Bistra	1.00	
Roland Kamden	1.00	
Daniel Gebremichael	1.00	
Mahmoud Elsayed	1.00	
Raju Shrestha	1.00	
Daniel Albano	0.50	
Ovidiu Carpiuc	0.50	
FTE Equivalent:	8.00	
Total Number:	9	

Names of Post Doctorates

<u>NAME</u>	<u>PERCENT SUPPORTED</u>
FTE Equivalent:	
Total Number:	

Names of Faculty Supported

<u>NAME</u>	<u>PERCENT SUPPORTED</u>	National Academy Member
Dr. Paul Cotae	1.00	No
FTE Equivalent:	1.00	
Total Number:	1	

Names of Under Graduate students supported

<u>NAME</u>	<u>PERCENT SUPPORTED</u>	Discipline
Ayele Woldemarian	1.00	BS Electrical and Computer Engineering
Missi Sogbohossou	1.00	BS Electrical and Computer Engineering
Saroj Tiwani	1.00	BS Electrical and Computer Engineering
Silva Abdradridge	1.00	BS Electrical and Computer Engineering
Abayomi Dairo	1.00	BS Electrical and Computer Engineering
Ashenafi Lambebo	1.00	BS Electrical and Computer Engineering
Nikola Jovic	1.00	BS Electrical and Computer Engineering
Ashenafi Tesfaye	1.00	BS Electrical and Computer Engineering
John Brandon	1.00	BS Electrical and Computer Engineering
Babatunde Taiwo	1.00	BS Electrical and Computer Engineering
Mahmoud Elsayed	1.00	BS Electrical and Computer Engineering
Aime Mbakop	1.00	BS Electrical and Computer Engineering
Charles Williams	1.00	BS Electrical and Computer Engineering
Laith Athoum	1.00	BS Electrical and Computer Engineering
FTE Equivalent:	14.00	
Total Number:	14	

Student Metrics

This section only applies to graduating undergraduates supported by this agreement in this reporting period

The number of undergraduates funded by this agreement who graduated during this period: 14.00

The number of undergraduates funded by this agreement who graduated during this period with a degree in science, mathematics, engineering, or technology fields:..... 14.00

The number of undergraduates funded by your agreement who graduated during this period and will continue to pursue a graduate or Ph.D. degree in science, mathematics, engineering, or technology fields:..... 10.00

Number of graduating undergraduates who achieved a 3.5 GPA to 4.0 (4.0 max scale):..... 8.00

Number of graduating undergraduates funded by a DoD funded Center of Excellence grant for Education, Research and Engineering:..... 0.00

The number of undergraduates funded by your agreement who graduated during this period and intend to work for the Department of Defense 11.00

The number of undergraduates funded by your agreement who graduated during this period and will receive scholarships or fellowships for further studies in science, mathematics, engineering or technology fields:..... 3.00

Names of Personnel receiving masters degrees

NAME

Roland Kamden
Suresh Regmi
Hadis Dashtestani
Daniel Ghebremichael
Birajan Bistra (project)
Raju Shrestha
Mahmoud Elsayed
Daniel Albano (project)

Total Number: 8

Names of personnel receiving PHDs

NAME

Total Number:

Names of other research staff

NAME

PERCENT SUPPORTED

FTE Equivalent:

Total Number:

Sub Contractors (DD882)

Inventions (DD882)

Scientific Progress

1)Foreword

This Final Report is organized in four parts as following. Part I covers the period between August 1st 2014 and April 14, 2015 (the last period of project). Part II covers the results obtained from 1-Aug-2013 to 31-July-2014 and it is based on the Interim progress report 3 submitted for this period. Part III covers the results obtained from 1-Aug-2012 to 31-July-2013 and Part II is also based on the Interim Progress Report 2 submitted in that time frame. Part IV covers the period April 6, 2011 (when this grant was awarded) until July 31, 2012. Part IV is mostly based on the Interim Progress Report 1.

In this project, we used an experimental approach to enhance the performance of the underwater acoustic sensor networks and to decrease the network power consumption. For a Distributed Underwater Wireless Sensor Networks (UWSN), we estimated the number of operating receivers based on the knowledge of the Bit-Error-Rate (BER) and the signal detection performance of the transmitted message. In our experimental observations, we considered two network models: multi hop relay acoustic sensors network and parallel acoustic sensors network.

We have used the information theoretic aspects to analyze and to study the impact of using mobile/moving sensor nodes, as opposed to fixed nodes in UWSN. Also, we developed software platform named "SAM Control" which is a GUI written in MATLAB programming language to facilitate our experiments. The SAM Control unit coordinates and manages the communications between the acoustic modems used in our experiments, while at the same time is allowing data gathering of all experimental observations and the performance analysis of power consumption, BER, mutual information, and information loss.

We investigated the performance of underwater acoustic sensor networks in underwater wireless communication in terms of mutual information, channel capacity, bit error rate, and information loss based on the transmission power, distance, carrier frequency and the bandwidth of the underwater channel. Moreover, we used the information theoretic aspects to analyze and study the impact of using mobile/moving sensor nodes, as opposed to fixed nodes used in UWSN. A placement of multiple acoustic sensors in a multi-hop relay form is needed in numerous applications where data transmission has to be accomplished beyond short distances. This network is effective since the bandwidth of an underwater acoustic communication is severely limited and decays with increase in distances. It is advantageous to accomplish such transmission using sensors in a multi-hop relay network keeping constraints such as transmission rate, transmission delay, Signal-to-Interference and Noise Ratio (SINR) under consideration.

Table of Content

1)Foreword.....	1
2)Table of Content.....	2
3) List of Appendices, Illustrations and Tables.....	3
4)Part I (Period August 1st 2014 and April 14, 2015).....	5
I.1)Statement of problem studied.....	5
I.2)Summary of the most important results.....	6
I.3)Accomplishments.....	11
5)Part II (Period August 1st 2013 and July 31st , 2014).....	11
II.1)Foreword.....	11
II.2) Statement of problem studied.....	12
II.3) Summary of the most important results.....	13
II.4)Accomplishments.....	16
6)Part III (Period August 1st 2012-July 31st 2013).....	16
III.1)Foreword.....	16
III.2)Statement of problem studied.....	17
III.3)Summary of the most important results.....	18
III.4)Accomplishments.....	26
7)Part IV (Period April 6 2011 and July 31st 2012).....	27
IV.1)Foreword.....	27
IV.2)Statement of problem studied.....	27
IV.3)Summary of the most important results.....	28
IV.4)Accomplishments.....	32
8) Bibliography.....	32

3)List of Appendices, Illustrations and Tables

List of Figures

- Figure 1: The global picture of the overall project
- Figure 2: SAM Control GUI
- Figure 3: Cascaded underwater wireless sensor network
- Figure 4: Parallel underwater wireless sensor network
- Figure 5: Underwater Mobile Acoustic Sensor Network
- Figure 6: Experimental approach setup
- Figure 7. PSD of Noise (No (f)) experimentally measured in underwater
- Figure 8 Illustration of Multihop network
- Figure 9. Delay between Relays
- Figure 10. Acoustic Sensors by Vendor and Experimental set up in Underwater Communications
- Figure 11. PSD of Noise (No(f)) experimentally measured in underwater
- Figure 12. Matlab simulation Set Up for multi-hop network sensor model
- Figure 13. Transmitted and Received Modulated m-Sequence Signals (17 kHz)
- Figure 14. Experimental set up and its components
- Figure 15. Autocorrelation of Noise Measured in Swimming Pool
- Figure 16. PSD of Measured Noise in Swimming Pool
- Figure 17. PSD Estimation by Parametric Methods
- Figure 18. PSD Estimation by Blind Methods
- Figure 19. Comparisons of Parametric and Blind Spectral Estimation Methods
- Figure 20. Linear Frequency Modulation Cosine, and its PSD
- Figure 21. Periodic Autocorrelation of PN-Sequences
- Figure 22. Initial Transmitted (a) and Received (b) m-sequence signal
- Figure 23. Frequency Modulated Transmitted Signal
- Figure 24. Frequency Modulated m-Sequence Received Signals (17 kHz)
- Figure 25. Autocorrelation of Transmitted and Received 52-m –Sequences
- Figure 26. Partial Autocorrelation of Received Signals Showing 48 to 52 m-Sequences
- Figure 27. Power Spectral Density of Transmitted and Received Signal [Water Tank]
- Figure 28. Partial PSD of a Received Signal [Results for Water Tank]
- Figure 29. PSD of Received Signal [Results for Swimming pool]
- Figure 30. Transmitted and Received Signal for LFM m- Sequences [Pool]
- Figure 31. Autocorrelation, PSD and Partial Autocorrelation of LFM 52- m- Sequences
- Figure 32. Estimation of Instantaneous and Average Doppler Shift Using Oerder and Meyr Algorithm
- Figure 33. 4 level tree structured network with 2 children nodes
- Figure 34. Optimal distance (on the top) for ideal and imperfect channels including BER and interference for a tree shaped topology with 7 levels.
- Figure 35. The distances for different imperfect channel scenarios and their improved situations after applying CC
- Figure 36. The ratio of the sensor power of the imperfect channel compared to the sensor power of the ideal channel
- Figure 37. Optimal frequency at each distance associated with a specific level for an ideal channel in a 7 level tree structured network
- Figure 38. Optimal frequency at each distance associated with a specific level for an imperfect channel (BER = 0.001) in a 7-level tree structured UWSN
- Figure 39. Optimal frequency at each distance associated with a specific level for an ideal channel in a 7-level tree structured network
- Figure 40. Frequency dependent portion of narrow-band SNR.
- Figure 41. Optimal placement of the sensor nodes when the transmitting power is constant
- Figure 42. The optimal power allocations for the scenario 1 are shown near each sensor node (in Watts)
- Figure 43. The optimal power allocations for the scenario 2 are shown near each sensor node (in Watts)
- Figure 44. The optimal sensors' locations and power allocations (in Watts).
- Figure 45. BSC/SE capacity
- Figure 46. Capacity of BAC/SE
- Figure 47. Capacity of BSC/SE for threshold values
- Figure 48. (2,3) DMC and Pinsker capacity Bound
- Figure 49. (2,3) DMC and Helgert capacity Bound
- Figure 50. Capacity(C), Pinsker (L) and Helgert (U) bounds for different values of threshold
- Figure 51. Optimal noise power and threshold for stochastic resonance, with a scalable factor

List of Tables

Table 1: Bit loss test for different distance of sensors
 Table 2: Result analysis for Tx1 and Rx1 (d=5 m)
 Table 3: Result analysis for Tx2 and Rx2 (d=5 m)
 Table 4: Result analysis for Tx3 and Rx3 (d=5 m)
 Table 5: Result analysis for Tx1 and Rx4 (d=15 m)
 Table 6: Result analysis for cascaded sensors network
 Table 7: Result analysis for Tx1 and Rx1
 Table 8: Bit loss test for mobile sensor nodes of maximum distances $d = 15\text{m}$.
 Table 9: Bit loss test for mobile sensor nodes moving in vertical direction.
 Table 10: Performance results of using mobile sensor nodes
 Table 11: Numerical results for scenario #1
 Table 12: Numerical results for scenario #2
 Table 13: Result analysis of using fixed sensor nodes
 Table 14: Summary results for using mobile sensor nodes
 Table 15: Numerical results for scenario #1 (no target is moving):
 Table 16: Approach results in noisy UAC (Scenario#2)
 Table 17: Modem Specifics and Operating Function
 Table 18: Bit loss test for different distance of sensors
 Table 19: Result analysis for First Hop Tx1 and Rx1 (d=5 m)
 Table 20: Result analysis for Second Hop Tx2 and Rx2 (d=5 m)
 Table 21: Result analysis for third Hop Tx3 and Rx3 (d=5 m)
 Table 22: Result analysis for Tx1 and Rx4 (d=15 m)
 Table 23: Result analysis for Multihop relay link and direct link
 Table 24: Optimized placements and other related parameters when the transmitting power of each node is constant and equal to 1 watt
 Table 25: Optimized energy allocation and other related parameters when the sensor nodes are fixed in their locations, first scenario
 Table 26: Optimized energy allocation and other related parameters when the sensor nodes are fixed in their locations, second scenario
 Table 27: Optimized placements, optimized power other related parameters
 Table 28: Summary of (2,3) DMC

4)Part I (August 1st 2014 and April 14, 2015)

I.1)Statement of problem studied

The potential contributions of this project consist of improving the understanding of the information theory aspects of a distributed underwater sensor network in the context of noncoherent communication techniques. The research goals of this proposal are in line with Army vision and mission, and they are integrated in the exiting research interests of Office of Naval Research (ONR) at the Naval Research Laboratories in Washington DC (Acoustic Division, Code 7120 and the Center for High Assurance Computing, Code 5540).

The novelty of our approach is to investigate the performance of acoustic sensor networks in underwater wireless communication in terms of mutual information, channel capacity, bit error rate, and information loss based on the transmission power, distance, carrier frequency and the bandwidth of the channel. UWSN are typically characterized by severely energy limited nodes. The reason is the nodes have small batteries and therefore cannot afford much energy to complete tasks. As the life time of any individual sensor in the UWSN is limited, the number sensor nodes that stop working due to power loss increases with a lengthened deployment time, therefore the coverage area of UWSN will be reduced. In our approach, we estimated the number of operating receivers within the network based on the knowledge of the Bit-Error-Rate (BER) and the signal detection of the transmitted message, and, therefore, take advantage of the BER variation, which depends on the underwater acoustic channel environment.

In the sensor system architecture presented in Figure 1, the underwater sensor nodes with acoustic modems are distributed in the underwater space. Each underwater sensor node can measure a specific bit rate of the data around it. The sensors are positioned in clusters and they communicate with the Command and Control center via the Monitoring Center (MC). The MC will eventually communicate with Command and Control unit on the shipboard through high capacity wavelength optical fiber links. Different goals in this project can be summarized as [34]:

- To analyze and improve the non-data aided methods for Doppler shift estimation and compensation (squaring time phase recovery method, power spectrum method, and partial autocorrelation method);

- To determine the necessary quantity and deployment strategy of a sensors in a given region and to provide a required security level;

- To minimize the probability of false alarm and the bit error rate;

- To improve decision-making on target detection with sensor collaboration in the context of blind Doppler shift estimation

and detection, and

To improve the ability of a distributed sensor system to detect intruders (targets) and determine how the network wireless sensor design is affected.

Figure 1: The global picture of the overall project

1.2) Summary of the most important results

Our contribution for this period is related to the performance of the UWSN and it consists in how to practically apply our knowledge and education background to enhance the capabilities of UWSN. In order to understand these contributions the reader should be familiarized with the results obtained in the Interim Reports 1-3 because they are not repeated here.

To improve the ability of a distributed sensor system, we concentrated on improving mutual information between two data signals in terms of minimum bit error rate, maximum data rate communication, and channel performance. We focus on the sensor placement in multi-hop to minimize the bandwidth consumption and mitigate the risk of acoustic link failure and information loss. In order to reduce the communication load for each sensor we develop new distributed algorithms for underwater communication similar to those developed in wireless communication in [2]. The advantage of this sensor placement will help in fulfilling the increasing demand for reliable maximum data rate wireless communication links to accommodate the wide range of underwater application.

We developed a Software development (SAM Control) which is a GUI interface program that was designed for these experiments. The program is written in MATLAB, which reads and writes data to the serial buffer of the modem. SAM Control greatly streamlines the data collection and data analysis process by automating commonly used functions of the modem. Its main features are:

- COM settings: Configure the COM port settings that are connected to the modem.
- Modem Settings: These sets of control are used to configure the sensor communication parameters, such as receiver threshold, transmission speed (data rate) and receive speed.
- TX Mode: mainly responsible of generating the transmitting data which are the m-sequences of 1023 length so to be send through the sensor.
- RX Mode: managing all operations need to be done by the receiver, including reading the received data and storing it in a desired file type, so it can be ready for performing our analysis and evaluation on the data.

Figure 2: SAM Control GUI

During our experiments, we configured the sensors for serial communication, generated PN-sequence of the code length of 1024 by choosing the 10th order polynomial. We chose 10th order polynomial so that we could generate the sequences with period length of 1023bits. In our practical experiments we transmitted baseband m-sequences of length 1023. Initially, we were not able to receive 1023 bits because of 32 bytes buffer memory of the sensors used. The buffer memory size was only 32 bytes and each bit sent via serial port was coded as 8 bits. As a result, we were only able to send maximum of 30 bits plus 2 bytes handshaking at a time from the m-sequences of length 1023. Therefore, practically the length of the sequence could be considered 30 for one transmission.

In cascaded sensor network given in Figure 3, we transmitted data from sensor 1 (upper left) and we received the output data in sensor 2 (upper right). Then we transmitted the received data from sensor 2 exactly as it was received to sensor 3(lower left). The same process was repeated to send data from sensor 3 to sensor 4. The output at sensor 4 was compared with input data at sensor 3 and then we calculated mutual information. Besides, bit error rate, probability error, and information loss is calculated at each communication channel. The obtained results are given in the following in many tables presented below.

Figure 3: Cascaded underwater wireless sensor network

For a collaborative network, we obtained the experimental result for cascaded wireless sensor network in an underwater acoustic communication for four sensors. The bit loss and bit error were computed in an underwater channel sending 1023 bits of 1's and 0's alternately for couple of times for different location of sensors.

Table 1: Bit loss test for different distance of sensors

For the data obtained in Table 1, we transmitted 1023 bits of binary sequences data to the receiver sensor node at a distance of 5 m. This channel transmitted all 1023 bits; however it has bit error of 8 bits in average.

Table 2: Result analysis for Tx1 and Rx1 (d=5 m)

In Table 2, the transmitted data were exactly the received data from first sensor node; however we filtered the error bits that were incurred in first channel. This channel was also set for distance of 5 m between transmitter and receiver. We were able to handle a communication of data between sensor nodes with bit error of 7 -8 bits in average.

Table 3: Result analysis for Tx2 and Rx2 (d=5 m)

In Table 3, we load the received data from sensor node 3 and transmitted exactly to another sensor node in cascaded network. This receiver was at a distance of 5 m. The channel had full communication of data with bit error of approximately 7-8 bits.

Table 4: Result analysis for Tx3 and Rx3 (d=5 m)

Table 4 shows our improvement regarding drop in bit loss and bit error compare to direct transmission between two sensor nodes and cascaded network. The channel distance was approx. 15 m. The output result shows that the channel has bit error along with bit loss. This proves that transmission loss in underwater acoustic communication depends on distance.

Table 5: Result analysis for Tx1 and Rx4 (d=15 m)

Table 5 shows that underwater acoustic communication (UAC) capacity is strongly dependent on transmission distance. Using more than one sensor in cascaded network system will increase in the mutual information and rate of data transmission with minimum bit error probability. A summary of all results are given in Table 6.

Table 6: Result analysis for cascaded sensors network

A similar experiment was performed in parallel sensor network system. In this system, we have one transmitter and 3 receivers, acting system as Single Input Multiple Output (SIMO) system. The optimum output was recorded each time and the experiment was carried out several times for m sequences of length 1023 bits. The result obtained for probability of error, BER, mutual information, entropy estimation is displayed in numerical results in Tables.

Figure 4: Parallel underwater wireless sensor network

Similarly, an experimental result for parallel sensor network model shows the following outcomes shown in Table 7. This channel network is more effective than cascaded sensors network channel; however cascaded network can transmit data to larger distance for available sensor nodes. In parallel sensor network channel, bit error rate is significantly low compared to cascaded sensor networks. This tells us that data transmission in parallel sensor network has low probability error. The bit loss and bit error in data transmission between transmitter sensor and any received sensor might be fixed during data transmission with second or third sensor node.

Table 7: Result analysis for Tx1 and Rx1

The maximum distances between two communicating sensors were 15 meters. The sensors were positioned such that they could float in water and move freely. We are optimizing the sensors locations and sensitivity analysis to increase the mutual information and channel capacity [6-8]. In the experimental model, we studied the impact of using moving acoustic sensor node in a point to point communication system to accomplish same work done in the cascaded network model above.

Figure 5: Underwater Mobile Acoustic Sensor Network

The receiver has been moving while receiving the transmitted data in both vertical and horizontal directions, the maximum distances reached between the two sensor nodes is 15m, as we were limited it by the size of the indoor pool, where the experiments took place. We have done the transmission of the data several times over different distances with different velocities. All the experimental observations and result we obtained for probability of error (BER) mutual information, entropy estimation is displayed in numerical results in section below. In Table 8, the bit loss and bit error were computed in an underwater channel sending 1023 bits of 1's and 0's alternately for a couple of times for different velocities of the moving sensor over 15m maximum distance apart between the sensors. In Table 9, the bit loss and bit error were computed in an underwater channel sending 1023 bits of 1's and 0's alternately for a couple of times for different velocities of the moving sensor over 15m maximum distance apart between the sensors.

Table 8: Bit loss test for mobile sensor nodes of maximum distances $d = 15m$.

Table 9: Bit loss test for mobile sensor nodes moving in vertical direction.

In the table below, we show the information theoretic aspects, we use to evaluate the performance of our point to point communication system model using mobile sensors nodes moving with velocities $v_1= 1$ knot, $v_2=2$ knots and $v_3= 3$ knots.

Table 10: Performance results of using mobile sensor nodes

X and Y are the transmitter and receiver nodes respectively in our communication system. As shown in Table 4, we achieve maximum mutual information ($I(X, Y) = 1$), since we have received same sequence length of the transmitted data. However, there is a small probability of error in reconstructing the transmitted bits. In conclusion, after estimating a simulation study of the UAC model, we used the information theory aspects tools to compare the performance of our UWSN model using mobile sensor nodes to the UWSN model that the author proposed [3]. We observed remarkable results in terms of the performance based on probability of error, mutual information and loss of information. The result of this work indicates that the use of few mobile sensors in UWSN can accomplish the same work as a larger group of static networks and achieve comparable results with low probability of error ~ 0.001 . The experimental approach is presented in Fig.6.

Figure 6: Experimental approach setup

In the distributed sensor network model shown in Figure 4, we have one transmitter and 3 receivers optimally distributed, acting system as a Single Input Multiple Output (SIMO) system. We have started by transmitting the data while only one operating receiver (sensor) and the rest of the sensors were not functioning. The optimum output was recorded each time for m-sequences of length 1023 bits. Our developed software is continuously analyzing the received data and based on the results calculations of the loss of information, BER and mutual information, it sends a signal to operate other sensors. While collecting the data from multiple sensors/receivers, the software process compares and combines the data to achieve the desired BER value and signal detection quality with the least number of operated receivers. The user can set a threshold for the BER and the MI, so it compares it to the results and maintain that desired threshold. Several Experiments have been done in the University of the District of Columbia's indoor pool over different environments (existence and nonexistence of moving targets) to verify our approach and results.

In Table 11, the bit loss and bit error were computed for this scenario (we call this scenario #1) where no moving target or in clear underwater channel sending 1023 bits of 1's and 0's alternately for a couple of times with no effect of noise by moving target or high disturbance waves. The maximum distances were 15m between the sensors. We set the threshold BER = 0.003. It means that the least number of sensors will be used to maintain signal quality or the BER for the transmitted sequences no more than 0.003 (3bits error out of every 1000 transmitted bits) and since The BER less than desired value, only one sensor is functioning and collecting data while the rest of the deployed sensors are not functioning and result in reducing power consumption by the network.

Table 11: Numerical results for scenario #1

Now, we consider the case when the target is moving. In the table below, we show the analysis and results for scenario #2 where there is a target moving and making noise. During the transmission we used a moving boat to have a similar effect of moving object as well as increase the noise level in the underwater channel while the BER threshold was set to 0.003.

Table 12: Numerical results for scenario #2

As shown in Table 12, the BER of the transmitted data decreasing regularly. Since, the BER for the first sequence transmitted data is less than the threshold, the software sends signal to turn on the next adjacent sensor to start recording data and as a result we can see the BER decreased to 0.005. But, since the BER still less than the desired value (0.003), it turns another sensor to collect the data from the three sensors and by combining and selecting the data with lowest probability of error, so that it achieves a better signal detection and BER.

As mentioned before, based on Interim report 1-3, we used the hydrophone to practically find the PSD of the noise in UAC and its relation with the transmitted frequency. The transmitted signal has a carrier frequency of 17 kHz and the sampling rate of 8000. From the Figure 7, we can see that the power of noise is high for frequency range of 0 to 5 kHz. As the frequency increases we can observe that the power of noise is less than 38dB. So if we are able to transmit the signal in the frequency range where the noise power is relatively less, we can obtain better performance. Therefore, we choose 17 kHz of carrier frequency for our experiments.

Figure:7. PSD of Noise (No (f)) experimentally measured in underwater

Table 13: Result analysis of using fixed sensor nodes

In conclusion, we used the information theory aspects tools to compare the performance of our UWSN model using mobile sensor, as opposed to fixed sensor nodes in UWSN. We observed remarkable results in terms of the performance based on the probability of error, mutual information and loss of information. Our result indicates that the use of few mobile sensors in UWSN can accomplish the same work as a larger group of static networks and achieve comparable results with low probability of error

~0.001.

Table 14: Summary results for using mobile sensor nodes

Also, another significant contribution is we show the results of applying our experimental approach to UWSN can reduce the BER of the communications system while at the same time maintaining low power consumption depending on the underwater environment.

Table 15 Numerical results for scenario #1 (no target is moving):

Table 16: Approach results in noisy UAC (Scenario#2)

In Table 15 & 16, we can notice the relation between BER and number of operated sensors. The more sensors operate, the less BER goes where result in better signal detection. Also, the number operating sensors vary depends on the underwater channel environment. If there is low level of noise, fewer sensors will be working and then noticeable reduction in the power consumption will be observed.

I.3)Accomplishments for this period included in Part I:

Paper published: 4 conferences (1 IEEE, 3 ASEE)

Paper under in progress: 2 (1 under review, 1 going to be submitted this fall)

5 MSEE students presentations at the University of the District of Columbia, Research meetings, and ASEE UDC Conference in the fall of 2014.

2 Undergraduate students supported for conference travel to Philadelphia, Fall 2014 and San Antonio Spring 2015.

3 Graduate students supported: 2 Master Thesis successfully defended in Fall 2014 and Spring 2015. One graduate student defended his master project in Spring 2015.

5)Part II (August 1st 2013 and July 31st , 2014)

II.1) Foreword

The results obtained between August 1st 2013 and July 31st 2014 are along with the objectives of this grant. We investigated the performance of wireless sensors in cascaded multi-hop relay network in Underwater Acoustic Communication (UAC). We focused on the optimizing the mutual information between transmitted data and received data for a specific network model in underwater channel. Specifically, we use multiple sensor nodes in a relay network to transfer the data signal into long distance for maximum mutual information. In addition, we studied the relationship of channel capacity to transmission power, bandwidth and carrier frequency. In comparison with the free space wireless communication, the underwater acoustic communication suffers from the limits of the less available bandwidth and complex noise caused by the underwater channel. Therefore, we derived an algorithm for the placement of sensor nodes at an optimal distance in a multi-hop relay network.

We use information theoretic analysis tools to demonstrate the effect of delay, carrier frequency, noise, and link distance on the maximizing the mutual information. In the second part of our research, we worked on experimental data received from a pair of SAM-1 acoustic sensors provided by Desert Star Systems. We used information theoretic tools of entropy, conditional entropy, probability mass function etc. of input and output data signal to analyze the mutual information, information loss, bit error rate, and channel capacity. The significant research of this thesis is observing the multi-hop relay network model and to analyze the optimal distance, frequency, and capacity for available bandwidth in Underwater Wireless Sensor Network (UWSN). Various algorithms are discussed emphasizing on non-coherent approaches.

II.2)Statement of problem studied

The potential contributions of this project for this period consist of improving the understanding of the information theory aspects of a distributed underwater sensor network in the context of noncoherent communication techniques. The research goals of this proposal are in line with Army vision and mission, and they are integrated in the exiting research interests of Office of Naval Research (ONR) at the Naval Research Laboratories in Washington DC (Acoustic Division, Code 7120 and the Center for High Assurance Computing, Code 5540).

The novelty of our approach is to investigate the performance of acoustic sensor networks in underwater wireless

communication in terms of mutual information, channel capacity, bit error rate, and information loss based on the transmission power, distance, carrier frequency and the bandwidth of the channel. A placement of multiple acoustic sensors in a multi-hop relay form is needed in numerous applications where data transmission has to be accomplished beyond short distances. This network is effective since the bandwidth of an underwater acoustic communication is severely limited and decays with increase in distances. It is advantageous to accomplish such transmission using sensors in a multi-hop relay form keeping constraints such as transmission rate, transmission delay, Signal-to-Interference and Noise Ratio (SINR) under consideration. In particular, we consider a communication scenario where a certain number of bits have to be transmitted over a distance d .

Our result analyzes the optimal number of sensor nodes, N to use over a link distance d to increase the mutual information between transmitted data and received data in terms of link capacity, delay, information loss, and bit error rate. So far, different goals of our projects can be summarized as [11]:

- To analyze and improve the non-data aided methods for Doppler shift estimation and compensation (squaring time phase recovery method, power spectrum method, and partial autocorrelation method);

- To determine the necessary quantity and deployment strategy of sensors in a given region, and to provide a required security level;

- To minimize the probability of false alarm and the bit error rate;

- To improve decision-making on target detection with sensor collaboration in the context of blind Doppler shift estimation and detection, and

- To improve the ability of a distributed sensor system to detect intruders (targets) and determine how the network wireless sensor design is affected.

There are some scientific barriers related to problem studied: 1) Lack of experimental results on improving mutual information between two data signals in terms of minimum bit error rate, maximum data rate communication, and channel performance. 2) What is the optimum sensor placement in multi-hop in order to minimize the bandwidth consumption and to mitigate the risk of acoustic link failure and information loss. For reducing the communication load for each sensor we developed new distributed algorithms for underwater communication similar to those developed in wireless communication in [14].

The advantage of this sensor placement will help in fulfilling the increasing demand for reliable maximum data rate wireless communication links to accommodate the wide range of underwater application. We also focused on algorithms that reduce the significant challenges to the development of underwater wireless systems such as complex channel noise, bandwidth limitations, and frequency and distance dependent signal attenuation [5]. Scientific progress and accomplishments including significant theoretical and experimental advances are given in the next section.

II.3) Summary of the most important results

We modeled our sensors as a multi-hop relay network to maximize mutual information for point to point Gaussian channels between transmitter and receiver in the underwater environment. Our contribution is on UWSN design for long range acoustic communication placing an optimum number of sensor nodes at an optimum distance for certain average transmission power. By maximizing the mutual information with an upper bounded average power yields the same channel capacity [6]. We focused on non-coherent channels for maximizing the mutual information between transmitter and receiver. We study the transmission distance, data rate, and channel noise to get the maximum of the digital information embedded in the received signal to maximize the mutual information. We applied a multi-hop relay sensor node by dividing the total link into multiple hops, where a relay acoustic node is employed at each hop as in Fig.8

Figure 8 Illustration of Multihop network.

The relay node receives the signal, regenerates it, and passes it on to the next hop, until the final destination is reached. The question of interest to our design is how exactly does this approach gives improvement in terms of maximizing the mutual information, total power consumed, energy per bit, overall cost and delay. We use an information theoretic tool to accomplish the assumption that the capacity of relay channel is equal to the capacity of each of its hops, and are shown to increase with the number of relays. Here, we show that relaying also helps to reduce the total transmission power and its benefits are even more pronounced in view of energy per bit savings. We consider system optimization in the light of minimizing both bit error rate and the information loss as in Fig.9

Figure 9. Delay between Relays

We focused on an experimental approach for placement of sensors in underwater for minimum BER and maximum mutual information. Our experimental model consisted of an indoor swimming pool, two pairs of SAM-1 acoustic transducers provided by Desert Star Systems, two portable computers both equipped with MATLAB software, signal processing toolbox, communication toolbox, a hydrophone to measure sound underwater, and an acoustic speaker to generate noise as in Fig.10. The data is transferred using transducers and is processed in Matlab. In our experiment, the transmitted signal has a carrier frequency of 17 kHz and the sampling rate of 8000 as in Figs. 10 , 11 and 12.

Figure 10. Acoustic Sensors by Vendor and Experimental set up in Underwater Communications

Figure 11. PSD of Noise ($N(f)$) experimentally measured in underwater

Figure 12 shows that power of noise is high for frequency range of 0 to 5 kHz.

As the frequency increases we observe that the power of noise decreases up to -12 dB. Therefore, we choose to transmit the signal in the frequency range where the noise power is relatively less, and gives better performance in terms of BER and mutual information bound.

Figure 12. Matlab simulation Set Up for multi-hop network sensor model

Figure 13 gives the insight of how the multi-hop relay network is setup. In Matlab simulation, we connect an output from first hop to second hop as an input and transmit data with some delay and noise. Before transmitting a data to second hop, BER and mutual information is calculated and data are regenerated such that noise and error does not get accumulated throughout the transmission.

Figure 13. Transmitted and Received Modulated m-Sequence Signals (17 KHz)

Table 17. Modem Specifics and Operating Function

We perform a serial data communication via serial port using RS-232 levels. The data are transmitted at 4800 baud and 8 data bits. To perform serial communication from Matlab software, we first define the serial port object and then configure device parameters for communication. Values sent, received, transfer status and bytes available are recorded in Matlab for tracking purpose. We increase the buffer size of Matlab software to 1023 bytes (by default it is 512 byte). The received data is then loaded to workspace as in Fig.5. We do the similar experiment using Simulink and record the data to the workspace. Since there are only four stationary nodes in our network, we use a static routing table that lists the routing paths for all possible source-destination pairs. For example, we place the four nodes on a straight line, and label them as A, B, C and D respectively. If node A generates a message with the source field as A and the destination field as D, then the next-hop is node B and then node C in the routing table for the (A, D) source-destination pair.

Table 18. Bit loss test for different distance of sensors

In Table 19, we transmit 1023 bits of binary sequences data to the receiver sensor node at a distance of 5 m. This channel transmits all 1023 bits; however it has bit error of 8 bits in average.

Table 19. Result analysis for First Hop Tx1 and Rx1 (d=5 m)

In Table 20, the transmitting data are exactly the received data from first sensor node; however we filter the error bits that are incurred in first channel. This channel is also set for distance of 5 m between transmitter and receiver. We get a full communication of data between sensor nodes with bit error of 7-8 bits in average.

Table 20. Result analysis for Second Hop Tx2 and Rx2 (d=5 m)

In Table 21, we load the received data from sensor node 3 and transmit exactly to another sensor node in a relay network. This receiver is again at a distance of 5 m. The channel has full communication of data with bit error of approximately 7-8 bits.

Table 21. Result analysis for third Hop Tx3 and Rx3 (d=5 m)

Table 22 shows our improvement regarding minimization in bit loss and bit error compare to direct transmission between two sensor nodes and a relay network. The channel distance is approximately 15 m. The output result shows that the channel has bit error along with bit loss. This proves that transmission loss in underwater acoustic communication depends on distance.

Table 22. Result analysis for Tx1 and Rx4 (d=15 m)

Table 23 shows that underwater acoustic communication (UAC) capacity is strongly dependent on transmission distance. Using more than one sensor as multi-hop network system model, increases the mutual information and rate of data transmission with minimum bit error probability.

Table 23. Result analysis for Multihop relay link and direct link

The problem of an optimum placement of sensors in a multi-hop relay structure for long range acoustic communication in underwater channel have been investigated to maximize the mutual information and channel capacity. The optimum communication frequencies for given link distance and bandwidth available have been calculated where noise power is low. The deployment of sensors in multi-hop relay structure for large transmission range has been considered to minimize bit error rate and information loss as well.

Additionally, an analytical and experimental result of multi-hop sensor network model in a relay has been investigated to optimize the mutual information and maximize rate of data communication. It was advantageous to accomplish such transmission using relays since the available acoustic bandwidth decayed with increase in distance. Moreover, numerous applications required a relay acoustic link where data transmission had to be accomplished beyond short distances. The multi-hop relay structured that we have used would be suitable fit to address the issues of power and energy consumption, and link delay along with maximizing mutual information.

The improvement in mutual information and data rate transmission has been investigated using information theoretic tools such as entropy, conditional entropy, and information loss between transmitted and received data signals. Based on our experiment and simulation result, we concluded that the mutual information between transmitted and received data signal can be maximized by placing extra sensor nodes in between a transmission range which also decreased BER and information loss. The problem occurred in our analytical result was an additional delay due to relay link. However, we observed that delay depended on the rate at which the information is transmitted as well. This fact implied an interesting property of an acoustic link: although each relay introduces an additional delay, as the hops become shorter transmission can be accomplished faster over each hop. This improvement is specific to the underwater acoustic environment, where bounds of mutual information and bandwidth are dependent on the transmission distance.

During our experiment we had several issues with data compatibility with the software. It took several hours to run the Matlab programs. Memory buffer size of sensors was another issue, which only transmit real data signal through serial communication. We also observed that Matlab serial communication does not support complex signals. We had problems with the sensors since they transmitted some random signals by themselves due to unknown internal error.

We can expand our work for movable sensor nodes in underwater channel to address the issues with Doppler spread. Along with a relay network, we can address a multi-path channel model and use the wireless communications knowledge of MRC (Maximal Ratio Combination) to increase the detection quality of received signal.

II.4) Accomplishments for this period included in Part II

Paper published: 6 conferences (4 IEEE, 1 IEEE invited paper, 1 ASEE)

Paper under in progress: 4 (1 under review, 3going to be submitted this fall)

Invited talks: 1 (University "Polytechnica", May 2014).

5 MSEE students presentations at the University of the District of Columbia, Research meetings, and ASEE UDC Conference in the fall of 2013.

3 presentations at Engineering week at UDC, Graduate and undergraduate research day at UDC

4 Undergraduate students supported: 2 Undergraduate students supported for conference travel to Philadelphia, Fall 2013.

5 Graduate students supported: 2 Master Thesis successfully defended Spring 2014. Another 2 students will defend in the AY2014-2015.

6) Part III (Period August 1st 2012-July 31st 2013)

III.1)Foreword

The results obtained between August 1st 2012 and July 31st 2013 are along with the objectives of this grant. We investigated different methods for blind Doppler shift estimation and compensation in underwater acoustic wireless sensor networks. Our study is based on the data collected from our experiments. We conducted experiments for underwater acoustic wireless communication using a pair of SAM-1 sensors provided by Desert Star Systems. MATLAB software was used to send data via the serial port for transmission and acquire data from a sensor into a PC. We analyzed the data collected from the experiment using non-data aided techniques such as Power Spectrum analysis, Autocorrelation, and Squaring Time Phase Recovery (Oerder & Meyr) to estimate Doppler shift in collaborative distributed underwater sensor networks.

We also extensively investigate optimal sensor placement in a tree structured multi-hop hierarchical network. We focused on optimization of the consuming energy by each sensor node for this specific network. We assume that our network contains a number of sensor nodes, distributed at different water depth levels, and that the nodes communicate with each other for purposes of monitoring and tracking. Specifically, we focused on a symmetric tree like multi-hop hierarchical routing topology, which can potentially cover larger areas as we go deeper in the water than flat placement of underwater sensor networks. We derived an optimization algorithm for the locations of sensor nodes in the mentioned network. This algorithm applies to both symmetric as well as asymmetric tree shaped hierarchical networks and it provides the optimum distances between children nodes and their parent nodes.

III.2) Statement of problem studied

The novelty of our approach is to estimate Doppler shift by blind methods. We explored different types of parametric and blind spectral estimation techniques and compared them. We generated different types of random processes corrupted by noise of 25dB signal to noise ratio (SNR). We analyzed the PSD for different types of random processes. We observed that the Periodogram spectral estimation technique is better to locate the dominant frequency than other blind spectral estimation methods. It gives sharp and a highest spectral peak at frequencies with high power and distinguishes nearby frequencies clearly. In addition, we observed that the Welch's method is smoother and covers a large window. Therefore we choose both the Periodogram and the Welch's methods for blind Doppler shift estimation performance bounds for channels communication which are more accurate and less computationally expensive.

We examined different modulation techniques that would increase the bandwidth of a waveform while maintaining pulse duration. We focused on the linear frequency modulation (LFM), and spread spectrum techniques. Specifically, we modulated the transmitted signal using LFM and maximal length sequence, also called m-sequence. We used 2 kHz of sweeping frequency for LFM and m-sequence of length 1023 bits. We observed that these two modulations, when used together, give better signal resolution and are more robust to noise and Doppler spread.

We developed an algorithm for optimum placement of the underwater sensors which can be used for different possible communications channels. We considered the ideal channel scenario, the imperfect channel scenario without having interference between sensor nodes and the imperfect channel scenario considering the interference only between children sensor nodes and their parent nodes. We found the exact optimal locations of sensor nodes using the Karush–Kuhn–Tucker (KKT) conditions by considering the interference between the sensor nodes. Using the same approach, we find the optimized consuming energy for each sensor node having fixed locations. It is worth mentioning that the energy consumption and the efficient usage of energy are of notable importance to Underwater Wireless Sensor Networks (UWSNs).

There are some scientific barriers related to problem studied: 1) Lack of the information theoretical bounds for the binary underwater communication channels in the presence of the Additive White Gaussian Noise (AWGN). How the information about the target is processed in a faster way with a limited computational resources. 2) How the non-coherent communication methods can be used for extracting more information from a cooperative underwater sensor network for tracking the target. 3) The protocols used in actual acoustic networks (usually inspired from terrestrial wireless ad hoc networks) cannot be employed to handle self-organized sensors with slow data rates and high random dispersion rates. Scientific progress and accomplishments including significant theoretical and experimental advances are given in the next section.

III.3) Summary of the most important results

Our experimental model consisted of an indoor water tank, and an indoor swimming pool, a pair of SAM-1 acoustic transducers provided by Desert Star Systems, two portable computers both equipped with MATLAB software, signal processing toolbox, a communication toolbox, a hydrophone to measure sound underwater, and an acoustic speaker to generate noise. The data was transferred using a pair of acoustic modems and was processed in MATLAB. Figure 1 illustrates our prototype environment where the sensors are connected to the computer via a serial port and are floating in the water.

Figure 14 Experimental set up and its components

To carry out the experiment on daily basis, we used a plastic water tank by assuming the acoustic environment to be anechoic: an environment without reverberation of signals. However, the acoustic environment had surrounding noise and human made noise. The distance between the sensors were kept 7ft apart all the time (diagonal) so that we would have the longest time lag. After our experiments in the water tank, we performed our experiment in the swimming pool. The distance between two communicating sensors were 15 yards and the depth of the swimming pool was 11ft and 8 inches. The surface temperature of the swimming pool was seventy degrees Fahrenheit and the water was chlorinated.

The sensors were positioned such that they could float in water and move freely. We have used a pair of acoustic modems provided by Desert Star Systems to perform practical experiments. The modems can operate in the range of 250 meters. The

transmitting power of the sensors depends on the voltage supply (ranging from 183dB at 8V to 189dB at 16V). We configured the sensors to operate at 13 bits per second. The main problem in our experiment was the limited storage of the modems. The buffer memory size was only 32 bytes and each bits sent via the serial port were encoded as 8 bits. As a result, we were only able to send a maximum of 32 bits at a time from the m-sequences of length 1023. So practically the length of the sequence could be considered to be 32 for one transmission.

The acoustic modems transferred serial data at 4800 baud, 8 data bits, no parity, and 1 stop bit. Flow control was set to software handshaking. We used Matlab Simulink to transmit the whole 1023 length sequence. Initially, we measured underwater channel noise and plotted its PSD. The purpose of this study was to find the suitable frequency range for transmission, such that noise would be relatively less dominant in that frequency ranges than others. We measured the noise during our experiment for the length of 3.65 minutes sampled at the rate of .01s and plotted its autocorrelation and PSD.

Figure 15 Autocorrelation of Noise Measured in Swimming Pool

From Figure 15 we can observe that the autocorrelation of the measured noise is 1 at time 366 milliseconds which refers to the 0 time lag. As the time lag increases, the autocorrelation of the measured noise decreases.

Figure 16. PSD of Measured Noise in Swimming Pool

From Figure 16 we see that the power of noise is high for frequency range of 0 to 5 kHz. As the frequency increases we observe that the power of noise is less than -11.86 dB. So if we are able to transmit the signal in the frequency range where the noise power is relatively less, we can obtain better performance. Therefore, we have chosen 17 kHz of carrier frequency for our experiments. We could use any frequencies above 5 kHz and below 40 kHz, but to be consistent with [1], [3], [5], [6], we preferred 17 kHz. Besides noise, we investigated different spectral estimation techniques for different types of random signals/processes.

We generated an AR process by filtering a unit variance white noise with an all pole filter, a MA process by all zero filters, and ARMA process with pole-zero filters. From all of the PSD's of generated random processes, we observed that the magnitude of the spectrum was higher for dominant frequency components. It is clear that, we could extrapolate the information contained in the random process by using a band pass filter that would pass only the dominant frequency components. It was observed that for different stochastic process we had different dominant frequency components.

Furthermore, we used the stochastic processes generated using different models described earlier in this thesis for spectral estimation using parametric and non-parametric methods. We used the Periodogram and the Welch's methods for non-parametric spectral estimation, and the Yule-Walker, and the Burg methods for parametric spectral estimation. We compared the results for parametric and non-parametric spectral estimation methods. We observed that non-parametric spectral estimation techniques gave us almost similar results but with a higher magnitude. We have plotted the estimated PSD for all parametric in Figure 17 and blind methods in Figure 18.

Figure 17. PSD Estimation by Parametric Methods

From Figure 17 (a), (b), (c), and (d), we observed that Yule's method of parametric spectral estimation is smoother and covers a large window than the Burg method. Yule's method is preferred in extracting information contained in the signal because it avoids information leakage during windowing. For detection purpose, we preferred Burg's method because it gives a high frequency resolution. Therefore it is useful in detecting underlying frequency component of the signal in environment where the noise spectrum is relatively high. In Figures 5 (a),(b),(c), and (d), we have plotted the spectral estimation results for blind methods.

Figure 18. PSD Estimation by Blind Methods

From the simulation of non-parametric spectral estimation techniques, in Figure 18, we observe that the Periodogram spectral estimation technique gives a sharp peak while the Welch method is smoother and has a larger window that will prevent data leakage while windowing for certain range of frequencies. It is also clear that periodogram method gives many sharp peaks and clearly distinguishes adjacent frequency components. Therefore it is useful in frequency estimation. However, in underwater acoustic communication due to the Doppler shift, adjacent frequency components might result in false frequency estimation. Since the spectrum of Welch's method has a lower magnitude, it is not preferable for higher noise environment. Periodogram techniques are more preferred for fast varying environment for blind estimation of frequency for target detection. In Figure 19 we compared parametric with blind methods for an ARMA random process.

Figure 19. Comparisons of Parametric and Blind Spectral Estimation Methods

We advanced our experimental results further by performing cosine linear frequency modulation and m-sequence modulation.

These modulation techniques were used in data transmission in our experiments. The swiping frequency of LFM was 2kHz (17kHz to 19kHz). Figure 7 shows the chirp cosine signal with swiping frequency of 2kHz, spectrogram and its PSD. It is clear from the spectrum that LFM increases bandwidth. The ripples in the spectrum is due to FFT routine of Matlab. We have also plotted the autocorrelation function for three m-sequences.

Figure 20. Linear Frequency Modulation Cosine, and its PSD

From Figure 20 we see that the LFM increases the pulse bandwidth. As a result, pulse will compress in the time domain. This pulse compression enables us to decouple the duration of the pulse from its energy by effectively creating different durations for the transmitted pulse and the processed echo. We further plotted the autocorrelation function of three m-sequences. Spread spectrum technology is used to broaden the bandwidth of a signal in the frequency domain. In [12], it is proved that spread spectrum technology is more robust to noise and doppler spread than LFM. Therefore, in this thesis, we studied the autocorrelation and PSD maximal length sequences. In Figure 21, we observe the discrete components for each m-sequences at time lag 1023 bits length. It is also observed that the amplitude of autocorrelation for different m-sequences is different. This shows that the correlation between 1st and the second m-sequences is relatively more than first and the third.

Figure 21. Periodic Autocorrelation of PN- Sequences

To examine the performance of the blind methods and to find the Doppler shift, we used MATLAB as user interface to receive and transfer data through SAM-1 acoustic modems. The received data were acquired via serial data acquisition processes in MATLAB. The acoustic modems were operated at baud rate of 4800 symbols per sec and 8 data bits. The data rate of transfer was 13 bits per sec. We used three different types of data for transmission: m-sequence of length 1023, m-sequence of length 1023 modulated with carrier of frequency 17 kHz, m-sequence of length 1023 modulated with LFM signal of sweeping frequency of 2 kHz. The received data for the 1st two types of modulations were analyzed using the spectral characteristics: autocorrelation and PSD, and the last one were analyzed using Oerder and Meyr squaring timing recovery.

In our experiment the transmitted signal had a carrier frequency of 17 kHz and a sampling rate of 8000 samples/sec. The transmitted spectrum in both the cases (tank and pool) had almost a flat spectrum. We plotted the PSD of the received signal and observed the different spectral components for both tank and pool. Initially we plotted the transmitted baseband and received signal in Figure 22.

Figure 22. Initial Transmitted (a) and Received (b) m-sequence signal

We see in Figure 22 that the transmitted data consist of m-sequences with 1023 symbols and the received data is m-sequences with 34 symbols. There was a problem in transmission of the 1023 symbols because the maximum buffer size was only 32 bytes. So basically it was a data overflow problem. We addressed to the problem by writing a program that could send a data in packets of 32 bits at one time. It is equivalent to 4 symbols per transmission with 8 samples per symbol. We choose 32 bits because we observed highest accuracy for a 32-36 bit transmission range during our multiple experiments. We were able to receive all the bits transmitted when 32-36 bits were sent. It is worth mentioning that each bit is encoded in 8 bits by the hardware. In addition the sensors were half duplex. After fixing the data overflow problem, we transmitted the modulated m-sequence. Figures 23-25 shows the signals and their autocorrelation.

Figure 23 Frequency Modulated Transmitted Signal

Figure 24 Frequency Modulated m-Sequence Received Signals (17 kHz)

Figure 25 Autocorrelation of Transmitted and Received 52-m -Sequences

It is clear from Figure 25(b) that on the received signal we were able to distinguish the transmitted 52 m-sequences clearly. However, the received signal is not free of noise and some multipath components. The dark lines refer to the cross-spectral correlation effect. The dark line on the autocorrelation of the transmitted signal is due to modulation effect. So we plotted the partial autocorrelation of the received signal and find out the transmitted m-sequences associated with it.

Figure 26 Partial Autocorrelation of Received Signals Showing 48th to 52nd m-Sequences

In Figure 26, we noticed that the length between each m-sequence is not 1023 bits (in the transmitted signal it was 1023 bits). From this observation we concluded that the multipath effect must have induced additional bits into the received signal during the period of 1023 millisecond.

Figure 27 Power Spectral Density of Transmitted and Received Signal [Water Tank]

In Figure 27, it can be seen that the PSD of transmitted m-sequences is flat and the PSD of received signal is nearly flat as well

but with greater magnitude. This means there might be very less of an effect of multipath components (which are very less because the tank is supposedly anechoic) but more of an effect of noise, and most importantly the data sequence overlap because of the limited buffer memory. In the case of the water tank experiment, we were able to receive same data that was sent with a bit error rate of 0.0078 (we had 8 bits error in 1023 bits). Looking at the partial PSD around the carrier frequency and its period, we can see the Doppler shift.

Figure 28 Partial PSD of a Received Signal [Results for Water Tank]

The partial PSD spectrum in Figure 28 shows that the Doppler shift is 50 Hz at carrier frequency 17KHz and 20 Hz at double of carrier frequency. Taking average we conclude that the estimated Doppler shift is approximately 35 Hz. After measuring the Doppler shift in the water tank, we performed experiments in the swimming pool. In the swimming pool, the transmission range was longer (25 yards) and the environment is echoic, so we experienced more of multipath effect.

Figure 29 PSD of Received Signal [Results for Swimming pool]

We searched for the local maxima around the carrier and found the Doppler shift to be 130 Hz at frequency of 17 KHz and 170Hz in average 150Hz. Then, we transmitted the LFM m-sequences signal and analyzed the signal using Oerder & Meyr squaring recovery circuit. Figures 30 and

Figure 31 show the transmitted signal, received signal, their autocorrelation, and phase shift.

Figure 30 Transmitted and Received Signal for LFM m- Sequences [Pool]

Figure 31 Autocorrelation, PSD and Partial Autocorrelation of LFM 52- m- Sequences

The results obtained in Figure 31 (e) and (f), the Doppler frequency shift is almost consistent with the one from cosine modulated m-sequences for the water tank experiment. One should carefully note the magnitude of spectrum or cosine modulated and LFM modulated m-sequences. We observe same Doppler frequency shift but with different powers of received signal. We should also note that the Doppler shift for cosine modulated m-sequence signal in the swimming pool experiment was approximately 150 Hz, but the Doppler shift for LFM m-sequences is 35 Hz. From this observation we concluded that the double modulation technique is more robust to Doppler spread. We used Oerder & Meyr algorithm to find the instantaneous and average phase shift and plotted in Figure 32.

Figure 32. Estimation of Instantaneous and Average Doppler Shift Using Oerder & Meyr Algorithm

From Figure 32, we see that average Doppler shift is 0.85 and the instantaneous shift of range [0-2.86]. From the experiments, we claim that Doppler shift could be minimized by using double modulation technique instead of using either the LFM or m-sequence technique separately. This can be validated by the minimal shift obtained in Figure 32. It can be observed that, for the double modulation technique, phase shift is less than the one provided in [1]. The results provided in [1] were for m-sequence modulation and the average phase shift was 1.12 for the same parameters ($k=100$ symbols).

In the next we present the numerical results from applying the optimal distance/frequency algorithm (developed under this grant) for different underwater communications channel scenarios. We also provide some explanations for our observations according to the channel model and our assumptions. As seen in Figure 33 and Figure 34 the optimal distances in case of the ideal channel scenario are almost two times longer than the optimal distances in the case of imperfect channel scenario.

Figure 33. 4 level tree structured network with 2 children nodes

Moreover, according to Figure 33 and for the ideal channel scenario, the optimal distance for the leaf sensor nodes successfully transmit the measured information to their parent nodes can be up to 16 Km. According to the results, using CDMA could improve the system performance and the distances could be even longer indicating that for the same amount of transferring information, a channel with CDMA utilization needs less capacity than a regular channel. However, this placement may not provide adequate coverage at those depths since every sensor can cover up to a specific distance. Thus, there is a tradeoff between optimal distance in terms of reliable communication and optimal distance in terms of coverage for the nodes at deeper water. In summary, the optimal placement for the nodes closer to the water surface should follow the non-uniform distance needed for reliable communication and the optimal placement for the nodes farther away from the water surface should follow the coverage rule.

Figure 34. Optimal distance (on the top) for ideal and imperfect channels including BER and interference for a tree shaped topology with 7 levels

As it can be seen from Figure 34, the distances for transmitting the same amount of information at each level can be longer in the case of ideal channel comparing to the same level for imperfect channel. For both scenarios, the optimum frequency at

higher level (corresponding to lower transmitting data rate) would be much more than the required frequency at lower levels. The lower part of Figure 34 has been plotted separately in Figure 35 since it represents the imperfect channel scenarios, which are more realistic ones. Figure 35 also shows how imperfect channels would be enhanced after CC usage. From the results we can conclude that the optimal distances can be longer in the case of ideal channel compared to the imperfect channel, whereas, in the case of using CDMA, distances could be even longer.

Figure 35. The distances for different imperfect channel scenarios and their improved situations after applying CC

Another important research question is the amount of power boost required in the imperfect channel case in order to achieve the same links' lengths as of the ideal channel scenario. As shown in the Figure 36, the power boost depends on the level at which the sensor is located in the underwater acoustic network. However, the power boost in our case is between (660 - 690, i. e., 28.1 dB – 28.3 dB).

Figure 36. The ratio of the sensor power of the imperfect channel compared to the sensor power of the ideal channel

Moreover, the channel characteristics for the 7 level symmetric tree structured sensor network, the optimum transmission frequencies have been numerically calculated and illustrated in Figure 37 under the case of ideal channel scenario. Figure 38 depicts the optimal frequency in the case of imperfect channel with BER of 0.001.

Figure 37. Optimal frequency at each distance associated with a specific level for an ideal channel in a 7-level tree structured network

Figure 38. Optimal frequency at each distance associated with a specific level for an imperfect channel (BER = 0.001) in a 7-level tree structured UWSN

On the other hand, the improved system by using convolutional codes has been shown in Figure 39 [16], [17]. Figure 39 shows the effect of convolutional code on optimal frequency of a tree structured underwater wireless sensor network in which optimal frequency is closer to that one corresponding to the ideal channels. The highest optimal frequency in the case of ideal channel is 8.9 kHz at level 7, while this goes up to 13.69 kHz in the case of imperfect condition and after utilization of convolutional coding this amount decreases slightly to 12.8 kHz. Also, the optimal frequency at higher levels (corresponding to lower transmitting data rate) would be larger than the optimal frequency at lower levels.

Figure 39. Optimal frequency at each distance associated with a specific level for an imperfect channel (BER = 0.001) improved with convolutional code in a 7-level tree structured network

Figure 40 shows the variation of the path-loss in tree structured wireless sensor network as a function of frequency and networking level in the described model. Interestingly, we can see that the optimum operating frequency at each level is in the area around the minimum path-loss, where the inverse amount of path-loss as in the Figure 40 has its pick for each curve. In other words, for any given distances between children nodes and their parents, the narrowband SNR is a function of frequency, and from the Figure 40 it is obvious that the acoustic bandwidth depends on the transmission distance.

Figure 40. Frequency dependent portion of narrow-band SNR.

Now, let us assume that the system operating frequency f and the system bandwidth frequency are equal to 10 KHz and 100 Hz, respectively. This is consistent with the narrowband assumption. Also, the sensor powers are all identical to each other and equal to 1 Watt and the spreading factor for the ambient noise is also 1. We solve the optimization problem for the optimal sensors' location under the above assumptions using a MATLAB codes. Figure 28 shows the optimal sensors' placement.

Figure 41. Optimal placement of the sensor nodes when the transmitting power is constant

Using the optimal sensors' locations, Table I shows the optimal signal to noise ratios over links 1, 3 and link 4.

Table 24. Optimized placements and other related parameters when the transmitting power of each node is constant and equal to 1 watt

The main result of this optimization problem is: with the underwater acoustic sensor network topology in Figure 41, and with the policy explained earlier, under the optimization problem constraints, and with sensors transmit power of 1 Watt, the highest information rate than be transmitted to the root node 0 is equal to 453.37 bps, assuming optimal sensors' locations obtained in the optimization problem. It is interesting to notice that although the tree structured sensor network is symmetric with respect to the root node, the optimal locations of the nodes 3 and 4 are not at the same depth. As expected, since sensor node 3 has fewer number of neighbor nodes, and is less affected by the interference of the other sensor nodes, the optimal distance between child node 3 and the parent node 1 (16.8 km) is larger than the optimal distance between child node 4 and the parent

node 1 (14.2 km). In the next, we assume that the system operating frequency and the system bandwidth frequency are equal to 10 KHz and 100 Hz, respectively. The optimal sensor's power allocation for the tree structured UWSN when its sensors are fixed at the places plotted in the Figure 41.

From Figure 42 we can see that if sensors are located at the same depth assuming they are transmitting the same amount of information, the energy consumption would be more for the ones who are exposed to more interference. In Figure 42, sensors 4 and 5 need more energy than the sensors 3 and 6.

Table 25 shows the coordinates of each sensor node, optimal transferring energy, optimal SINR for each sensor node and the optimal links' capacities.

Figure 42. The optimal power allocations for the scenario 1 are shown near each sensor node (in Watts)

Table 25. Optimized energy allocation and other related parameters when the sensor nodes are fixed in their locations, first scenario

Therefore, the optimal aggregate rate of information of this underwater acoustic sensor network would be 283.37 bps. Now, let us obtain the optimal sensors' power allocation in another network somehow little asymmetric compared to the previous graph, where the nodes are located in the following locations (Figure 43). The optimization problem and the parameters are the same as the first scenario. Table III also depicts all the related parameters of this scenario.

Figure 43. The optimal power allocations for the scenario 2 are shown near each sensor node (in Watts)

In this scenario, the optimal aggregate rate of information of this underwater acoustic sensor network as a result of optimal power allocation would be 437.56 bps.

Table 26. Optimized energy allocation and other related parameters when the sensor nodes are fixed in their locations, second scenario

In the next we assume that both sensors' placement and their consuming power are unknown and we try to find the optimal solution for the cases at the same time, given the mentioned policy. We take the same network parameters we had for previous sections: the system operating frequency f and the system bandwidth frequency are equal to 10 KHz and 100 Hz, respectively which is consistent with the narrowband assumption. But in this part, the power constraint is 1.2.

Figure 44. The optimal sensors' locations and power allocations (in Watts)

Figure 44 shows the optimized locations and the optimized consuming energies for each sensor node at the tree structured network explained earlier. According to the Figure 44 and also the calculated information inserted in the Table 27 we can see that the optimal tree structured UWSN is the one which is symmetric. This could play an important role in the network configuration design. For the UWSNs with more levels, we can consider a symmetric structure and then find the optimal locations and transmitting power for each sensor node.

Table 27. Optimized placements, optimized power other related parameters

Table 27 also shows other the related parameters in the network. It is clear that, the power consumption in the levels closer to the water surface is dramatically larger. The SINRs for each acoustic link could be another proof for that saying, as the SINR for the links 1 and 2 is more than 20 times of that of the links in the higher levels corresponding to lower rate of transferring data. One possible solution for this huge difference between the power consumption, channel capacity and SINR of acoustic links at different levels would be deploying more sensors in the levels closer to the water surface. This can be led to change the tree structured configuration of the network so that we start with a specific shape and we can end up with another structure in order to improve the network parameters.

III.4) Accomplishments for this period included in Part III

Paper published: 3 conferences (IEEE, ASEE, IASTED)

Paper under in progress: 4 (1 under review, 3going to be submitted this fall)

Invited talks: 1 (Technical University of lassy, May 2013)).

Poster Presentation: 2 (Dynamics Days 2013, Denver CO, January 2012 and UDC May 2013)

5 MSEE students at the University of the District of Columbia, Research meetings, Fall 2012.

5 presented at Engineering week at UDC, Graduate and undergraduate research day at UDC

6 Undergraduate students supported: 4 Senior student presentation, 2 Undergraduate students supported for conference travel to Philadelphia, Fall 2012.

6 Graduate students supported: 2 Master Thesis successfully defended Spring 2013. Another students to be defended in the AY2013-2014.

New laboratory facility: Advanced Communication Laboratory, Building 32, Room A04, UDC. (New research laboratory at ECE, renovated during the Fall 2011, operational Spring/Summer 2012 and 2013.

7) Part IV (April 6 2011 and July 31st 2012)

IV.1) Foreword

The results obtained between April 6 2011 and July 31st 2012 are along with the objectives of this grant. We focused on the information theoretical aspects of the threshold Discrete Memoryless Channels and wireless MIMO channels. We derived the upper and the lower theoretical capacity bounds and we studied the stochastic resonance effect associated with the DMC channels. All findings and research results were published in collaboration with Naval Research Laboratory researchers, Center for High Assurance Computer System-5540, in Washington DC.

IV.2) Statement of problem studied

The potential contributions of this project consist of improving the understanding of the information theory aspects of a distributed underwater sensor network and optimizing the noncoherent communication techniques. The research goals of this proposal are in line with Army vision and mission, and they are integrated in the exiting research interests of Office of Naval Research (ONR) at the Naval Research Laboratories in Washington DC (Acoustic Division, Code 7120 and the Center for High Assurance Computing, Code 5540).

The novelty of our approach is to provide new information performance bounds for channels communication which are more accurate and less computationally expensive. We focused on noncoherent communications methods to be used by a distributed underwater wireless sensor network to extract and process the tactical information about the target. We studied new non-data-aided techniques for Doppler shift estimation and compensation to be used by a collaborative distributed underwater sensor network communicating at physical layer. In addition, the proposed research project includes developing information theory based tools for tracking the target by maximizing the mutual information between the moving target and each sensor location.

There are some scientific barriers related to problem studied: 1) Lack of the information theoretical bounds for the binary underwater communication channels in the presence of the Additive White Gaussian Noise (AWGN). How the information about the target is processed in a faster way with a limited computational resources. 2) How the non-coherent communication methods can be used for extracting more information from a cooperative underwater sensor network for tracking the target. 3) The protocols used in actual acoustic networks (usually inspired from terrestrial wireless ad hoc networks) cannot be employed to handle self-organized sensors with slow data rates and high random dispersion rates.

IV.3) Summary of the most important results

We studied the performance of Discrete Memoryless Channels (DMCs) arising in the context of cooperative underwater wireless sensor networks. We introduced a partial ordering for the binary-input ternary output (2,3) DMC. In the particular case of the Binary Symmetric Channel with Symmetric Erasure (BSC/SE), we used majorization theory, channel convexity and directional derivative in order to obtain a partial solution to the open problem of partial ordering of the DMCs. In addition, we analyzed the stochastic resonance (SR) phenomenon impact upon the performance limits of a distributed underwater wireless sensor networks operating with limited transmitted power and computational capabilities.

We focused on the threshold communication systems where, due to the underwater environment, non-coherent communication techniques are affected both by noise and threshold level. The binary-input ternary-output channel is used as a theoretical model for the DMC. We derived the capacity of the threshold (2,3) DMC in the presence of additive noise. The plots of BSC/SE and BAC/SE capacities are represented in Figures 45 and 46, respectively.

Figure 45. BSC/SE capacity

Figure 46. Capacity of BAC/SE

In order to evaluate stochastic resonance, we modeled the theoretical (2,3) DMC as a physical communication channel corrupted by additive noise with different probability distributions. The (2,3) DMC becomes the BSC/SE when the probability density function of the additive noise is an even function such as Gaussian, Laplace, and Cauchy distribution. Capacity of BSC/SE for threshold values is plotted in Figure 47.

Figure 47. Capacity of BSC/SE for threshold values.

Due to the complexity and the non-linearity of the channel capacity analytical expression, the Pinsker and Helgert capacity bounds were also used to evaluate the stochastic resonance in the case of the (2,3) DMC. Our contribution consists in improving the state of the art on the issue of partial ordering for the (2,3) DMC and deriving the optimal noise level required to obtain the maximum capacity for a given threshold decision level in the case of the binary-input ternary-output DMC. These results are plotted in Figures 48, 49 and 50.

Figure 48. (2,3) DMC and Pinsker capacity Bound

Figure 49. (2,3) DMC and Helgert capacity Bound

Figure 50. Capacity(C), Pinsker (L) and Helgert (U) bounds for different values of threshold

We analyzed the stochastic resonance phenomenon which is a non-linear effect wherein a communication system can enhance the transmission of the information in the presence of the additive noise [2-5]. Various performance metrics in the presence of stochastic resonance such as signal to noise ratio, mutual information, and channel capacity improvement, under a certain range of power noise levels, were discussed in [5]. It is observed that the channel capacity increases, as the noise level increases, until the channel capacity reaches a resonance peak. This increase of the channel capacity is not in concordance with the intuition that increasing the noise power level will decrease the channel capacity. We analyzed the physical communication model of the (2,3) DMC for threshold based stochastic resonance due to additive noise. A summary of our results are given in Table 28 Summary of (2,3) DMC.

Table 28 Summary of (2,3) DMC.

In [5] we focused on partial ordering in the case of the BSC/SE. The BSC/SE is of interest because it is known that in presence of additive Gaussian noise (AGN), the general (2,3) channel becomes the BSC/SE (2,3). The partial ordering of DMC consists of comparing DMC capacity based on the noise components without the computation of the analytical relation of the channel capacity, which in general, is very complex and non-linear. The ordering is critical, especially for wireless sensor communication links at the physical layer operating in very noisy environments with limited computational and power capability as we proposed in our grant. Our partial ordering is based on channel convexity and majorization theory. We reviewed the partial ordering for the particular case of the BSC and BEC and we proved three theorems (Theorems 4.2.1, 4.2.2 and 4.2.3) based on channel convexity and majorization theory. These theorems are used to provide a partial ordering for the BSC/SE (see the Appendices).

Our research results clearly indicate how one could compare the channel capacity under the stochastic resonance by using our analytical relation of the capacity and/or including the capacity bounds. They also demonstrate how one could improve the capacity of the binary threshold communication channel by changing the noise power or the threshold level as plotted in Figure 51.

Figure 51. Optimal noise power and threshold for stochastic resonance, with a scalable factor

In regarding the experimental results, we focused on four different projects in order to do our experimental work and collect data. The graduate students mentored the undergraduate students in teams as it was specified in the educational goals of this grant.

In the first project titled "Low Cost Frequency Shift Keying Acoustic Modem for Underwater Wireless Sensor Networks", we designed and build a prototype acoustic modem to serve as a physical transport layer for underwater digital communications. It converts between a digital communications scheme (function generator) and an acoustically coupled communications scheme required by our grant design. Specifically our project consisted of a pair of modems to operate as transmit/receive pairs and supports duplex communications. Although our modem operates in air, it is a proof-of-concept experiment in data transmission techniques that will be used to design a system capable of communicating over some distance in the underwater environment.

Determining the distance was the most challenging aspect of our design of the acoustic modem project. We did a lot of research in comparing different design of acoustic modems and the application used for each implementation. We considered three approaches available in order to design an acoustic modem. This can be implemented using microcontroller, FPGA board, and XR-2206 function generator with the appropriate electronics components. Finally, we focused on acoustic modem circuitry using electronics components to implement both the transmitter and the receiver.

We used the XR-2206 which is a monolithic function generator integrated circuit capable of producing high quality sine, square, triangle, ramp, and pulse waveforms of high-stability and accuracy. The output waveforms can be both amplitude and frequency modulated by an external voltage. Frequency of operation can be selected externally over a range of 0.01Hz to more than 1MHz. The circuit is ideally suited for communications instrumentation, and function generator applications requiring sinusoidal tone, AM, FM, or FSK generation. It has a typical drift specification of 20ppm/°C. The oscillator frequency can be linearly swept over a 2000:1 frequency range with an external control voltage, while maintaining low distortion.

We also used the XR-2211 which is a monolithic phase-locked loop (PLL) system especially designed for data communications applications. It is particularly suited for low rate FSK modem applications. It operates over a wide supply voltage range of 4.5 to 20V and a wide frequency range of 0.01Hz to 300kHz. It can accommodate analog signals between 10mV and 3V, and can interface with conventional DTL, TTL, and ECL logic families. The circuit consists of a basic PLL for tracking an input signal within the pass band, a quadrature phase detector which provides carrier detection, and an FSK voltage comparator which provides FSK demodulation. External components are used to independently set center frequency, bandwidth, and output delay.

In the second project titled "Localization of an Underwater Object" we used the LabView software. The scope of the project was to develop a system interface that would provide the velocity and distance of a remote operated vehicle. This remote operated vehicle will glide in a tank of water that is 8 feet by 10 inches in length. An active sonar was used in order to send a ping (signal) to the vehicle at differing locations. Depending of its location on some fixed axis, the ping will bounce off the vehicle, bounce from the bottom-surface interface of the tank, bounce from the air-water interface, and finally hit the hydrophone. Some signal reflections will not make as many transitions depending on their location from a fixed axis in the tank.

We tried different design methodologies. Our first design methodology was to use the remote operated vehicle, hydrophone, X-bee communication and LabView software package in order to track the position of the object in free space. We were using GPS technology, to locate the object above water. The location information would have been sent to a central hub via RF communication. Then by LabView visual programming, an interface would have been designed to gather the actual position of the remote operated vehicle. The remote operated vehicle was then to be submerged underwater. Once underwater, a passive series of hydrophones would have been used to locate the object.

The speed would have also been determined. The information from the hydrophone was to be sent serially to a computer. This computer was to be connected to an X-bee network to form a RF communication node between the GPS and the underwater hydrophone. Consequently, the central hub which would have been the LabView software would have done a comparison and contrast analysis of the information sent from the GPS and the computer linked to the hydrophones determining the remote operated vehicle's actual position above and underwater. We have since then disregarded of the idea of using the GPS and X-bee for the more cost efficient design.

Our second design method consists of everything mentioned above except of the X-bee communication module and the GPS. It was necessary to construct active SONAR (Sound Navigation And Ranging) as well as a LabView interface. The active Sonar transmits a generated pulse signal to the remote operated vehicle. We anticipated the sonar signal reflect from the ROV then be received at the hydrophone. The LabView interface displays the Sonar signal as well as the Noise from the hydrophone. The Sonar system consists of LM 386 Audio Power Amplifier, a standard speaker enclosed in PVC piping and a pulse generating program. The hydrophone used was the Dolphin Ear 100 which is a low cost, high quality hydrophone used in professional and academic research, as well as recreationally.

The purpose of the third project titled "Wireless GPS Tracking System with Graphical User Interface" was to design a GPS tracking system which works in real time by using a GPS receiver and radio frequency transceivers. This device can be used for tracking ships or any moving objects and monitors its location, speed and direction. In this project, main focus was to track a ship. The design of this project consisted of two main parts: hardware and software. The hardware part includes components needed in designing the GPS tracking system and designing the circuit interface of the hardware used, so that the functionality of the wireless tracking system can be observed. The software part represented in the developed code which can extract and process the received GPS data and using it to generate a final map showing the transfer location done by the object used to track.

In the last project we worked with SAM-1 Miniature Acoustic Modem in helping undergraduate students to understand how underwater communication modems work. This is related to the grant goal which is to create clusters of underwater sensors that will be able to detect intruders and communicate wirelessly with acoustic waves. Working with SAM-1 improved the undergraduate student understanding of the current state of technology in commercial underwater communications, it helped understanding some principle on which this technology works, they learned about data rate and about acceptable noise levels.

In working with SAM-1, students learned about other issues that characterize underwater communication as: refraction of acoustic waves due to shallow waters and properties of water creating different time of arrival for acoustic waves which could

increase or decrease S/N ratio. In our laboratory setting, water tank of 1m x 3m x 0.6m, the signal send by SAM-1 was strong enough and it was well received for threshold level over T40. Our set up was noisy due to existence of different machinery in our lab. This ambient noise has created errors in rare occasions, and in those occasions no data were received. Also, students learned that there is a significant time delay between data transmission and data being received. This is due to sound propagation, signal processing and data processing.

IV.4)Accomplishments for this period included in Part IV

Paper published: 1 Journal (AECE), 4 conferences (3 IEEE, 1 ASEE).

Paper under in progress: 2 (going to be submitted this fall)

Invited talks: 1 (University of Macao, China, January 2012).

Poster Presentation: 2 (Dynamics Days 2012, Baltimore, January 2012 and UDC May 2012)

Student Presentations: external 4 (QMDNS 2012, April 30-May 1, 2012, George Mason University)

internal 4 (MSEE students at the University of the District of Columbia, Research meetings, Fall 2011)

internal 5 (Engineering week at UDC, Graduate and undergraduate research day at UDC)

6 Undergraduate students supported: 4 Senior design projects finalized in Spring 2012

2 Undergraduate students supported for conference travel to Philadelphia, Fall 2011.

6 Graduate students supported: 1 Master Thesis successfully defended Spring 2012. Another 3 students to be defended in the Spring of 2013.

New laboratory facility: Advanced Communication Laboratory, Building 32, Room A04, UDC. (New research laboratory at ECE, renovated during the Fall 2011, operational Spring/Summer 2012).

8) Bibliography

B. J. Rao and T. Prabhakar, "Underwater Acoustic Wireless Communications Channel Model and Bandwidth," International Journal of Applied Engineering Research, ISSN 0973-4562 Vol. 6. No. 18 (2011).

I. Akyildiz, D. Pompeili and T. Melodia, (2005), "Underwater Acoustic Sensor Networks: Research Challenges," Elsevier Journal on Ad Hoc Networks, Vol. 3, issue 3, pp. 257-279.

M. Stojanovic, "On the Relationship between Capacity and Distance in an Underwater Acoustic Communication Channel," WUWNet, 2006, pp 41-47.

S. Ali, A. Fakoorian, G. R. Solat, H. Eidi, "Maximizing Capacity in Wireless Sensor Networks by Optimal Placement of Cluster Heads," Canadian conference on Electrical and Computer Engineering , May 2008, pp. 001245-001250.

H. Nouri and M. Uysal, "Information Theoretic Analysis and Optimization of Underwater Acoustic Communication Systems," IEEE. 978-1-4673-2232. EuroCon 2013.

D. Lucani, M. Stojanovic, M. Medard, "On the Relationship between Transmission Power and Capacity of an Underwater Acoustic Communication Channel", WUWNet, 2006, pp.41-47.

M. Stojanovic, "Capacity of a Relay Acoustic Channel," IEEE Transactions on Communications. Massachusetts Institute of Technology. 0-933957-35-1. 2007 MTS.

S. Ali, A. Fakoorian, G.R. Solat, H. Taheri, A. Eidi, "Maximizing Capacity in Wireless Sensor Networks by Optimal Placement of Clusterheads," IEEE, 978-1-4244-1643, January 2008.

P. Cotae, I. S. Moskowitz and M. H. Kang, "Eigenvalue Characterization of the Capacity of Discrete Memoryless Channels with Invertible Channel Matrices," Proceedings IEEE 44th Annual Conference on Information Science and Systems- CISS 2010, Princeton University, March 17-19, pp. 1-6, March 2010.

T. Schurmann and P. Grassberger, "Entropy Estimation of Symbol Sequences," Department of Theoretical Physics, University of Wuppertal, D-42097 Wuppertal, Germany.

P. Cotae, S. Yalamanchili, C. L. P. Chen, A. Ayon, "Optimization of Sensor Locations and Sensitivity Analysis for Engine Health Monitoring Using Minimum Interference Algorithm," EURASIP Journal on Advances in Signal Processing.

T. C. Yang and W. Yang, "Performance Analysis of Direct-Sequence Spread Spectrum Underwater Acoustic Communications with low signal-to-noise ratio input signals," Journal of Acoustical Society of America, pp. 842-855, February 2008.

D. Guo, S. Shamai(Shitz) and S. Verdu, "Mutual Information and minimum Mean Square Error in Gaussian Channels," IEEE Transaction on Information theory, Vol. 51, no. 4, April 2005.

- P. Cotae, "Transmitter Adaptation Algorithm for Multicellular Synchronous CDMA Systems with Multipath," IEEE Journal of Selected Areas in Communications (Special Issue on Next Generation CDMA Technologies), vol. 24, no. 1. Pp. 94-103, Jan. 2006.
- R. Cao, F. Qu, L. Yang, "On the Capacity and System Design of Relay-Aided Underwater Acoustic Communications," IEEE, 2010, 978-1-4244-6398-5/10.
- B. C. Geiger, G. Kubin, "On the Rate of Information Loss in Memoryless Systems," IEE Signal Processing, April 2013.
- F. Zhao, J. Shin, J. Reich, "Information Driven Dynamic Sensor Collaboration for Tracking Applications," IEEE Signal Processing Magazine, Vol. 19, no. 2, pp 61-72, 2002.
- A. G. Bessios and F. M. Caimi, "High-rate Wireless data Communications: An Underwater Acoustic Communications Framework at the Physical Layer," Department of Electrical Engineering, Harbor Branch Oceanographic Institution, Inc., 5600 U.S. 1 North, Fort Pierce, FL 34946.
- W. Alsali, H. Hassanein, and S. Akl, "Placement of multiple mobile data collectors in underwater acoustic sensor networks," IEEE ICC, 2008, pp. 2113-2118.
- T.M. Cover and J. A. Thomas, 'Elements of Information Theory,' 2nd ed., New York: Wiley, 2006.
- J.G. Proakis, Digital Communications, 5th ed., McGraw-Hill, 2008.
- E. Ertin, "Maximum Mutual Information Principle for Dynamic Sensor Query Problems", IPSN 2003, LNCS 2634, pp. 405-416, 2003.
- R. Shrestha, P. Cotae, "On the mutual information of sensor networks in Underwater Wireless Communication: An experimental Approach," ASEE Zone I Conference, University of Bridgeport, Bridgeport, CT, USA. April 3-5, 2014.
- Matlab Signal Processing Toolbox, <http://www.mathworks.com/products/signal/>
- Matlab Communication toolbox, <http://www.mathworks.com/products/communications/>
- Ira S. Moskowitz, Paul Cotae, Myong H. Kang, Pedro N. Safier, "Capacity Approximations for a Deterministic MIMO Channel", Advances in Electrical and Computer Engineering, Vol. 11, no. 1, pp. 3-10. Sept. 2011
- Roland Kamdem, Ira S. Moskowitz, Paul Cotae, "Threshold Based Stochastic Resonance for the Binary-Input Ternary-Output Discrete Memoryless Channels", Proceedings of Seventh IASTED International Conference, Communication, Internet, and Information Technology (CIIT 2012), Baltimore 14-16 May, DOI: 10.2316/P.2012.773-041, pp. 398-404, May 2012.
- Ira S Moskowitz, Paul Cotae, Pedro Safier and Daniel Kang "Capacity Bounds and Stochastic Resonance for Binary Input Binary Output Channels", Proceedings of the IEEE ComCompAp 2012, Hong Kong, China, January 11-13, pp. 61-66, Jan. 2012
- Ira S Moskowitz, Paul Cotae, Pedro Safier "Algebraic Information Theory and Stochastic Resonance for Binary Input Binary Output Channels", Proceedings IEEE 46th Annual Conference on Information Sciences and Systems-CISS 2012, Princeton University, March 21 – 23, pp.1-6, March 2012.
- Roland Yannick Kamdem Kenmogne "Partial Ordering and Stochastic Resonance in Discrete Memoryless Channels", UDC ECE Department, Defended May 1st, 2012.
- Nikola Jovic, Abayomi Dairo, Ashenafi Tesfaye, Aime Valere, Yannick Roland Kamdem, Sasan Haghani and Paul Cotae "Detecting Falls Among Elderly Patients in Nursing Homes by Using Wireless Sensor Networks", Proceedings of the ASEE MidAtlantic Section Fall Conference 2011 (Hosted by College of Engineering, Temple University, Philadelphia), pp. 422 -431, Oct. 2011.
- C.E Shannon and W.W Weaver, "The Mathematical Theory of Communication," University of Illinois press, Urbana, IL, 1949.
- Thomas M. Cover and Joy A. Thomas, "Elements of Information Theory," Second Edition, John Wiley and Sons, 2006.
- Paul Cotae "Blind Doppler Estimation and Compensation in the Underwater Communications" Technical report submitted to the Naval Research Laboratories, Washington DC, Sept 2009.
- François Chapeau-Blondeau, "Noise Enhanced Capacity via Stochastic Resonance in an Asymmetric Binary Channel," Physical Review E, 55(2):2016-2019, 1997.
- François Chapeau-Blondeau, "Periodic and Aperiodic Stochastic Resonance with Output Signal-to-noise Ratio Exceeding that at the Input," International Journal of Bifurcation and Chaos, vol.9, No1:267-272, 1999.
- K. Chatzikokolaskis and K. Martin, "A monotonicity principle for information theory", Electronic Notes in Theoretical computer science 218(2008)111-129.
- Paul Cotae and Ira S. Moskowitz, "On the Partial Ordering of the Discrete Memoryless Channels Arising in Cooperative Sensor Networks," 4th IFIP International Conference on New Technologies, Mobility and Security, NTMS 2011, pp.1-6, Paris, France, February 2011.
- H.J. Helgert, "A Partial Ordering of Discrete Memoryless Channels", IEEE Transactions on Information Theory, vol. IT-3, no. 3, pp.360-365, July 1967.
- Ira S. Moskowitz, Paul Cotae, Pedro N. Safier, and Daniel L. Kang, "Capacity Bounds and Stochastic Resonance for Binary Input Binary Output Channels," Proc. of the IEEE Computing, Communications & Applications conference, ComComAP 2012, Hong Kong, pp.61-66, Jan. 2012.
- François Chapeau-Blondeau, "Stochastic Resonance and the Benefit of Noise in Nonlinear Systems," Noise, Oscillators and Algebraic Randomness – From Noise in Communication Systems to Number Theory. pp. 137-155; M. Planat, ed., Lecture Notes in Physics, Vol. 550, Springer (Berlin) 2000.
- Paul Cotae, Ira S. Moskowitz and Myong H. Kang, "Eigenvalue Characterization of the Capacity of Discrete Memoryless Channels with Invertible Channel Matrices," Proceedings IEEE 44th Annual Conference on Information Sciences and Systems-

CISS 2010, Princeton University, pp.1-6, March 2010.

Ira S. Moskowitz, "Approximations for the Capacity of Binary Input Discrete Memoryless Channels," In Proceedings 44th Annual Conf. on Information Science and Systems, CISS 2010, Princeton, NJ, USA, March 2010.

Ira S. Moskowitz, "An Approximation of the Capacity of a Simple Channel," 43rd Annual Conf. on Information Science and Systems, CISS 2009, Baltimore, MD, USA, June 2009.

Paul Cotae and T.C. Yang "A cyclostationary blind Doppler estimation method for underwater acoustic communications using direct-sequence spread spectrum signals," 8th International conf. on Communications, COMM 2010, Bucharest, July 2010.

Ira S. Moskowitz and Paul Cotae, "Channel Capacity Behavior for Simple Models of Optical Fiber Communication," 8th International conf. on Communications, COMM 2010, Bucharest, pp.1-6, July 2010.

Roland Kamdem, Paul Cotae and Ira S. Moskowitz, "Threshold Based Stochastic Resonance for the Binary-Input Ternary-Output Discrete Memoryless Channel," accepted at 7th IASTED International Conf. on Communication, Internet and Information Technology, CIIT 2012, Baltimore, May 2012.

François Chapeau-Blondeau, "Stochastic Resonance and the Benefit of Noise in Nonlinear Systems," Noise, Oscillators and Algebraic Randomness – From Noise in Communication Systems to Number Theory. pp. 137-155; M. Planat, ed., Lecture Notes in Physics, Vol. 550, Springer (Berlin) 2000.

Sanya Mitaim, Bart Kosko, "Adaptive Stochastic Resonance in Noisy Neurons Based on Mutual Information," IEEE Trans on Neural Networks Vol.15, No.6, Nov 2004.

Mark Damian McDonnell, "Theoretical Aspects of Stochastic Signal Quantization and Suprathreshold Stochastic Resonance," PhD thesis, The University of Adelaide, Australia, Feb.2006.

Bart Kosko, Sanya Mitaim, Ashok Patel and Mark M. Wilde, "Applications of Forbidden Interval Theorem in Stochastic Resonance," In Applications of Nonlinear Dynamics, Understanding Complex Systems, pages 71-89. Springer-Verlag, 2009.

Ira S. Moskowitz, Paul Cotae, Pedro N. Safier, "Algebraic Information Theory and Stochastic Resonance for Binary-Input Binary-Output Channels," Proceedings IEEE 46th Annual Conference on Information Sciences and Systems-CISS 2012, Princeton University, March 17-19, pp.1-6, March 2012.

Paul Cotae, et. all "Design and Application of a Distributed and Scalable Underwater Wireless Sensor Acoustic Networks" 2009 Annual ASEE Global Colloquium on Engineering Education, Budapest, Hungary, Oct. 12-15, 2009.

R. A. Silverman, "On Binary Channels and their Cascades," IRE Trans. Information Theory, Vol.1, no., pp.19-27, Dec 1995.

C. E. Shannon, "A note on a partial ordering for communication channels," Information and control, Vol.1, pp.390-397, 1958.

H. J. Helgert, "A Partial Ordering of Discrete Memoryless Channel," IEEE Transactions on Information Theory, vol.1, no.3, pp.360-365, July 1967.

A.W. Marshall and I. Olkin, Inequalities: Theory of Majorization and its applications. New York: Academic, 1979.

Patrick M. Fitzpatrick "Advanced Calculus," American Mathematical Society, 2009.

Technology Transfer

All computer codes for Matlab simulations and technical reports will be transferred to NRL, Washington DC.

Dr. Ira S. Moskowitz from the Naval Research Laboratory, Center for High Assurance Computer System - code 5540, Washington DC was on the graduate committee for the 6 Master Thesis.

During the Spring of 2011-2015 the PI received a ONR Faculty Fellowship under the ONR ASEE Summer Faculty Research Program. He spent 10 weeks each summer at the Center for High Assurance Computing (Code 5540) collaborating with Drs: Ira S Moskowitz, Myong H. Kang and Pedro Safier. With the freed money for the Summer of 2013, the PI is able to hire one more graduate student working under this grant. The PI published one journal and seven conference papers with the NRL Washington DC researchers. Another two conference papers, also in collaboration with NRL are in progress right now. Recently The PI is doing his sabbatical at NRL under the supervision of Dr. Myong Kang.

Report Type: **Final Report**
Proposal Number: **58962NSREP**
Agreement Number: **W911NF1110144**
Proposal Title: **Information-Driven Blind Doppler Shift Estimation and Compensation Methods for Underwater Wireless Sensor Networks**
ReportPeriod Begin Date: **04/06/2011**
Report Period End Date: **04/14/2015**

1) Foreword

This Final Report is organized in four parts as following. Part I covers the period between August 1st 2014 and April 14, 2015 (the last period of project). Part II covers the results obtained from 1-Aug-2013 to 31-July-2014 and it is based on the Interim progress report 3 submitted for this period. Part III covers the results obtained from 1-Aug-2012 to 31-July-2013 and Part II is also based on the Interim Progress Report 2 submitted in that time frame. Part IV covers the period April 6, 2011 (when this grant was awarded) until July 31, 2012. Part IV is mostly based on the Interim Progress Report 1.

In this project, we used an experimental approach to enhance the performance of the underwater acoustic sensor networks and to decrease the network power consumption. For a Distributed Underwater Wireless Sensor Networks (UWSN), we estimated the number of operating receivers based on the knowledge of the Bit-Error-Rate (BER) and the signal detection performance of the transmitted message. In our experimental observations, we considered two network models: multi hop relay acoustic sensors network and parallel acoustic sensors network.

We have used the information theoretic aspects to analyze and to study the impact of using mobile/moving sensor nodes, as opposed to fixed nodes in UWSN. Also, we developed software platform named "SAM Control" which is a GUI written in MATLAB programming language to facilitate our experiments. The SAM Control unit coordinates and manages the communications between the acoustic modems used in our experiments, while at the same time is allowing data gathering of all experimental observations and the performance analysis of power consumption, BER, mutual information, and information loss.

We investigated the performance of underwater acoustic sensor networks in underwater wireless communication in terms of mutual information, channel capacity, bit error rate, and information loss based on the transmission power, distance, carrier frequency and the bandwidth of the underwater channel. Moreover, we used the information theoretic aspects to analyze and study the impact of using mobile/moving sensor nodes, as opposed to fixed nodes used in UWSN. A placement of multiple acoustic sensors in a multi-hop relay form is needed in numerous applications where data transmission has to be accomplished beyond short distances. This network is effective since the bandwidth of an underwater acoustic communication is severely limited and decays with increase in distances. It is advantageous to accomplish such transmission using sensors in a multi-hop relay network keeping constraints such as transmission rate, transmission delay, Signal-to-Interference and Noise Ratio (SINR) under consideration.

Table of Content

1) Foreword.....	1
2) Table of Content.....	2
3) List of Appendices, Illustrations and Tables.....	3
4) Part I (Period August 1 st 2014 and April 14, 2015).....	5
I.1 Statement of problem studied.....	5
I.2 Summary of the most important results.....	6
I.3 Accomplishments.....	10
5) Part II (Period August 1 st 2013 and July 31 st , 2014).....	11
II.1 Foreword.....	11
II.2 Statement of problem studied.....	12
II.3 Summary of the most important results.....	13
II.4 Accomplishments.....	16
6) Part III (Period August 1 st 2012-July 31 st 2013).....	16
III.1 Foreword.....	16
III.2 Statement of problem studied.....	17
III.3 Summary of the most important results.....	18
III.4 Accomplishments.....	26
7) Part IV (Period April 6 2011 and July 31 st 2012).....	27
IV.1 Foreword.....	27
IV.2 Statement of problem studied.....	27
IV.3 Summary of the most important results.....	28
IV.4 Accomplishments.....	31
8) Bibliography.....	32

3) List of Appendices, Illustrations and Tables

List of Figures

- Figure 1: The global picture of the overall project
- Figure 2: SAM Control GUI
- Figure 3: Cascaded underwater wireless sensor network
- Figure 4: Parallel underwater wireless sensor network
- Figure 5: Underwater Mobile Acoustic Sensor Network
- Figure 6: Experimental approach setup
- Figure 7. PSD of Noise ($N_o(f)$) experimentally measured in underwater
- Figure 8 Illustration of Multihop network
- Figure 9. Delay between Relays
- Figure 10. Acoustic Sensors by Vendor and Experimental set up in Underwater Communications
- Figure 11. PSD of Noise ($N_o(f)$) experimentally measured in underwater
- Figure 12. Matlab simulation Set Up for multi-hop network sensor model
- Figure 13. Transmitted and Received Modulated m-Sequence Signals (17 kHz)
- Figure 14. Experimental set up and its components
- Figure 15. Autocorrelation of Noise Measured in Swimming Pool
- Figure 16. PSD of Measured Noise in Swimming Pool
- Figure 17. PSD Estimation by Parametric Methods
- Figure 18. PSD Estimation by Blind Methods
- Figure 19. Comparisons of Parametric and Blind Spectral Estimation Methods
- Figure 20. Linear Frequency Modulation Cosine, and its PSD
- Figure 21. Periodic Autocorrelation of PN-Sequences
- Figure 22. Initial Transmitted (a) and Received (b) m-sequence signal
- Figure 23. Frequency Modulated Transmitted Signal
- Figure 24. Frequency Modulated m-Sequence Received Signals (17 kHz)
- Figure 25. Autocorrelation of Transmitted and Received 52-m –Sequences
- Figure 26. Partial Autocorrelation of Received Signals Showing 48 to 52 m-Sequences
- Figure 27. Power Spectral Density of Transmitted and Received Signal [Water Tank]
- Figure 28. Partial PSD of a Received Signal [Results for Water Tank]
- Figure 29. PSD of Received Signal [Results for Swimming pool]
- Figure 30. Transmitted and Received Signal for LFM m- Sequences [Pool]
- Figure 31. Autocorrelation, PSD and Partial Autocorrelation of LFM 52- m- Sequences
- Figure 32. Estimation of Instantaneous and Average Doppler Shift Using Oerder and Meyr Algorithm
- Figure 33. 4 level tree structured network with 2 children nodes
- Figure 34. Optimal distance (on the top) for ideal and imperfect channels including BER and interference for a tree shaped topology with 7 levels.
- Figure 35. The distances for different imperfect channel scenarios and their improved situations after applying CC
- Figure 36. The ratio of the sensor power of the imperfect channel compared to the sensor power of the ideal channel
- Figure 37. Optimal frequency at each distance associated with a specific level for an ideal channel in a 7 level tree structured network
- Figure 38. Optimal frequency at each distance associated with a specific level for an imperfect channel (BER = 0.001) in a 7-level tree structured UWSN

Figure 39. Optimal frequency at each distance associated with a specific level for an ideal channel in a 7-level tree structured network

Figure 40. Frequency dependent portion of narrow-band SNR.

Figure 41. Optimal placement of the sensor nodes when the transmitting power is constant

Figure 42. The optimal power allocations for the scenario 1 are shown near each sensor node (in Watts)

Figure 43. The optimal power allocations for the scenario 2 are shown near each sensor node (in Watts)

Figure 44. The optimal sensors' locations and power allocations (in Watts).

Figure 45. BSC/SE capacity

Figure 46. Capacity of BAC/SE

Figure 47. Capacity of BSC/SE for threshold values

Figure 48. (2,3) DMC and Pinsker capacity Bound

Figure 49. (2,3) DMC and Helgert capacity Bound

Figure 50. Capacity(C), Pinsker (L) and Helgert (U) bounds for different values of threshold

Figure 51. Optimal noise power and threshold for stochastic resonance, with a scalable factor

List of Tables

Table 1: Bit loss test for different distance of sensors

Table 2: Result analysis for Tx1 and Rx1 (d=5 m)

Table 3: Result analysis for Tx2 and Rx2 (d=5 m)

Table 4: Result analysis for Tx3 and Rx3 (d=5 m)

Table 5: Result analysis for Tx1 and Rx4 (d=15 m)

Table 6: Result analysis for cascaded sensors network

Table 7: Result analysis for Tx1 and Rx1

Table 8: Bit loss test for mobile sensor nodes of maximum distances $d = 15\text{m}$.

Table 9: Bit loss test for mobile sensor nodes moving in vertical direction.

Table 10: Performance results of using mobile sensor nodes

Table 11: Numerical results for scenario #1

Table 12: Numerical results for scenario #2

Table 13: Result analysis of using fixed sensor nodes

Table 14: Summary results for using mobile sensor nodes

Table 15: Numerical results for scenario #1 (no target is moving):

Table 16: Approach results in noisy UAC (Scenario#2)

Table 17: Modem Specifics and Operating Function

Table 18: Bit loss test for different distance of sensors

Table 19: Result analysis for First Hop Tx₁ and Rx₁ (d=5 m)

Table 20: Result analysis for Second Hop Tx₂ and Rx₂ (d=5 m)

Table 21: Result analysis for third Hop Tx₃ and Rx₃ (d=5 m)

Table 22: Result analysis for Tx₁ and Rx₄ (d=15 m)

Table 23: Result analysis for Multihop relay link and direct link

Table 24: Optimized placements and other related parameters when the transmitting power of each node is constant and equal to 1 watt

Table 25: Optimized energy allocation and other related parameters when the sensor nodes are

fixed in their locations, first scenario

Table 26. Optimized energy allocation and other related parameters when the sensor nodes are fixed in their locations, second scenario

Table 27. Optimized placements, optimized power other related parameters

Table 28. Summary of (2,3) DMC

4) Part I (August 1st 2014 and April 14, 2015)

I.1 Statement of problem studied

The potential contributions of this project consist of improving the understanding of the information theory aspects of a distributed underwater sensor network in the context of noncoherent communication techniques. The research goals of this proposal are in line with Army vision and mission, and they are integrated in the exiting research interests of Office of Naval Research (ONR) at the Naval Research Laboratories in Washington DC (Acoustic Division, Code 7120 and the Center for High Assurance Computing, Code 5540).

The novelty of our approach is to investigate the performance of acoustic sensor networks in underwater wireless communication in terms of mutual information, channel capacity, bit error rate, and information loss based on the transmission power, distance, carrier frequency and the bandwidth of the channel. UWSN are typically characterized by severely energy limited nodes. The reason is the nodes have small batteries and therefore cannot afford much energy to complete tasks. As the life time of any individual sensor in the UWSN is limited, the number sensor nodes that stop working due to power loss increases with a lengthened deployment time, therefore the coverage area of UWSN will be reduced. In our approach, we estimated the number of operating receivers within the network based on the knowledge of the Bit-Error-Rate (BER) and the signal detection of the transmitted message, and, therefore, take advantage of the BER variation, which depends on the underwater acoustic channel environment.

In the sensor system architecture presented in Figure 1, the underwater sensor nodes with acoustic modems are distributed in the underwater space. Each underwater sensor node can measure a specific bit rate of the data around it. The sensors are positioned in clusters and they communicate with the Command and Control center via the Monitoring Center (MC). The MC will eventually communicate with Command and Control unit on the shipboard through high capacity wavelength optical fiber links. Different goals in this project can be summarized as [34]:

- 1) To analyze and improve the non-data aided methods for Doppler shift estimation and compensation (squaring time phase recovery method, power spectrum method, and partial autocorrelation method);
- 2) To determine the necessary quantity and deployment strategy of a sensors in a given region and to provide a required security level;
- 3) To minimize the probability of false alarm and the bit error rate;
- 4) To improve decision-making on target detection with sensor collaboration in the context of blind Doppler shift estimation and detection, and
- 5) To improve the ability of a distributed sensor system to detect intruders (targets) and determine how the network wireless sensor design is affected.

Figure 1: The global picture of the overall project

I.2 Summary of the most important results

Our contribution for this period is related to the performance of the UWSN and it consists in how to practically apply our knowledge and education background to enhance the capabilities of UWSN. In order to understand these contributions the reader should be familiarized with the results obtained in the Interim Reports 1-3 because they are not repeated here.

To improve the ability of a distributed sensor system, we concentrated on improving mutual information between two data signals in terms of minimum bit error rate, maximum data rate communication, and channel performance. We focus on the sensor placement in multi-hop to minimize the bandwidth consumption and mitigate the risk of acoustic link failure and information loss. In order to reduce the communication load for each sensor we develop new distributed algorithms for underwater communication similar to those developed in wireless communication in [2]. The advantage of this sensor placement will help in fulfilling the increasing demand for reliable maximum data rate wireless communication links to accommodate the wide range of underwater application.

We developed a Software development (SAM Control) which is a GUI interface program that was designed for these experiments. The program is written in MATLAB, which reads and writes data to the serial buffer of the modem. SAM Control greatly streamlines the data collection and data analysis process by automating commonly used functions of the modem. Its main features are:

- COM settings: Configure the COM port settings that are connected to the modem.
- Modem Settings: These sets of control are used to configure the sensor communication parameters, such as receiver threshold, transmission speed (data rate) and receive speed.
- TX Mode: mainly responsible of generating the transmitting data which are the m-sequences of 1023 length so to be send through the sensor.
- RX Mode: managing all operations need to be done by the receiver, including reading the received data and storing it in a desired file type, so it can be ready for performing our analysis and evaluation on the data.

Figure 2: SAM Control GUI

During our experiments, we configured the sensors for serial communication, generated PN-sequence of the code length of 1024 by choosing the 10th order polynomial. We chose 10th order polynomial so that we could generate the sequences with period length of 1023bits. In our practical experiments we transmitted baseband m-sequences of length 1023. Initially, we were not able to receive 1023 bits because of 32 bytes buffer memory of the sensors used. The buffer memory size was only 32 bytes and each bit sent via serial port was coded as 8 bits. As a result, we were only able to send maximum of 30 bits plus 2 bytes handshaking at a time from the m-sequences of length 1023. Therefore, practically the length of the sequence could be considered 30 for one transmission.

In cascaded sensor network given in Figure 3, we transmitted data from sensor 1 (upper left) and we received the output data in sensor 2 (upper right). Then we transmitted the received data from sensor 2 exactly as it was received to sensor 3(lower left). The same process was repeated to send data from sensor 3 to sensor 4. The output at sensor 4 was compared with input data at sensor 3 and then we calculated mutual information. Besides, bit error rate, probability error, and information loss is calculated at each communication channel. The obtained results are given in the following in many tables presented below.

Figure 3: Cascaded underwater wireless sensor network

For a collaborative network, we obtained the experimental result for cascaded wireless sensor network in an underwater acoustic communication for four sensors. The bit loss and bit error were computed in an underwater channel sending 1023 bits of 1's and 0's alternately for couple of times for different location of sensors.

Table 1: Bit loss test for different distance of sensors

For the data obtained in Table 1, we transmitted 1023 bits of binary sequences data to the receiver sensor node at a distance of 5 m. This channel transmitted all 1023 bits; however it has bit error of 8 bits in average.

Table 2: Result analysis for Tx1 and Rx1 (d=5 m)

In Table 2, the transmitted data were exactly the received data from first sensor node; however we filtered the error bits that were incurred in first channel. This channel was also set for distance of 5 m between transmitter and receiver. We were able to handle a communication of data between sensor nodes with bit error of 7-8 bits in average.

Table 3: Result analysis for Tx2 and Rx2 (d=5 m)

In Table 3, we load the received data from sensor node 3 and transmitted exactly to another sensor node in cascaded network. This receiver was at a distance of 5 m. The channel had full communication of data with bit error of approximately 7-8 bits.

Table 4: Result analysis for Tx3 and Rx3 (d=5 m)

Table 4 shows our improvement regarding drop in bit loss and bit error compare to direct transmission between two sensor nodes and cascaded network. The channel distance was approx. 15 m. The output result shows that the channel has bit error along with bit loss. This proves that transmission loss in underwater acoustic communication depends on distance.

Table 5: Result analysis for Tx1 and Rx4 (d=15 m)

Table 5 shows that underwater acoustic communication (UAC) capacity is strongly dependent on transmission distance. Using more than one sensor in cascaded network system will increase in the mutual information and rate of data transmission with minimum bit error probability. A summary of all results are given in Table 6.

Table 6: Result analysis for cascaded sensors network

A similar experiment was performed in parallel sensor network system. In this system, we have one transmitter and 3 receivers, acting system as Single Input Multiple Output (SIMO) system. The optimum output was recorded each time and the experiment was carried out several times for m sequences of length 1023 bits. The result obtained for probability of error, BER, mutual information, entropy estimation is displayed in numerical results in Tables.

Figure 4: Parallel underwater wireless sensor network

Similarly, an experimental result for parallel sensor network model shows the following outcomes shown in Table 7. This channel network is more effective than cascaded sensors network channel; however cascaded network can transmit data to larger distance for available sensor nodes. In parallel sensor network channel, bit error rate is significantly low compared to cascaded sensor networks. This tells us that data transmission in parallel sensor network has low probability error. The bit loss and bit error in data transmission between transmitter sensor and any received sensor might be fixed during data transmission with second or third sensor node.

Table 7: Result analysis for Tx1 and Rx1

The maximum distances between two communicating sensors were 15 meters. The sensors were positioned such that they could float in water and move freely. We are optimizing the sensors locations and sensitivity analysis to increase the mutual information and channel capacity [6-8]. In the experimental model, we studied the impact of using moving acoustic sensor node in a point to point communication system to accomplish same work done in the cascaded network model above.

Figure 5: Underwater Mobile Acoustic Sensor Network

The receiver has been moving while receiving the transmitted data in both vertical and horizontal directions, the maximum distances reached between the two sensor nodes is 15m, as we were limited it by the size of the indoor pool, where the experiments took place. We have done the transmission of the data several times over different distances with different velocities. All the experimental observations and result we obtained for probability of error (BER) mutual information, entropy estimation is displayed in numerical results in section below. In Table 8, the bit loss and bit error were computed in an underwater channel sending 1023 bits of 1's and 0's alternately for a couple of times for different velocities of the moving sensor over 15m maximum distance apart between the sensors. In Table 9, the bit loss and bit error were computed in an underwater channel sending 1023 bits of 1's and 0's alternately for a couple of times for different velocities of the moving sensor over 15m maximum distance apart between the sensors.

Table 8: Bit loss test for mobile sensor nodes of maximum distances $d = 15\text{m}$.

Table 9: Bit loss test for mobile sensor nodes moving in vertical direction.

In the table below, we show the information theoretic aspects, we use to evaluate the performance of our point to point communication system model using mobile sensors nodes moving with velocities $v_1 = 1 \text{ knot}$, $v_2 = 2 \text{ knots}$ and $v_3 = 3 \text{ knots}$.

Table 10: Performance results of using mobile sensor nodes

X and Y are the transmitter and receiver nodes respectively in our communication system. As shown in Table 4, we achieve maximum mutual information ($I(X, Y) = 1$), since we have received same sequence length of the transmitted data, However, there is a small probability of error in reconstructing the transmitted bits. In conclusion, after estimating a simulation study of the UAC model, we used the information theory aspects tools to compare the performance of our UWSN model using mobile sensor nodes to the UWSN model that the author proposed [3]. We observed remarkable results in terms of the performance based on probability of error, mutual information and loss of information. The result of this work indicates that the use of few mobile sensors in UWSN can accomplish the same work as a larger group of static networks and achieve comparable results with low probability of error ≈ 0.001 . The experimental approach is presented in Fig.6.

Figure 6: Experimental approach setup

In the distributed sensor network model shown in Figure 4, we have one transmitter and 3 receivers optimally distributed, acting system as a Single Input Multiple Output (SIMO) system. We have started by transmitting the data while only one operating receiver (sensor) and the rest of the sensors were not functioning. The optimum output was recorded each time for m-sequences of length 1023 bits. Our developed software is continuously analyzing the received data and based on the results calculations of the loss of information, BER and mutual information, it sends a signal to operate other sensors. While collecting the data from multiple sensors/receivers, the software process compares and combines the data to achieve the desired BER value and signal detection quality with the least number of operated receivers. The user can set a threshold for the BER and the MI, so it compares it to the results and maintain that desired threshold. Several Experiments have been done in the University of the District of Columbia's indoor pool over different environments (existence and nonexistence of moving targets) to verify our approach and results.

In Table 11, the bit loss and bit error were computed for this scenario (we call this scenario #1) where no moving target or in clear underwater channel sending 1023 bits of 1's and 0's alternately for a couple of times with no effect of noise by moving target or high disturbance waves. The maximum distances were 15m between the sensors. We set the threshold BER = 0.003. It means that the least number of sensors will be used to maintain signal quality or the BER for the transmitted sequences no more than 0.003 (3bits error out of every 1000 transmitted bits)

and since The BER less than desired value, only one sensor is functioning and collecting data while the rest of the deployed sensors are not functioning and result in reducing power consumption by the network.

Table 11: Numerical results for scenario #1

Now, we consider the case when the target is moving. In the table below, we show the analysis and results for scenario #2 where there is a target moving and making noise. During the transmission we used a moving boat to have a similar effect of moving object as well as increase the noise level in the underwater channel while the BER threshold was set to 0.003.

Table 12: Numerical results for scenario #2

As shown in Table 12, the BER of the transmitted data decreasing regularly. Since, the BER for the first sequence transmitted data is less than the threshold, the software sends signal to turn on the next adjacent sensor to start recording data and as a result we can see the BER decreased to 0.005. But, since the BER still less than the desired value (0.003), it turns another sensor to collect the data from the three sensors and by combining and selecting the data with lowest probability of error, so that it achieves a better signal detection and BER.

As mentioned before, based on Interim report 1-3, we used the hydrophone to practically find the PSD of the noise in UAC and its relation with the transmitted frequency. The transmitted signal has a carrier frequency of 17 kHz and the sampling rate of 8000. From the Figure 7, we can see that the power of noise is high for frequency range of 0 to 5 kHz. As the frequency increases we can observe that the power of noise is less than 38dB. So if we are able to transmit the signal in the frequency range where the noise power is relatively less, we can obtain better performance. Therefore, we choose 17 kHz of carrier frequency for our experiments.

Figure:7. PSD of Noise ($N_o(f)$) experimentally measured in underwater

Table 13: Result analysis of using fixed sensor nodes

In conclusion, we used the information theory aspects tools to compare the performance of our UWSN model using mobile sensor, as opposed to fixed sensor nodes in UWSN. We observed remarkable results in terms of the performance based on the probability of error, mutual information and loss of information. Our result indicates that the use of few mobile sensors in UWSN can accomplish the same work as a larger group of static networks and achieve comparable results with low probability of error ≈ 0.001 .

Table 14: Summary results for using mobile sensor nodes

Also, another significant contribution is we show the results of applying our experimental approach to UWSN can reduce the BER of the communications system while at the same time maintaining low power consumption depending on the underwater environment.

Table 15 Numerical results for scenario #1 (no target is moving):

Table 16: Approach results in noisy UAC (Scenario#2)

In Table 15 & 16, we can notice the relation between BER and number of operated sensors. The more sensors operate, the less BER goes where result in better signal detection. Also, the number operating sensors vary depends on the underwater channel environment. If there is low level of noise, fewer sensors will be working and then noticeable reduction in the power consumption will be observed.

I.3 Accomplishments for this period included in Part I:

Paper published: 4 conferences (1 IEEE, 3 ASEE)

Paper under in progress: 2 (1 under review, 1 going to be submitted this fall)

5 MSEE students presentations at the University of the District of Columbia, Research meetings, and ASEE UDC Conference in the fall of 2014.

2 Undergraduate students supported for conference travel to Philadelphia, Fall 2014 and San Antonio Spring 2015.

3 Graduate students supported: 2 Master Thesis successfully defended in Fall 2014 and Spring 2015. One graduate student defended his master project in Spring 2015.

5) Part II (August 1st 2013 and July 31st , 2014)

II.1 Foreword

The results obtained between August 1st 2013 and July 31st 2014 are along with the objectives of this grant. We investigated the performance of wireless sensors in cascaded multi-hop relay network in Underwater Acoustic Communication (UAC). We focused on the optimizing the mutual information between transmitted data and received data for a specific network model in underwater channel. Specifically, we use multiple sensor nodes in a relay network to transfer the data signal into long distance for maximum mutual information. In addition, we studied the relationship of channel capacity to transmission power, bandwidth and carrier frequency. In comparison with the free space wireless communication, the underwater acoustic communication suffers from the limits of the less available bandwidth and complex noise caused by the underwater channel. Therefore, we derived an algorithm for the placement of sensor nodes at an optimal distance in a multi-hop relay network. We use information theoretic analysis tools to demonstrate the effect of delay, carrier frequency, noise, and link distance on the maximizing the mutual information. In the second part of our research, we worked on experimental data received

from a pair of SAM-1 acoustic sensors provided by Desert Star Systems. We used information theoretic tools of entropy, conditional entropy, probability mass function etc. of input and output data signal to analyze the mutual information, information loss, bit error rate, and channel capacity. The significant research of this thesis is observing the multi-hop relay network model and to analyze the optimal distance, frequency, and capacity for available bandwidth in Underwater Wireless Sensor Network (UWSN). Various algorithms are discussed emphasizing on non-coherent approaches.

II.2 Statement of problem studied

The potential contributions of this project for this period consist of improving the understanding of the information theory aspects of a distributed underwater sensor network in the context of noncoherent communication techniques. The research goals of this proposal are in line with Army vision and mission, and they are integrated in the exiting research interests of Office of Naval Research (ONR) at the Naval Research Laboratories in Washington DC (Acoustic Division, Code 7120 and the Center for High Assurance Computing, Code 5540).

The novelty of our approach is to investigate the performance of acoustic sensor networks in underwater wireless communication in terms of mutual information, channel capacity, bit error rate, and information loss based on the transmission power, distance, carrier frequency and the bandwidth of the channel. A placement of multiple acoustic sensors in a multi-hop relay form is needed in numerous applications where data transmission has to be accomplished beyond short distances. This network is effective since the bandwidth of an underwater acoustic communication is severely limited and decays with increase in distances. It is advantageous to accomplish such transmission using sensors in a multi-hop relay form keeping constraints such as transmission rate, transmission delay, Signal-to-Interference and Noise Ratio (SINR) under consideration. In particular, we consider a communication scenario where a certain number of bits have to be transmitted over a distance d .

Our result analyzes the optimal number of sensor nodes, N to use over a link distance d to increase the mutual information between transmitted data and received data in terms of link capacity, delay, information loss, and bit error rate. So far, different goals of our projects can be summarized as [11]:

- a) To analyze and improve the non-data aided methods for Doppler shift estimation and compensation (squaring time phase recovery method, power spectrum method, and partial autocorrelation method);
- b) To determine the necessary quantity and deployment strategy of sensors in a given region, and to provide a required security level;
- c) To minimize the probability of false alarm and the bit error rate;
- d) To improve decision-making on target detection with sensor collaboration in the context of blind Doppler shift estimation and detection, and
- e) To improve the ability of a distributed sensor system to detect intruders (targets) and determine how the network wireless sensor design is affected.

There are some scientific barriers related to problem studied: 1) Lack of experimental results on improving mutual information between two data signals in terms of minimum bit error rate, maximum data rate communication, and channel performance. 2) What is the optimum sensor

placement in multi-hop in order to minimize the bandwidth consumption and to mitigate the risk of acoustic link failure and information loss. For reducing the communication load for each sensor we developed new distributed algorithms for underwater communication similar to those developed in wireless communication in [14].

The advantage of this sensor placement will help in fulfilling the increasing demand for reliable maximum data rate wireless communication links to accommodate the wide range of underwater application. We also focused on algorithms that reduce the significant challenges to the development of underwater wireless systems such as complex channel noise, bandwidth limitations, and frequency and distance dependent signal attenuation [5]. Scientific progress and accomplishments including significant theoretical and experimental advances are given in the next section.

II.3 Summary of the most important results

We modeled our sensors as a multi-hop relay network to maximize mutual information for point to point Gaussian channels between transmitter and receiver in the underwater environment. Our contribution is on UWSN design for long range acoustic communication placing an optimum number of sensor nodes at an optimum distance for certain average transmission power. By maximizing the mutual information with an upper bounded average power yields the same channel capacity [6]. We focused on non-coherent channels for maximizing the mutual information between transmitter and receiver. We study the transmission distance, data rate, and channel noise to get the maximum of the digital information embedded in the received signal to maximize the mutual information. We applied a multi-hop relay sensor node by dividing the total link into multiple hops, where a relay acoustic node is employed at each hop as in Fig.8

Figure 8 Illustration of Multihop network.

The relay node receives the signal, regenerates it, and passes it on to the next hop, until the final destination is reached. The question of interest to our design is how exactly does this approach gives improvement in terms of maximizing the mutual information, total power consumed, energy per bit, overall cost and delay. We use an information theoretic tool to accomplish the assumption that the capacity of relay channel is equal to the capacity of each of its hops, and are shown to increase with the number of relays. Here, we show that relaying also helps to reduce the total transmission power and its benefits are even more pronounced in view of energy per bit savings. We consider system optimization in the light of minimizing both bit error rate and the information loss as in Fig.9

Figure 9. Delay between Relays

We focused on an experimental approach for placement of sensors in underwater for minimum BER and maximum mutual information. Our experimental model consisted of an indoor swimming pool, two pairs of SAM-1 acoustic transducers provided by Desert Star Systems, two portable computers both equipped with MATLAB software, signal processing toolbox, communication toolbox, a hydrophone to measure sound underwater, and an acoustic speaker to

generate noise as in Fig.10. The data is transferred using transducers and is processed in Matlab. In our experiment, the transmitted signal has a carrier frequency of 17 kHz and the sampling rate of 8000 as in Figs. 10 , 11 and 12.

Figure 10. Acoustic Sensors by Vendor and Experimental set up in Underwater Communications

Figure 11. PSD of Noise ($N_o(f)$) experimentally measured in underwater

Figure 12 shows that power of noise is high for frequency range of 0 to 5 kHz. As the frequency increases we observe that the power of noise decreases up to -12 dB. Therefore, we choose to transmit the signal in the frequency range where the noise power is relatively less, and gives better performance in terms of BER and mutual information bound.

Figure 12. Matlab simulation Set Up for multi-hop network sensor model

Figure 13 gives the insight of how the multi-hop relay network is setup. In Matlab simulation, we connect an output from first hop to second hop as an input and transmit data with some delay and noise. Before transmitting a data to second hop, BER and mutual information is calculated and data are regenerated such that noise and error does not get accumulated throughout the transmission.

Figure 13. Transmitted and Received Modulated m-Sequence Signals (17 KHz)

Table 17. Modem Specifics and Operating Function

We perform a serial data communication via serial port using RS-232 levels. The data are transmitted at 4800 baud and 8 data bits. To perform serial communication from Matlab software, we first define the serial port object and then configure device parameters for communication. Values sent, received, transfer status and bytes available are recorded in Matlab for tracking purpose. We increase the buffer size of Matlab software to 1023 bytes (by default it is 512 byte).The received data is then loaded to workspace as in Fig.5. We do the similar experiment using Simulink and record the data to the workspace. Since there are only four stationary nodes in our network, we use a static routing table that lists the routing paths for all possible source-destination pairs. For example, we place the four nodes on a straight line, and label them as A, B, C and D respectively. If node A generates a message with the source field as A and the destination field as D, then the next-hop is node B and then node C in the routing table for the (A, D) source-destination pair.

Table 18. Bit loss test for different distance of sensors

In Table 19, we transmit 1023 bits of binary sequences data to the receiver sensor node at a distance of 5 m. This channel transmits all 1023 bits; however it has bit error of 8 bits in average.

Table 19. Result analysis for First Hop Tx₁ and Rx₁ (d=5 m)

In Table 20, the transmitting data are exactly the received data from first sensor node; however we filter the error bits that are incurred in first channel. This channel is also set for distance of 5 m between transmitter and receiver. We get a full communication of data between sensor nodes with bit error of 7-8 bits in average.

Table 20. Result analysis for Second Hop T_{x2} and R_{x2} ($d=5$ m)

In Table 21, we load the received data from sensor node 3 and transmit exactly to another sensor node in a relay network. This receiver is again at a distance of 5 m. The channel has full communication of data with bit error of approximately 7-8 bits.

Table 21. Result analysis for third Hop T_{x3} and R_{x3} ($d=5$ m)

Table 22 shows our improvement regarding minimization in bit loss and bit error compare to direct transmission between two sensor nodes and a relay network. The channel distance is approximately 15 m. The output result shows that the channel has bit error along with bit loss. This proves that transmission loss in underwater acoustic communication depends on distance.

Table 22. Result analysis for T_{x1} and R_{x4} ($d=15$ m)

Table 23 shows that underwater acoustic communication (UAC) capacity is strongly dependent on transmission distance. Using more than one sensor as multi-hop network system model, increases the mutual information and rate of data transmission with minimum bit error probability.

Table 23. Result analysis for Multihop relay link and direct link

The problem of an optimum placement of sensors in a multi-hop relay structure for long range acoustic communication in underwater channel have been investigated to maximize the mutual information and channel capacity. The optimum communication frequencies for given link distance and bandwidth available have been calculated where noise power is low. The deployment of sensors in multi-hop relay structure for large transmission range has been considered to minimize bit error rate and information loss as well.

Additionally, an analytical and experimental result of multi-hop sensor network model in a relay has been investigated to optimize the mutual information and maximize rate of data communication. It was advantageous to accomplish such transmission using relays since the available acoustic bandwidth decayed with increase in distance. Moreover, numerous applications required a relay acoustic link where data transmission had to be accomplished beyond short distances. The multi-hop relay structured that we have used would be suitable fit to address the issues of power and energy consumption, and link delay along with maximizing mutual information.

The improvement in mutual information and data rate transmission has been investigated using information theoretic tools such as entropy, conditional entropy, and information loss between transmitted and received data signals. Based on our experiment and simulation result, we

concluded that the mutual information between transmitted and received data signal can be maximized by placing extra sensor nodes in between a transmission range which also decreased BER and information loss. The problem occurred in our analytical result was an additional delay due to relay link. However, we observed that delay depended on the rate at which the information is transmitted as well. This fact implied an interesting property of an acoustic link: although each relay introduces an additional delay, as the hops become shorter transmission can be accomplished faster over each hop. This improvement is specific to the underwater acoustic environment, where bounds of mutual information and bandwidth are dependent on the transmission distance.

During our experiment we had several issues with data compatibility with the software. It took several hours to run the Matlab programs. Memory buffer size of sensors was another issue, which only transmit real data signal through serial communication. We also observed that Matlab serial communication does not support complex signals. We had problems with the sensors since they transmitted some random signals by themselves due to unknown internal error.

We can expand our work for movable sensor nodes in underwater channel to address the issues with Doppler spread. Along with a relay network, we can address a multi-path channel model and use the wireless communications knowledge of MRC (Maximal Ratio Combination) to increase the detection quality of received signal.

II.4 Accomplishments for this period included in Part II

Paper published: 6 conferences (4 IEEE, 1 IEEE invited paper, 1 ASEE)

Paper under in progress: 4 (1 under review, 3going to be submitted this fall)

Invited talks: 1 (University “Polytechnica”, May 2014).

5 MSEE students presentations at the University of the District of Columbia, Research meetings, and ASEE UDC Conference in the fall of 2013.

3 presentations at Engineering week at UDC, Graduate and undergraduate research day at UDC

4 Undergraduate students supported: 2 Undergraduate students supported for conference travel to Philadelphia, Fall 2013.

5 Graduate students supported: 2 Master Thesis successfully defended Spring 2014. Another 2 students will defend in the AY2014-2015.

6) Part III (Period August 1st 2012-July 31st 2013)

III.1 Foreword

The results obtained between August 1st 2012 and July 31st 2013 are along with the objectives of this grant. We investigated different methods for blind Doppler shift estimation and

compensation in underwater acoustic wireless sensor networks. Our study is based on the data collected from our experiments. We conducted experiments for underwater acoustic wireless communication using a pair of SAM-1 sensors provided by Desert Star Systems. MATLAB software was used to send data via the serial port for transmission and acquire data from a sensor into a PC. We analyzed the data collected from the experiment using non-data aided techniques such as Power Spectrum analysis, Autocorrelation, and Squaring Time Phase Recovery (Oerder & Meyr) to estimate Doppler shift in collaborative distributed underwater sensor networks.

We also extensively investigate optimal sensor placement in a tree structured multi-hop hierarchical network. We focused on optimization of the consuming energy by each sensor node for this specific network. We assume that our network contains a number of sensor nodes, distributed at different water depth levels, and that the nodes communicate with each other for purposes of monitoring and tracking. Specifically, we focused on a symmetric tree like multi-hop hierarchical routing topology, which can potentially cover larger areas as we go deeper in the water than flat placement of underwater sensor networks. We derived an optimization algorithm for the locations of sensor nodes in the mentioned network. This algorithm applies to both symmetric as well as asymmetric tree shaped hierarchical networks and it provides the optimum distances between children nodes and their parent nodes.

III.2 Statement of problem studied

The novelty of our approach is to estimate Doppler shift by blind methods. We explored different types of parametric and blind spectral estimation techniques and compared them. We generated different types of random processes corrupted by noise of 25dB signal to noise ratio (SNR). We analyzed the PSD for different types of random processes. We observed that the Periodogram spectral estimation technique is better to locate the dominant frequency than other blind spectral estimation methods. It gives sharp and a highest spectral peak at frequencies with high power and distinguishes nearby frequencies clearly. In addition, we observed that the Welch's method is smoother and covers a large window. Therefore we choose both the Periodogram and the Welch's methods for blind Doppler shift estimation performance bounds for channels communication which are more accurate and less computationally expensive.

We examined different modulation techniques that would increase the bandwidth of a waveform while maintaining pulse duration. We focused on the linear frequency modulation (LFM), and spread spectrum techniques. Specifically, we modulated the transmitted signal using LFM and maximal length sequence, also called m-sequence. We used 2 kHz of sweeping frequency for LFM and m-sequence of length 1023 bits. We observed that these two modulations, when used together, give better signal resolution and are more robust to noise and Doppler spread.

We developed an algorithm for optimum placement of the underwater sensors which can be used for different possible communications channels. We considered the ideal channel scenario, the imperfect channel scenario without having interference between sensor nodes and the imperfect channel scenario considering the interference only between children sensor nodes and their parent nodes. We found the exact optimal locations of sensor nodes using the Karush–Kuhn–Tucker (KKT) conditions by considering the interference between the sensor nodes. Using the same approach, we find the optimized consuming energy for each sensor node having fixed

locations. It is worth mentioning that the energy consumption and the efficient usage of energy are of notable importance to Underwater Wireless Sensor Networks (UWSNs).

There are some scientific barriers related to problem studied: 1) Lack of the information theoretical bounds for the binary underwater communication channels in the presence of the Additive White Gaussian Noise (AWGN). How the information about the target is processed in a faster way with a limited computational resources. 2) How the non-coherent communication methods can be used for extracting more information from a cooperative underwater sensor network for tracking the target. 3) The protocols used in actual acoustic networks (usually inspired from terrestrial wireless ad hoc networks) cannot be employed to handle self-organized sensors with slow data rates and high random dispersion rates.

Scientific progress and accomplishments including significant theoretical and experimental advances are given in the next section.

III.3 Summary of the most important results

Our experimental model consisted of an indoor water tank, and an indoor swimming pool, a pair of SAM-1 acoustic transducers provided by Desert Star Systems, two portable computers both equipped with MATLAB software, signal processing toolbox, a communication toolbox, a hydrophone to measure sound underwater, and an acoustic speaker to generate noise. The data was transferred using a pair of acoustic modems and was processed in MATLAB. Figure 1 illustrates our prototype environment where the sensors are connected to the computer via a serial port and are floating in the water.

Figure 14 Experimental set up and its components

To carry out the experiment on daily basis, we used a plastic water tank by assuming the acoustic environment to be anechoic: an environment without reverberation of signals. However, the acoustic environment had surrounding noise and human made noise. The distance between the sensors were kept 7ft apart all the time (diagonal) so that we would have the longest time lag. After our experiments in the water tank, we performed our experiment in the swimming pool. The distance between two communicating sensors were 15 yards and the depth of the swimming pool was 11ft and 8 inches. The surface temperature of the swimming pool was seventy degrees Fahrenheit and the water was chlorinated.

The sensors were positioned such that they could float in water and move freely. We have used a pair of acoustic modems provided by Desert Star Systems to perform practical experiments. The modems can operate in the range of 250 meters. The transmitting power of the sensors depends on the voltage supply (ranging from 183dB at 8V to 189dB at 16V). We configured the sensors to operate at 13 bits per second. The main problem in our experiment was the limited storage of the modems. The buffer memory size was only 32 bytes and each bits sent via the serial port were encoded as 8 bits. As a result, we were only able to send a maximum of 32 bits at a time from the m-sequences of length 1023. So practically the length of the sequence could be considered to be 32 for one transmission. The acoustic modems transferred serial data at 4800 baud, 8 data bits, no parity, and 1 stop bit. Flow control was set to software handshaking. We used Matlab Simulink to transmit the whole 1023 length sequence. Initially, we measured

underwater channel noise and plotted its PSD. The purpose of this study was to find the suitable frequency range for transmission, such that noise would be relatively less dominant in that frequency ranges than others. We measured the noise during our experiment for the length of 3.65 minutes sampled at the rate of .01s and plotted its autocorrelation and PSD.

Figure 15 Autocorrelation of Noise Measured in Swimming Pool

From Figure 15 we can observe that the autocorrelation of the measured noise is 1 at time 366 milliseconds which refers to the 0 time lag. As the time lag increases, the autocorrelation of the measured noise decreases.

Figure 16. PSD of Measured Noise in Swimming Pool

From Figure 16 we see that the power of noise is high for frequency range of 0 to 5 kHz. As the frequency increases we observe that the power of noise is less than -11.86 dB. So if we are able to transmit the signal in the frequency range where the noise power is relatively less, we can obtain better performance. Therefore, we have chosen 17 kHz of carrier frequency for our experiments. We could use any frequencies above 5 kHz and below 40 kHz, but to be consistent with [1], [3], [5], [6], we preferred 17 kHz. Besides noise, we investigated different spectral estimation techniques for different types of random signals/processes.

We generated an AR process by filtering a unit variance white noise with an all pole filter, a MA process by all zero filters, and ARMA process with pole-zero filters. From all of the PSD's of generated random processes, we observed that the magnitude of the spectrum was higher for dominant frequency components. It is clear that, we could extrapolate the information contained in the random process by using a band pass filter that would pass only the dominant frequency components. It was observed that for different stochastic process we had different dominant frequency components.

Furthermore, we used the stochastic processes generated using different models described earlier in this thesis for spectral estimation using parametric and non- parametric methods. We used the Periodogram and the Welch's methods for non-parametric spectral estimation, and the Yule-Walker, and the Burg methods for parametric spectral estimation. We compared the results for parametric and non-parametric spectral estimation methods. We observed that non-parametric spectral estimation techniques gave us almost similar results but with a higher magnitude. We have plotted the estimated PSD for all parametric in Figure 17 and blind methods in Figure 18.

Figure 17. PSD Estimation by Parametric Methods

From Figure 17 (a), (b), (c), and (d), we observed that Yule's method of parametric spectral estimation is smoother and covers a large window than the Burg method. Yule's method is preferred in extracting information contained in the signal because it avoids information leakage during windowing. For detection purpose, we preferred Burg's method because it gives a high frequency resolution. Therefore it is useful in detecting underlying frequency component of the signal in environment where the noise spectrum is relatively high. In Figures 5 (a),(b),(c), and (d), we have plotted the spectral estimation results for blind methods.

Figure 18. PSD Estimation by Blind Methods

From the simulation of non-parametric spectral estimation techniques, in Figure 18, we observe that the Periodogram spectral estimation technique gives a sharp peak while the Welch method is smoother and has a larger window that will prevent data leakage while windowing for certain range of frequencies. It is also clear that periodogram method gives many sharp peaks and clearly distinguishes adjacent frequency components. Therefore it is useful in frequency estimation. However, in underwater acoustic communication due to the Doppler shift, adjacent frequency components might result in false frequency estimation. Since the spectrum of Welch's method has a lower magnitude, it is not preferable for higher noise environment. Periodogram techniques are more preferred for fast varying environment for blind estimation of frequency for target detection. In Figure 19 we compared parametric with blind methods for an ARMA random process.

Figure 19. Comparisons of Parametric and Blind Spectral Estimation Methods

We advanced our experimental results further by performing cosine linear frequency modulation and m-sequence modulation. These modulation techniques were used in data transmission in our experiments. The swiping frequency of LFM was 2kHz (17kHz to 19kHz). Figure 7 shows the chirp cosine signal with swiping frequency of 2kHz, spectrogram and its PSD. It is clear from the spectrum that LFM increases bandwidth. The ripples in the spectrum is due to FFT routine of Matlab. We have also plotted the autocorrelation function for three m-sequences.

Figure 20. Linear Frequency Modulation Cosine, and its PSD

From Figure 20 we see that the LFM increases the pulse bandwidth. As a result, pulse will compress in the time domain. This pulse compression enables us to decouple the duration of the pulse from its energy by effectively creating different durations for the transmitted pulse and the processed echo. We further plotted the autocorrelation function of three m-sequences. Spread spectrum technology is used to broaden the bandwidth of a signal in the frequency domain. In [12], it is proved that spread spectrum technology is more robust to noise and doppler spread than LFM. Therefore, in this thesis, we studied the autocorrelation and PSD maximal length sequences. In Figure 21, we observe the discrete components for each m-sequences at time lag 1023 bits length. It is also observed that the amplitude of autocorrelation for different m-sequences is different. This shows that the correlation between 1st and the second m-sequences is relatively more than first and the third.

Figure 21. Periodic Autocorrelation of PN- Sequences

To examine the performance of the blind methods and to find the Doppler shift, we used MATLAB as user interface to receive and transfer data through SAM-1 acoustic modems. The received data were acquired via serial data acquisition processes in MATLAB. The acoustic modems were operated at baud rate of 4800 symbols per sec and 8 data bits. The data rate of transfer was 13 bits per sec. We used three different types of data for transmission: m-sequence of length 1023, m-sequence of length 1023 modulated with carrier of frequency 17 kHz, m-

sequence of length 1023 modulated with LFM signal of sweeping frequency of 2 kHz. The received data for the 1st two types of modulations were analyzed using the spectral characteristics: autocorrelation and PSD, and the last one were analyzed using Oerder and Meyr squaring timing recovery.

In our experiment the transmitted signal had a carrier frequency of 17 kHz and a sampling rate of 8000 samples/sec. The transmitted spectrum in both the cases (tank and pool) had almost a flat spectrum. We plotted the PSD of the received signal and observed the different spectral components for both tank and pool. Initially we plotted the transmitted baseband and received signal in Figure 22.

Figure 22. Initial Transmitted (a) and Received (b) m-sequence signal

We see in Figure 22 that the transmitted data consist of m-sequences with 1023 symbols and the received data is m-sequences with 34 symbols. There was a problem in transmission of the 1023 symbols because the maximum buffer size was only 32 bytes. So basically it was a data overflow problem. We addressed to the problem by writing a program that could send a data in packets of 32 bits at one time. It is equivalent to 4 symbols per transmission with 8 samples per symbol. We choose 32 bits because we observed highest accuracy for a 32-36 bit transmission range during our multiple experiments. We were able to receive all the bits transmitted when 32-36 bits were sent. It is worth mentioning that each bit is encoded in 8 bits by the hardware. In addition the sensors were half duplex. After fixing the data overflow problem, we transmitted the modulated m-sequence. Figures 23-25 shows the signals and their autocorrelation.

Figure 23 Frequency Modulated Transmitted Signal

Figure 24 Frequency Modulated m-Sequence Received Signals (17 kHz)

Figure 25 Autocorrelation of Transmitted and Received 52-m -Sequences

It is clear from Figure 25(b) that on the received signal we were able to distinguish the transmitted 52 m-sequences clearly. However, the received signal is not free of noise and some multipath components. The dark lines refer to the cross-spectral correlation effect. The dark line on the autocorrelation of the transmitted signal is due to modulation effect. So we plotted the partial autocorrelation of the received signal and find out the transmitted m-sequences associated with it.

Figure 26 Partial Autocorrelation of Received Signals Showing 48th to 52nd m-Sequences

In Figure 26, we noticed that the length between each m-sequence is not 1023 bits (in the transmitted signal it was 1023 bits). From this observation we concluded that the multipath effect must have induced additional bits into the received signal during the period of 1023 millisecond.

Figure 27 Power Spectral Density of Transmitted and Received Signal [Water Tank]

In Figure 27, it can be seen that the PSD of transmitted m-sequences is flat and the PSD of received signal is nearly flat as well but with greater magnitude. This means there might be very less of an effect of multipath components (which are very less because the tank is supposedly anechoic) but more of an effect of noise, and most importantly the data sequence overlap because of the limited buffer memory. In the case of the water tank experiment, we were able to receive same data that was sent with a bit error rate of 0.0078 (we had 8 bits error in 1023 bits). Looking at the partial PSD around the carrier frequency and its period, we can see the Doppler shift.

Figure 28 Partial PSD of a Received Signal [Results for Water Tank]

The partial PSD spectrum in Figure 28 shows that the Doppler shift is 50 Hz at carrier frequency 17KHz and 20 Hz at double of carrier frequency. Taking average we conclude that the estimated Doppler shift is approximately 35 Hz. After measuring the Doppler shift in the water tank, we performed experiments in the swimming pool. In the swimming pool, the transmission range was longer (25 yards) and the environment is echoic, so we experienced more of multipath effect.

Figure 29 PSD of Received Signal [Results for Swimming pool]

We searched for the local maxima around the carrier and found the Doppler shift to be 130 Hz at frequency of 17 KHz and 170Hz in average 150Hz. Then, we transmitted the LFM m-sequences signal and analyzed the signal using Oerder & Meyr squaring recovery circuit. Figures 30 and Figure 31 show the transmitted signal, received signal, their autocorrelation, and phase shift.

Figure 30 Transmitted and Received Signal for LFM m- Sequences [Pool]

Figure 31 Autocorrelation, PSD and Partial Autocorrelation of LFM 52- m- Sequences

The results obtained in Figure 31 (e) and (f), the Doppler frequency shift is almost consistent with the one from cosine modulated m-sequences for the water tank experiment. One should carefully note the magnitude of spectrum or cosine modulated and LFM modulated m-sequences. We observe same Doppler frequency shift but with different powers of received signal. We should also note that the Doppler shift for cosine modulated m-sequence signal in the swimming pool experiment was approximately 150 Hz, but the Doppler shift for LFM m-sequences is 35 Hz. From this observation we concluded that the double modulation technique is more robust to Doppler spread. We used Order & Meyr algorithm to find the instantaneous and average phase shift and plotted in Figure 32.

Figure 32. Estimation of Instantaneous and Average Doppler Shift Using Oerder & Meyr Algorithm

From Figure 32, we see that average Doppler shift is 0.85 and the instantaneous shift of range [0-2.86]. From the experiments, we claim that Doppler shift could be minimized by using double modulation technique instead of using either the LFM or m-sequence technique separately. This can be validated by the minimal shift obtained in Figure 32. It can be observed that, for the double modulation technique, phase shift is less than the one provided in [1]. The results

provided in [1] were for m-sequence modulation and the average phase shift was 1.12 for the same parameters ($k=100$ symbols).

In the next we present the numerical results from applying the optimal distance/frequency algorithm (developed under this grant) for different underwater communications channel scenarios. We also provide some explanations for our observations according to the channel model and our assumptions. As seen in Figure 33 and Figure 34 the optimal distances in case of the ideal channel scenario are almost two times longer than the optimal distances in the case of imperfect channel scenario.

Figure 33. 4 level tree structured network with 2 children nodes

Moreover, according to Figure 33 and for the ideal channel scenario, the optimal distance for the leaf sensor nodes successfully transmit the measured information to their parent nodes can be up to 16 Km. According to the results, using CDMA could improve the system performance and the distances could be even longer indicating that for the same amount of transferring information, a channel with CDMA utilization needs less capacity than a regular channel. However, this placement may not provide adequate coverage at those depths since every sensor can cover up to a specific distance. Thus, there is a tradeoff between optimal distance in terms of reliable communication and optimal distance in terms of coverage for the nodes at deeper water. In summary, the optimal placement for the nodes closer to the water surface should follow the non-uniform distance needed for reliable communication and the optimal placement for the nodes farther away from the water surface should follow the coverage rule.

Figure 34. Optimal distance (on the top) for ideal and imperfect channels including BER and interference for a tree shaped topology with 7 levels

As it can be seen from Figure 34, the distances for transmitting the same amount of information at each level can be longer in the case of ideal channel comparing to the same level for imperfect channel. For both scenarios, the optimum frequency at higher level (corresponding to lower transmitting data rate) would be much more than the required frequency at lower levels. The lower part of Figure 34 has been plotted separately in Figure 35 since it represents the imperfect channel scenarios, which are more realistic ones. Figure 35 also shows how imperfect channels would be enhanced after CC usage. From the results we can conclude that the optimal distances can be longer in the case of ideal channel compared to the imperfect channel, whereas, in the case of using CDMA, distances could be even longer.

Figure 35. The distances for different imperfect channel scenarios and their improved situations after applying CC

Another important research question is the amount of power boost required in the imperfect channel case in order to achieve the same links' lengths as of the ideal channel scenario. As shown in the Figure 36, the power boost depends on the level at which the sensor is located in the underwater acoustic network. However, the power boost in our case is between (660 - 690, i.e., 28.1 dB – 28.3 dB).

Figure 36. The ratio of the sensor power of the imperfect channel compared to the sensor power of the ideal channel

Moreover, the channel characteristics for the 7 level symmetric tree structured sensor network, the optimum transmission frequencies have been numerically calculated and illustrated in Figure 37 under the case of ideal channel scenario. Figure 38 depicts the optimal frequency in the case of imperfect channel with BER of 0.001.

Figure 37. Optimal frequency at each distance associated with a specific level for an ideal channel in a 7-level tree structured network

Figure 38. Optimal frequency at each distance associated with a specific level for an imperfect channel (BER = 0.001) in a 7-level tree structured UWSN

On the other hand, the improved system by using convolutional codes has been shown in Figure 39 [16], [17]. Figure 39 shows the effect of convolutional code on optimal frequency of a tree structured underwater wireless sensor network in which optimal frequency is closer to that one corresponding to the ideal channels. The highest optimal frequency in the case of ideal channel is 8.9 kHz at level 7, while this goes up to 13.69 kHz in the case of imperfect condition and after utilization of convolutional coding this amount decreases slightly to 12.8 kHz. Also, the optimal frequency at higher levels (corresponding to lower transmitting data rate) would be larger than the optimal frequency at lower levels.

Figure 39. Optimal frequency at each distance associated with a specific level for an imperfect channel (BER = 0.001) improved with convolutional code in a 7-level tree structured network

Figure 40 shows the variation of the path-loss in tree structured wireless sensor network as a function of frequency and networking level in the described model. Interestingly, we can see that the optimum operating frequency at each level is in the area around the minimum path-loss, where the inverse amount of path-loss as in the Figure 40 has its pick for each curve. In other words, for any given distances between children nodes and their parents, the narrowband SNR is a function of frequency, and from the Figure 40 it is obvious that the acoustic bandwidth depends on the transmission distance.

Figure 40. Frequency dependent portion of narrow-band SNR.

Now, let us assume that the system operating frequency f and the system bandwidth frequency are equal to 10 KHz and 100 Hz, respectively. This is consistent with the narrowband assumption. Also, the sensor powers are all identical to each other and equal to 1 Watt and the spreading factor for the ambient noise is also 1. We solve the optimization problem for the optimal sensors' location under the above assumptions using a MATLAB codes. Figure 28 shows the optimal sensors' placement.

Figure 41. Optimal placement of the sensor nodes when the transmitting power is constant

Using the optimal sensors' locations, Table I shows the optimal signal to noise ratios over links 1, 3 and link 4.

Table 24. Optimized placements and other related parameters when the transmitting power of each node is constant and equal to 1 watt

The main result of this optimization problem is: with the underwater acoustic sensor network topology in Figure 41, and with the policy explained earlier, under the optimization problem constraints, and with sensors transmit power of 1 Watt, the highest information rate than be transmitted to the root node 0 is equal to 453.37 bps, assuming optimal sensors' locations obtained in the optimization problem. It is interesting to notice that although the tree structured sensor network is symmetric with respect to the root node, the optimal locations of the nodes 3 and 4 are not at the same depth. As expected, since sensor node 3 has fewer number of neighbor nodes, and is less affected by the interference of the other sensor nodes, the optimal distance between child node 3 and the parent node 1 (16.8 km) is larger than the optimal distance between child node 4 and the parent node 1 (14.2 km). In the next, we assume that the system operating frequency and the system bandwidth frequency are equal to 10 KHz and 100 Hz, respectively. The optimal sensor' power allocation for the tree structured UWSN when its sensors are fixed at the places plotted in the Figure 41.

From Figure 42 we can see that if sensors are located at the same depth assuming they are transmitting the same amount of information, the energy consumption would be more for the ones who are exposed to more interference. In Figure 42, sensors 4 and 5 need more energy than the sensors 3 and 6.

Table 25 shows the coordinates of each sensor node, optimal transferring energy, optimal SINR for each sensor node and the optimal links' capacities.

Figure 42. The optimal power allocations for the scenario 1 are shown near each sensor node (in Watts)

Table 25. Optimized energy allocation and other related parameters when the sensor nodes are fixed in their locations, first scenario

Therefore, the optimal aggregate rate of information of this underwater acoustic sensor network would be 283.37 bps. Now, let us obtain the optimal sensors' power allocation in another network somehow little asymmetric compared to the previous graph, where the nodes are located in the following locations (Figure 43). The optimization problem and the parameters are the same as the first scenario. Table 26 also depicts all the related parameters of this scenario.

Figure 43. The optimal power allocations for the scenario 2 are shown near each sensor node (in Watts)

In this scenario, the optimal aggregate rate of information of this underwater acoustic sensor network as a result of optimal power allocation would be 437.56 bps.

Table 26. Optimized energy allocation and other related parameters when the sensor nodes are fixed in their locations, second scenario

In the next we assume that both sensors' placement and their consuming power are unknown and we try to find the optimal solution for the cases at the same time, given the mentioned policy. We take the same network parameters we had for previous sections: the system operating frequency f and the system bandwidth frequency are equal to 10 KHz and 100 Hz, respectively which is consistent with the narrowband assumption. But in this part, the power constraint is 1.2.

Figure 44. The optimal sensors' locations and power allocations (in Watts)

Figure 44 shows the optimized locations and the optimized consuming energies for each sensor node at the tree structured network explained earlier. According to the Figure 44 and also the calculated information inserted in the Table 27 we can see that the optimal tree structured UWSN is the one which is symmetric. This could play an important role in the network configuration design. For the UWSNs with more levels, we can consider a symmetric structure and then find the optimal locations and transmitting power for each sensor node.

Table 27. Optimized placements, optimized power other related parameters

Table 27 also shows other the related parameters in the network. It is clear that, the power consumption in the levels closer to the water surface is dramatically larger. The SINRs for each acoustic link could be another proof for that saying, as the SINR for the links 1 and 2 is more than 20 times of that of the links in the higher levels corresponding to lower rate of transferring data. One possible solution for this huge difference between the power consumption, channel capacity and SINR of acoustic links at different levels would be deploying more sensors in the levels closer to the water surface. This can be led to change the tree structured configuration of the network so that we start with a specific shape and we can end up with another structure in order to improve the network parameters.

III.4 Accomplishments for this period included in Part III

Paper published: 3 conferences (IEEE, ASEE, IASTED)

Paper under in progress: 4 (1 under review, 3going to be submitted this fall)

Invited talks: 1 (Technical University of Iassy, May 2013)).

Poster Presentation: 2 (Dynamics Days 2013, Denver CO, January 2012 and UDC May 2013)

5 MSEE students at the University of the District of Columbia, Research meetings, Fall 2012.

5 presented at Engineering week at UDC, Graduate and undergraduate research day at UDC

6 Undergraduate students supported: 4 Senior student presentation, 2 Undergraduate students supported for conference travel to Philadelphia, Fall 2012.

6 Graduate students supported: 2 Master Thesis successfully defended Spring 2013. Another students to be defended in the AY2013-2014.

New laboratory facility: Advanced Communication Laboratory, Building 32, Room A04, UDC. (New research laboratory at ECE, renovated during the Fall 2011, operational Spring/Summer 2012 and 2013.

7) Part IV (April 6 2011 and July 31st 2012)

IV.1 Foreword

The results obtained between April 6 2011 and July 31st 2012 are along with the objectives of this grant. We focused on the information theoretical aspects of the threshold Discrete Memoryless Channels and wireless MIMO channels. We derived the upper and the lower theoretical capacity bounds and we studied the stochastic resonance effect associated with the DMC channels. All findings and research results were published in collaboration with Naval Research Laboratory researchers, Center for High Assurance Computer System-5540, in Washington DC.

IV.2 Statement of problem studied

The potential contributions of this project consist of improving the understanding of the information theory aspects of a distributed underwater sensor network and optimizing the noncoherent communication techniques. The research goals of this proposal are in line with Army vision and mission, and they are integrated in the exiting research interests of Office of Naval Research (ONR) at the Naval Research Laboratories in Washington DC (Acoustic Division, Code 7120 and the Center for High Assurance Computing, Code 5540).

The novelty of our approach is to provide new information performance bounds for channels communication which are more accurate and less computationally expensive. We focused on noncoherent communications methods to be used by a distributed underwater wireless sensor network to extract and process the tactical information about the target. We studied new non-data-aided techniques for Doppler shift estimation and compensation to be used by a collaborative distributed underwater sensor network communicating at physical layer. In addition, the proposed research project includes developing information theory based tools for tracking the target by maximizing the mutual information between the moving target and each sensor location.

There are some scientific barriers related to problem studied: 1) Lack of the information theoretical bounds for the binary underwater communication channels in the presence of the Additive White Gaussian Noise (AWGN). How the information about the target is processed in a faster way with a limited computational resources. 2) How the non-coherent communication methods can be used for extracting more information from a cooperative underwater sensor

network for tracking the target. 3) The protocols used in actual acoustic networks (usually inspired from terrestrial wireless ad hoc networks) cannot be employed to handle self-organized sensors with slow data rates and high random dispersion rates.

IV.3 Summary of the most important results

We studied the performance of Discrete Memoryless Channels (DMCs) arising in the context of cooperative underwater wireless sensor networks. We introduced a partial ordering for the binary-input ternary output (2,3) DMC. In the particular case of the Binary Symmetric Channel with Symmetric Erasure (BSC/SE), we used majorization theory, channel convexity and directional derivative in order to obtain a partial solution to the open problem of partial ordering of the DMCs. In addition, we analyzed the stochastic resonance (SR) phenomenon impact upon the performance limits of a distributed underwater wireless sensor networks operating with limited transmitted power and computational capabilities.

We focused on the threshold communication systems where, due to the underwater environment, non-coherent communication techniques are affected both by noise and threshold level. The binary-input ternary-output channel is used as a theoretical model for the DMC. We derived the capacity of the threshold (2,3) DMC in the presence of additive noise. The plots of BSC/SE and BAC/SE capacities are represented in Figures 45 and 46, respectively.

Figure 45. BSC/SE capacity

Figure 46. Capacity of BAC/SE

In order to evaluate stochastic resonance, we modeled the theoretical (2,3) DMC as a physical communication channel corrupted by additive noise with different probability distributions. The (2,3) DMC becomes the BSC/SE when the probability density function of the additive noise is an even function such as Gaussian, Laplace, and Cauchy distribution. Capacity of BSC/SE for threshold values is plotted in Figure 47.

Figure 47. Capacity of BSC/SE for threshold values.

Due to the complexity and the non-linearity of the channel capacity analytical expression, the Pinsker and Helgert capacity bounds were also used to evaluate the stochastic resonance in the case of the (2,3) DMC. Our contribution consists in improving the state of the art on the issue of partial ordering for the (2,3) DMC and deriving the optimal noise level required to obtain the maximum capacity for a given threshold decision level in the case of the binary-input ternary-output DMC. These results are plotted in Figures 48, 49 and 50.

Figure 48. (2,3) DMC and Pinsker capacity Bound

Figure 49. (2,3) DMC and Helgert capacity Bound

Figure 50. Capacity(C), Pinsker (L) and Helgert (U) bounds for different values of threshold

We analyzed the stochastic resonance phenomenon which is a non-linear effect wherein a communication system can enhance the transmission of the information in the presence of the additive noise [2-5]. Various performance metrics in the presence of stochastic resonance such as signal to noise ratio, mutual information, and channel capacity improvement, under a certain range of power noise levels, were discussed in [5]. It is observed that the channel capacity increases, as the noise level increases, until the channel capacity reaches a resonance peak. This increase of the channel capacity is not in concordance with the intuition that increasing the noise power level will decrease the channel capacity. We analyzed the physical communication model of the (2,3) DMC for threshold based stochastic resonance due to additive noise. A summary of our results are given in Table 28 Summary of (2,3) DMC.

Table 28 Summary of (2,3) DMC.

In [5] we focused on partial ordering in the case of the BSC/SE. The BSC/SE is of interest because it is known that in presence of additive Gaussian noise (AGN), the general (2,3) channel becomes the BSC/SE (2,3). The partial ordering of DMC consists of comparing DMC capacity based on the noise components without the computation of the analytical relation of the channel capacity, which in general, is very complex and non-linear. The ordering is critical, especially for wireless sensor communication links at the physical layer operating in very noisy environments with limited computational and power capability as we proposed in our grant. Our partial ordering is based on channel convexity and majorization theory. We reviewed the partial ordering for the particular case of the BSC and BEC and we proved three theorems (Theorems 4.2.1, 4.2.2 and 4.2.3) based on channel convexity and majorization theory. These theorems are used to provide a partial ordering for the BSC/SE (see the Appendices).

Our research results clearly indicate how one could compare the channel capacity under the stochastic resonance by using our analytical relation of the capacity and/or including the capacity bounds. They also demonstrate how one could improve the capacity of the binary threshold communication channel by changing the noise power or the threshold level as plotted in Figure 51.

Figure 51. Optimal noise power and threshold for stochastic resonance, with a scalable factor

In regarding the experimental results, we focused on four different projects in order to do our experimental work and collect data. The graduate students mentored the undergraduate students in teams as it was specified in the educational goals of this grant.

In the first project titled “Low Cost Frequency Shift Keying Acoustic Modem for Underwater Wireless Sensor Networks”, we designed and build a prototype acoustic modem to serve as a physical transport layer for underwater digital communications. It converts between a digital communications scheme (function generator) and an acoustically coupled communications scheme required by our grant design. Specifically our project consisted of a pair of modems to operate as transmit/receive pairs and supports duplex communications. Although our modem operates in air, it is a proof-of-concept experiment in data transmission techniques that will be

used to design a system capable of communicating over some distance in the underwater environment.

Determining the distance was the most challenging aspect of our design of the acoustic modem project. We did a lot of research in comparing different design of acoustic modems and the application used for each implementation. We considered three approaches available in order to design an acoustic modem. This can be implemented using microcontroller, FPGA board, and XR-2206 function generator with the appropriate electronics components. Finally, we focused on acoustic modem circuitry using electronics components to implement both the transmitter and the receiver.

We used the XR-2206 which is a monolithic function generator integrated circuit capable of producing high quality sine, square, triangle, ramp, and pulse waveforms of high-stability and accuracy. The output waveforms can be both amplitude and frequency modulated by an external voltage. Frequency of operation can be selected externally over a range of 0.01Hz to more than 1MHz. The circuit is ideally suited for communications instrumentation, and function generator applications requiring sinusoidal tone, AM, FM, or FSK generation. It has a typical drift specification of 20ppm/°C. The oscillator frequency can be linearly swept over a 2000:1 frequency range with an external control voltage, while maintaining low distortion.

We also used the XR-2211 which is a monolithic phase-locked loop (PLL) system especially designed for data communications applications. It is particularly suited for low rate FSK modem applications. It operates over a wide supply voltage range of 4.5 to 20V and a wide frequency range of 0.01Hz to 300kHz. It can accommodate analog signals between 10mV and 3V, and can interface with conventional DTL, TTL, and ECL logic families. The circuit consists of a basic PLL for tracking an input signal within the pass band, a quadrature phase detector which provides carrier detection, and an FSK voltage comparator which provides FSK demodulation. External components are used to independently set center frequency, bandwidth, and output delay.

In the second project titled “Localization of an Underwater Object” we used the LabView software. The scope of the project was to develop a system interface that would provide the velocity and distance of a remote operated vehicle. This remote operated vehicle will glide in a tank of water that is 8 feet by 10 inches in length. An active sonar was used in order to send a ping (signal) to the vehicle at differing locations. Depending of its location on some fixed axis, the ping will bounce off the vehicle, bounce from the bottom-surface interface of the tank, bounce from the air-water interface, and finally hit the hydrophone. Some signal reflections will not make as many transitions depending on their location from a fixed axis in the tank.

We tried different design methodologies. Our first design methodology was to use the remote operated vehicle, hydrophone, X-bee communication and LabView software package in order to track the position of the object in free space. We were using GPS technology, to locate the object above water. The location information would have been sent to a central hub via RF communication. Then by LabView visual programming, an interface would have been designed to gather the actual position of the remote operated vehicle. The remote operated vehicle was then

to be submerged underwater. Once underwater, a passive series of hydrophones would have been used to locate the object.

The speed would have also been determined. The information from the hydrophone was to be sent serially to a computer. This computer was to be connected to an X-bee network to form a RF communication node between the GPS and the underwater hydrophone. Consequently, the central hub which would have been the LabView software would have done a comparison and contrast analysis of the information sent from the GPS and the computer linked to the hydrophones determining the remote operated vehicle's actual position above and underwater. We have since then disregarded of the idea of using the GPS and X-bee for the more cost efficient design.

Our second design method consists of everything mentioned above except of the X-bee communication module and the GPS. It was necessary to construct active SONAR (Sound Navigation And Ranging) as well as a LabView interface. The active Sonar transmits a generated pulse signal to the remote operated vehicle. We anticipated the sonar signal reflect from the ROV then be received at the hydrophone. The LabView interface displays the Sonar signal as well as the Noise from the hydrophone. The Sonar system consists of LM 386 Audio Power Amplifier, a standard speaker enclosed in PVC piping and a pulse generating program. The hydrophone used was the Dolphin Ear 100 which is a low cost, high quality hydrophone used in professional and academic research, as well as recreationally.

The purpose of the third project titled "Wireless GPS Tracking System with Graphical User Interface" was to design a GPS tracking system which works in real time by using a GPS receiver and radio frequency transceivers. This device can be used for tracking ships or any moving objects and monitors its location, speed and direction. In this project, main focus was to track a ship. The design of this project consisted of two main parts: hardware and software. The hardware part includes components needed in designing the GPS tracking system and designing the circuit interface of the hardware used, so that the functionality of the wireless tracking system can be observed. The software part represented in the developed code which can extract and process the received GPS data and using it to generate a final map showing the transfer location done by the object used to track.

In the last project we worked with SAM-1 Miniature Acoustic Modem in helping undergraduate students to understand how underwater communication modems work. This is related to the grant goal which is to create clusters of underwater sensors that will be able to detect intruders and communicate wirelessly with acoustic waves. Working with SAM-1 improved the undergraduate student understanding of the current state of technology in commercial underwater communications, it helped understanding some principle on which this technology works, they learned about data rate and about acceptable noise levels.

In working with SAM-1, students learned about other issues that characterize underwater communication as: refraction of acoustic waves due to shallow waters and properties of water creating different time of arrival for acoustic waves which could increase or decrease S/N ratio. In our laboratory setting, water tank of 1m x 3m x 0.6m, the signal send by SAM-1 was strong enough and it was well received for threshold level over T40. Our set up was noisy due to

existence of different machinery in our lab. This ambient noise has created errors in rare occasions, and in those occasions no data were received. Also, students learned that there is a significant time delay between data transmission and data being received. This is due to sound propagation, signal processing and data processing.

IV.4 Accomplishments for this period included in Part IV

Paper published: 1 Journal (AECE), 4 conferences (3 IEEE, 1 ASEE).

Paper under in progress: 2 (going to be submitted this fall)

Invited talks: 1 (University of Macao, China, January 2012).

Poster Presentation: 2 (Dynamics Days 2012, Baltimore, January 2012 and UDC May 2012)

- i. Student Presentations: external 4 (QMDNS 2012, April 30-May 1, 2012, George Mason University)
- ii. internal 4 (MSEE students at the University of the District of Columbia, Research meetings, Fall 2011)
- iii. internal 5 (Engineering week at UDC, Graduate and undergraduate research day at UDC)

6 Undergraduate students supported: 4 Senior design projects finalized in Spring 2012
2 Undergraduate students supported for conference travel to Philadelphia, Fall 2011.

6 Graduate students supported: 1 Master Thesis successfully defended Spring 2012. Another 3 students to be defended in the Spring of 2013.

New laboratory facility: Advanced Communication Laboratory, Building 32, Room A04, UDC. (New research laboratory at ECE, renovated during the Fall 2011, operational Spring/Summer 2012).

8) Bibliography

- [1] B. J. Rao and T. Prabhakar, "Underwater Acoustic Wireless Communications Channel Model and Bandwidth," *International Journal of Applied Engineering Research*, ISSN 0973-4562 Vol. 6. No. 18 (2011).
- [2] I. Akyildiz, D. Pompeili and T. Melodia, (2005), "Underwater Acoustic Sensor Networks: Research Challenges," *Elsevier Journal on Ad Hoc Networks*, Vol. 3, issue 3, pp. 257-279.
- [3] M. Stojanovic, "On the Relationship between Capacity and Distance in an Underwater Acoustic Communication Channel," *WUWNet*, 2006, pp 41-47.

- [4] S. Ali, A. Fakoorian, G. R. Solat, H. Eidi, "Maximizing Capacity in Wireless Sensor Networks by Optimal Placement of Cluster Heads," *Canadian conference on Electrical and Computer Engineering*, May 2008, pp. 001245-001250.
- [5] H. Nouri and M. Uysal, "Information Theoretic Analysis and Optimization of Underwater Acoustic Communication Systems," *IEEE*, 978-1-4673-2232. EuroCon 2013.
- [6] D. Lucani, M. Stojanovic, M. Medard, "On the Relationship between Transmission Power and Capacity of an Underwater Acoustic Communication Channel", *WUWNet, 2006*, pp.41-47.
- [7] M. Stojanovic, "Capacity of a Relay Acoustic Channel," *IEEE Transactions on Communications*. Massachusetts Institute of Technology. 0-933957-35-1. 2007 MTS.
- [8] S. Ali, A. Fakoorian, G.R. Solat, H. Taheri, A. Eidi, "Maximizing Capacity in Wireless Sensor Networks by Optimal Placement of Clusterheads," *IEEE*, 978-1-4244-1643, January 2008.
- [9] P. Cotae, I. S. Moskowitz and M. H. Kang, "Eigenvalue Characterization of the Capacity of Discrete Memoryless Channels with Invertible Channel Matrices," *Proceedings IEEE 44th Annual Conference on Information Science and Systems- CISS 2010*, Princeton University, March 17-19, pp. 1-6, March 2010.
- [10] T. Schurmann and P. Grassberger, "Entropy Estimation of Symbol Sequences," *Department of Theoretical Physics, University of Wuppertal, D-42097 Wuppertal, Germany*.
- [11] P. Cotae, S. Yalamanchili, C. L. P. Chen, A. Ayon, "Optimization of Sensor Locations and Sensitivity Analysis for Engine Health Monitoring Using Minimum Interference Algorithm," *EURASIP Journal on Advances in Signal Processing*.
- [12] T. C. Yang and W. Yang, "Performance Analysis of Direct-Sequence Spread Spectrum Underwater Acoustic Communications with low signal-to-noise ratio input signals," *Journal of Acoustical Society of America*, pp. 842-855, February 2008.
- [13] D. Guo, S. Shamai(Shitz) and S. Verdú, "Mutual Information and minimum Mean Square Error in Gaussian Channels," *IEEE Transaction on Information theory*, Vol. 51, no. 4, April 2005.
- [14] P. Cotae, "Transmitter Adaptation Algorithm for Multicellular Synchronous CDMA Systems with Multipath," *IEEE Journal of Selected Areas in Communications (Special Issue on Next Generation CDMA Technologies)*, vol. 24, no. 1. Pp. 94-103, Jan. 2006.
- [15] R. Cao, F. Qu, L. Yang, "On the Capacity and System Design of Relay-Aided Underwater Acoustic Communications," *IEEE*, 2010, 978-1-4244-6398-5/10.
- [16] B. C. Geiger, G. Kubin, "On the Rate of Information Loss in Memoryless Systems," *IEE Signal Processing*, April 2013.
- [17] F. Zhao, J. Shin, J. Reich, "Information Driven Dynamic Sensor Collaboration for Tracking Applications," *IEEE Signal Processing Magazine*, Vol. 19, no. 2, pp 61-72, 2002.
- [18] A. G. Bessios and F. M. Caimi, "High-rate Wireless data Communications: An Underwater Acoustic Communications Framework at the Physical Layer," *Department of Electrical Engineering, Harbor Branch Oceanographic Institution, Inc.*, 5600 U.S. 1 North, Fort Pierce, FL 34946.
- [19] W. Alsalihi, H. Hassanein, and S. Akl, "Placement of multiple mobile data collectors in underwater acoustic sensor networks," *IEEE ICC*, 2008, pp. 2113-2118.
- [20] T.M. Cover and J. A. Thomas, 'Elements of Information Theory,' 2nd ed., New York: Wiley, 2006.
- [21] J.G. Proakis, *Digital Communications*, 5th ed., McGraw-Hill, 2008.
- [22] E. Ertin, "Maximum Mutual Information Principle for Dynamic Sensor Query Problems", *IPSN 2003, LNCS 2634*, pp. 405–416, 2003.
- [23] R. Shrestha, P. Cotae, "On the mutual information of sensor networks in Underwater Wireless Communication: An experimental Approach," *ASEE Zone I Conference, University of Bridgeport, Bridgeport, CT, USA*. April 3-5, 2014.
- [24] Matlab Signal Processing Toolbox, <http://www.mathworks.com/products/signal/>
- [25] Matlab Communication toolbox, <http://www.mathworks.com/products/communications/>
- [26] Ira S. Moskowitz, Paul Cotae, Myong H. Kang, Pedro N. Safier, "Capacity Approximations for a Deterministic MIMO Channel", *Advances in Electrical and Computer Engineering*, Vol. 11, no. 1, pp. 3-10. Sept. 2011
- [27] Roland Kamdem, Ira S. Moskowitz, Paul Cotae, "Threshold Based Stochastic Resonance for the Binary-Input Ternary-Output Discrete Memoryless Channels", *Proceedings of Seventh IASTED International Conference, Communication, Internet, and Information Technology (CIIT 2012)*, Baltimore 14-16 May, DOI: 10.2316/P.2012.773-041, pp. 398-404, May 2012.

- [28] Ira S Moskowitz, Paul Cotae, Pedro Safier and Daniel Kang "Capacity Bounds and Stochastic Resonance for Binary Input Binary Output Channels", *Proceedings of the IEEE ComCompAp 2012*, Hong Kong, China, January 11-13, pp. 61-66, Jan. 2012
- [29] Ira S Moskowitz, Paul Cotae, Pedro Safier "Algebraic Information Theory and Stochastic Resonance for Binary Input Binary Output Channels", *Proceedings IEEE 46th Annual Conference on Information Sciences and Systems-CISS 2012*, Princeton University, March 21 – 23, pp.1-6, March 2012.
- [30] Roland Yannick Kamdem Kenmogne "Partial Ordering and Stochastic Resonance in Discrete Memoryless Channels", UDC ECE Department, Defended May 1st, 2012.
- [31] Nikola Jovic, Abayomi Dairo, Ashenafi Tesfaye, Aime Valere, Yannick Roland Kamdem, Sasan Haghani and Paul Cotae "Detecting Falls Among Elderly Patients in Nursing Homes by Using Wireless Sensor Networks", *Proceedings of the ASEE MidAtlantic Section Fall Conference 2011* (Hosted by College of Engineering, Temple University, Philadelphia), pp. 422 -431, Oct. 2011.
- [32] C.E Shannon and W.W Weaver, "The Mathematical Theory of Communication," *University of Illinois press*, Urbana, IL, 1949.
- [33] Thomas M. Cover and Joy A. Thomas," Elements of Information Theory," *Second Edition, John Wiley and Sons*, 2006.
- [34] Paul Cotae "Blind Doppler Estimation and Compensation in the Underwater Communications" *Technical report submitted to the Naval Research Laboratories*, Washington DC, Sept 2009.
- [35] François Chapeau-Blondeau," Noise Enhanced Capacity via Stochastic Resonance in an Asymmetric Binary Channel," *Physical Review E*, 55(2):2016-2019, 1997.
- [36] François Chapeau-Blondeau, "Periodic and Aperiodic Stochastic Resonance with Output Signal-to-noise Ratio Exceeding that at the Input," *International Journal of Bifurcation and Chaos*, vol.9, No1:267-272, 1999.
- [37] K. Chatzikokolaskis and K. Martin ,"A monotonicity principle for information theory",*Electronic Notes in Theoretical computer science* 218(2008)111-129.
- [38] Paul Cotae and Ira S. Moskowitz," On the Partial Ordering of the Discrete Memoryless Channels Arising in Cooperative Sensor Networks," *4th IFIP International Conference on New Technologies, Mobility and Security, NTMS 2011*, pp.1-6, Paris, France, February 2011.
- [39] H.J. Helgert, "A Partial Ordering of Discrete Memoryless Channels", *IEEE Transactions on Information Theory* , vol. IT-3,no.3, pp.360-365,July 1967.
- [40] Ira S. Moskowitz, Paul Cotae, Pedro N. Safier, and Daniel L. Kang," Capacity Bounds and Stochastic Resonance for Binary Input Binary Output Channels," *Proc. of the IEEE Computing, Communications & Applications conference, ComComAP 2012*, Hong Kong,pp.61-66,Jan. 2012.
- [41] François Chapeau-Blondeau, "Stochastic Resonance and the Benefit of Noise in Nonlinear Systems," *Noise, Oscillators and Algebraic Randomness – From Noise in Communication Systems to Number Theory. pp. 137-155*; M. Planat, ed., *Lecture Notes in Physics, Vol. 550*, Springer (Berlin) 2000.
- [42] Paul Cotae, Ira S. Moskowitz and Myong H. Kang, "Eigenvalue Characterization of the Capacity of Discrete Memoryless Channels with Invertible Channel Matrices," *Proceedings IEEE 44th Annual Conference on Information Sciences and Systems-CISS 2010*, Princeton University,pp.1-6, March 2010.
- [43] Ira S. Moskowitz," Approximations for the Capacity of Binary Input Discrete Memoryless Channels," *In Proceedings 44th Annual Conf. on Information Science and Systems, CISS 2010*,Princeton ,NJ,USA, March 2010.
- [44] Ira S. Moskowitz," An Approximation of the Capacity of a Simple Channel," *43rd Annual Conf. on Information Science and Systems, CISS 2009*,Baltimore ,MD,USA, June 2009.
- [45] Paul Cotae and T.C. Yang "A cyclostationary blind Doppler estimation method for underwater acoustic communications using direct-sequence spread spectrum signals," *8th International conf. on Communications, COMM 2010*, Bucharest, July 2010.
- [46] Ira S. Moskowitz and Paul Cotae," Channel Capacity Behavior for Simple Models of Optical Fiber Communication," *8th International conf. on Communications, COMM 2010*, Bucharest, pp.1-6, July 2010.
- [47] Roland Kamdem, Paul Cotae and Ira S. Moskowitz, "Threshold Based Stochastic Resonance for the Binary-Input Ternary-Output Discrete Memoryless Channel," *accepted at 7th IASTED International Conf. on Communication, Internet and Information Technology, CIIT 2012*,Baltimore, May 2012.
- [48] François Chapeau-Blondeau," Stochastic Resonance and the Benefit of Noise in Nonlinear Systems," *Noise, Oscillators and Algebraic Randomness – From Noise in Communication Systems to Number Theory. pp. 137-155*; M. Planat, ed., *Lecture Notes in Physics, Vol. 550*, Springer (Berlin) 2000.
- [49] Sanya Mitaim, Bart Kosko,"Adaptive Stochastic Resonance in Noisy Neurons Based on Mutual Information ," *IEEE Trans on Neural Networks Vol.15,No.6*, Nov 2004.

- [50] Mark Damian McDonnell, "Theoretical Aspects of Stochastic Signal Quantization and Suprathreshold Stochastic Resonance," *PhD thesis, The University of Adelaide*, Australia, Feb.2006.
- [51] Bart Kosko, Sanya Mitiam, Ashok Patel and Mark M. Wilde, "Applications of Forbidden Interval Theorem in Stochastic Resonance," In *Applications of Nonlinear Dynamics ,Understanding Complex Systems*, pages 71-89.Springer-Verlag, 2009.
- [52] Ira S. Moskowitz, Paul Cotae, Pedro N. Safier,"Algebraic Information Theory and Stochastic Resonance for Binary-Input Binary-Output Channels ," *Proceedings IEEE 46th Annual Conference on Information Sciences and Systems-CISS 2012*, Princeton University, March 17-19, pp.1-6, March 2012.
- [53] Paul Cotae, et. all "Design and Application of a Distributed and Scalable Underwater Wireless Sensor Acoustic Networks" *2009 Annual ASEE Global Colloquium on Engineering Education*, Budapest, Hungary, Oct. 12-15, 2009.
- [54] R. A. Silverman,"On Binary Channels and their Cascades," *IRE Trans. Information Theory, Vol.1,no.,pp.19-27*,Dec 1995.
- [55] C. E. Shannon, "A note on a partial ordering for communication channels,"*Information and control*,Vol.1, pp.390-397,1958.
- [56] H. J. Helgert, "A Partial Ordering of Discrete Memoryless Channel," *IEEE Transactions on Information Theory*, vol.1, no.3, pp.360-365, July 1967.
- [57] A.W. Marshall and I. Olkin, *Inequalities: Theory of Majorization and its applications* .New York: Academic, 1979.
- [58] Patrick M. Fitzpatrick "Advanced Calculus," *American Mathematical Society*, 2009.

List of Figures and Tables

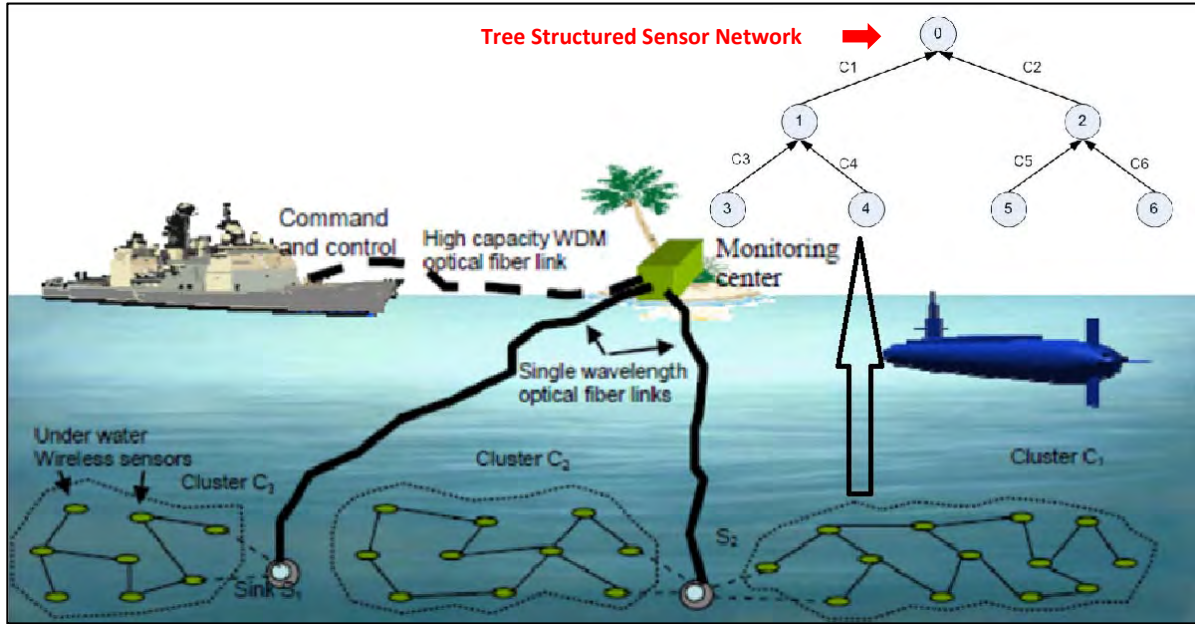


Figure 2: The global picture of the overall project

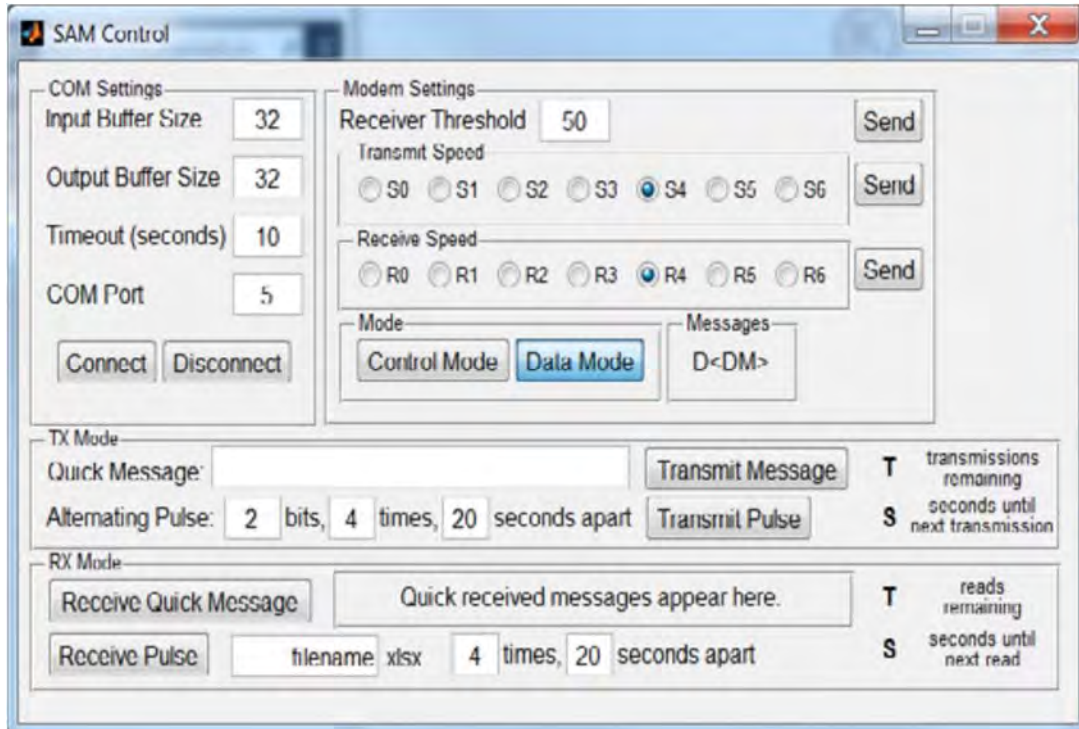


Figure 2 : SAM Control GUI

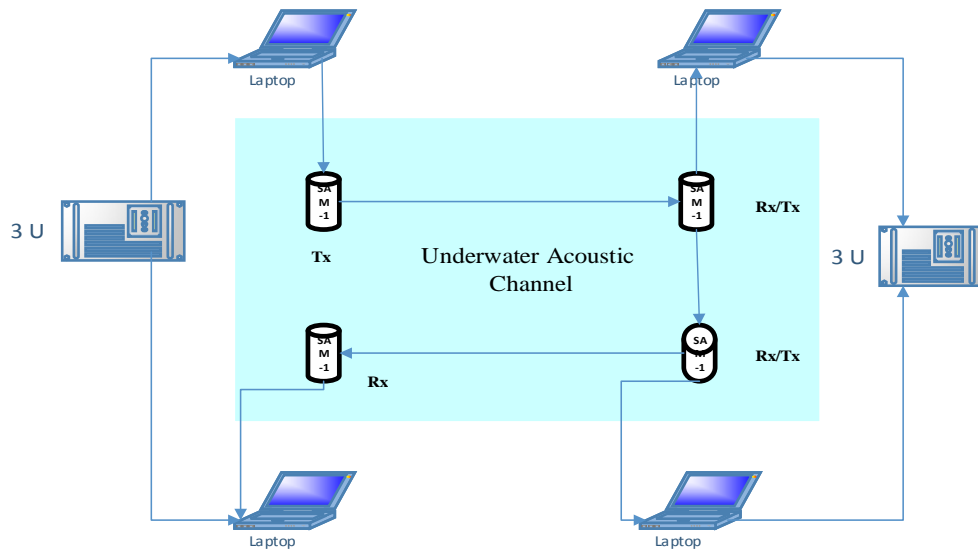


Figure 3: Cascaded underwater wireless sensor network

Table 1: Bit loss test for different distance of sensors

Distance between sensors	No. of bits transmitted	Received no. of bits	Bit loss	Bit error rate
5 m	1023	1015	8	0.007
7 m	1023	1011	12	0.011
10 m	1023	1011	12	0.011

Table 2: Result analysis for Tx1 and Rx1 (d=5 m)

Bits transmitted	Bits received	BER	$I(X;Y)$	Information loss $H(X/Y)$
1023	1023	0.0078	1.00	0.0
1023	1023	0.0087	1.00	0.00
1023	1023	0.0078	1.00	0.00

Table 3: Result analysis for Tx2 and Rx2 (d=5 m)

Bits transmitted	Bits received	BER	$I(X;Y)$	Information loss $H(X/Y)$
1015	1015	0.0068	1	0
1014	1014	0.0078	1	0
1015	1015	0.0088	1	0

Table 4: Result analysis for Tx3 and Rx3 (d=5 m)

Bits transmitted	Bits received	BER	$I(X;Y)$	Information loss $H(X/Y)$
1008	1008	0.0079	1	0
1007	1007	0.0079	1	0
1006	1006	0.0089	1	0

Table 5: Result analysis for Tx1 and Rx4 (d=15 m)

Bits transmitted	Bits received	BER	$I(X;Y)$	Information loss $H(X/Y)$
1023	1012	0.0185	0.9156	0.0844
1023	1015	0.0156	0.9419	0.0581
1023	1009	0.0215	0.8952	0.1048

Table 6: Result analysis for cascaded sensors network

S.N	Case study	$I(X:Y)$	BER	Information loss $H(X/Y)$
1	Tx ₁ and Rx ₁	1	0.0081	0
2	Tx ₂ and Rx ₂	1	0.0078	0
3	Tx ₃ and Rx ₃	1	0.0082	0
5	Tx ₁ and Rx ₄	0.9054	0.1853	0.0824

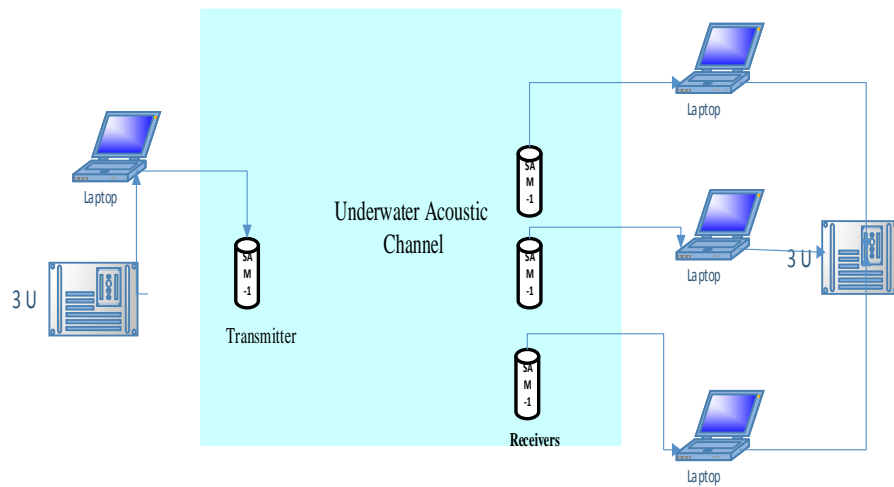


Figure 4. Parallel underwater wireless sensor network

Table 7 : Result analysis for Tx1 and Rx1

Bits transmitted	Bits received	BER	$I(X:Y)$	Information loss $H(X/Y)$
1023	1019	0.0039	0.9804	0.0196
1023	1016	0.0068	0.9645	0.0355
1023	1017	0.0058	0.9700	0.0300

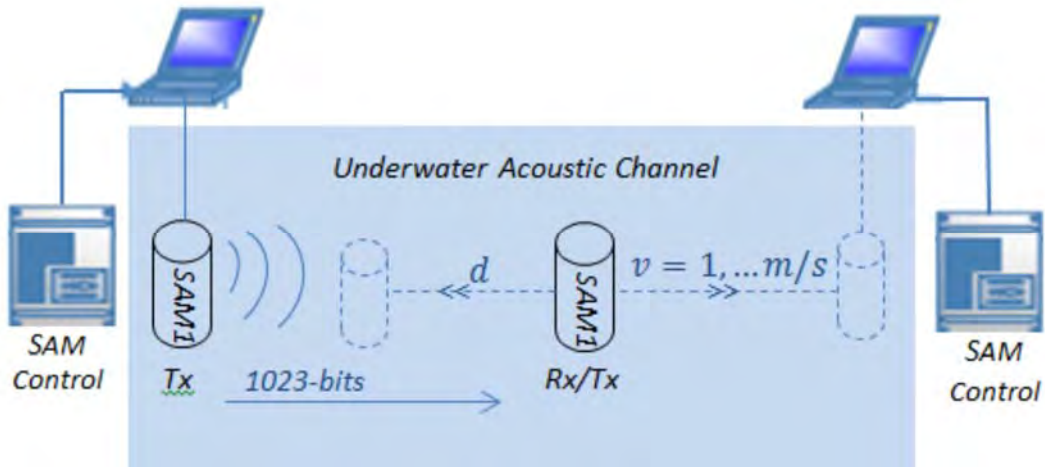


Figure 5 : Underwater Mobile Acoustic Sensor Network

Table 8 : Bit loss test for mobile sensor nodes of maximum distances = 15m.

Sensor Velocity	No. of bits transmitted	Received no. of bits	Bit loss	Bit error rate
1 Knot	1023	1018	5	0.004
2 knots	1023	1018	5	0.004
3 knots	1023	1015	8	0.007

Table 9: Bit loss test for mobile sensor nodes moving in vertical direction.

Sensor Velocity	No. of bits transmitted	Received no. of bits	Bit loss	Bit error rate
1 Knot	1023	1018	5	0.004
2 knots	1023	1018	5	0.004
3 knots	1023	1015	8	0.007

Table 10: Performance results of using mobile sensor nodes

V	Data length	Bits received	P (E)	$I(X;Y)$	Information loss $H(X/Y)$
v_1	1023	1023	0.004	1.00	0.0
v_2	1023	1023	0.004	1.00	0.00
v_3	1023	1023	0.007	1.00	0.00

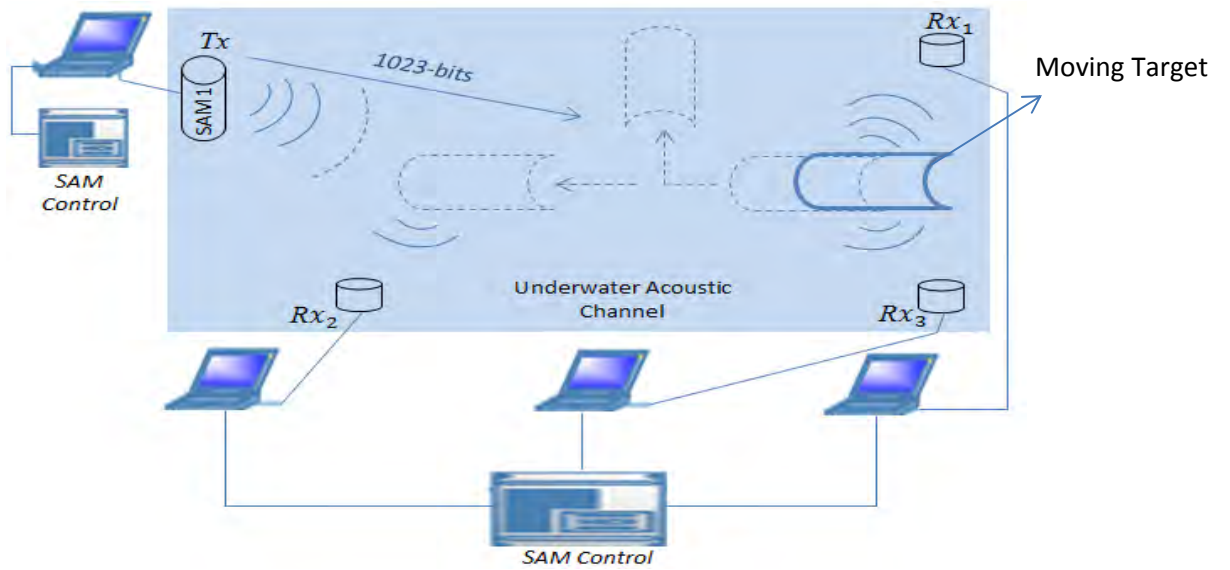


Figure 6 : Experimental approach setup

Table 11: Numerical results for scenario #1

No. of operated sensors	No. of bits transmitted	Received no. of bits	Bit loss	Bit error rate
1	1023	1021	2	0.0019
1	1023	1021	2	0.0019
1	1023	1022	1	0.0009

Table 12: Numerical results for scenario #2

No. of operated sensors	No. of bits transmitted	Received no. of bits	Bit loss	Bit error rate
1	1023	1011	12	0.01
2	1023	1017	6	0.005
3	1023	1015	2	0.001

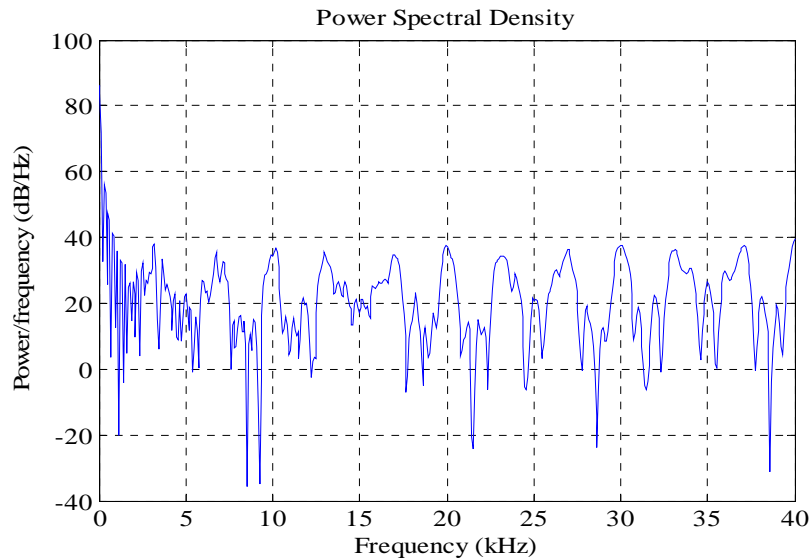


Figure: 7. PSD of Noise ($N_o(f)$) experimentally measured in underwater

Table 13 : Result analysis of using fixed sensor nodes

S.N	Case study	$I(X:Y)$	BER	Information loss $H(X/Y)$
1	Tx ₁ and Rx ₁	1	0.0081	0
2	Tx ₂ and Rx ₂	1	0.0078	0
3	Tx ₃ and Rx ₃	1	0.0082	0
5	Tx ₁ and Rx ₄	0.9054	0.1853	0.0824

Table 14: Summary results for using mobile sensor nodes

V	Data length	Bits received	P (E)	$I(X;Y)$	Information loss $H(X/Y)$
v_1	1023	1023	0.004	1.00	0.0
v_2	1023	1023	0.004	1.00	0.00
v_3	1023	1023	0.007	1.00	0.00

Table 15 (no target is moving): Numerical results for scenario #1

No. of operated sensors	No. of bits transmitted	Received no. of bits	Bit loss	Bit error rate
1	1023	1021	2	0.0019
1	1023	1021	2	0.0019
1	1023	1022	1	0.0009

Table 16: Approach results in Noisy UAC (Scenario#2)

No. of operated sensors	No. of bits transmitted	Received no. of bits	Bit loss	Bit error rate
1	1023	1011	12	0.01
2	1023	1017	6	0.005
3	1023	1015	2	0.001

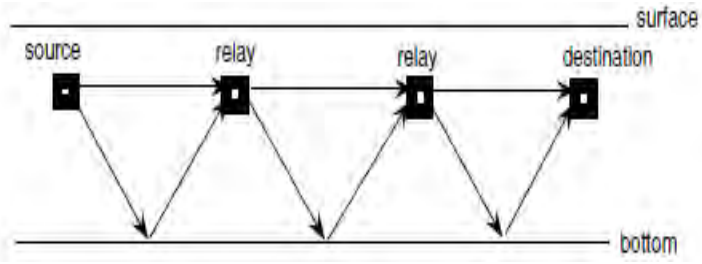


Figure 8 Illustration of Multihop network.

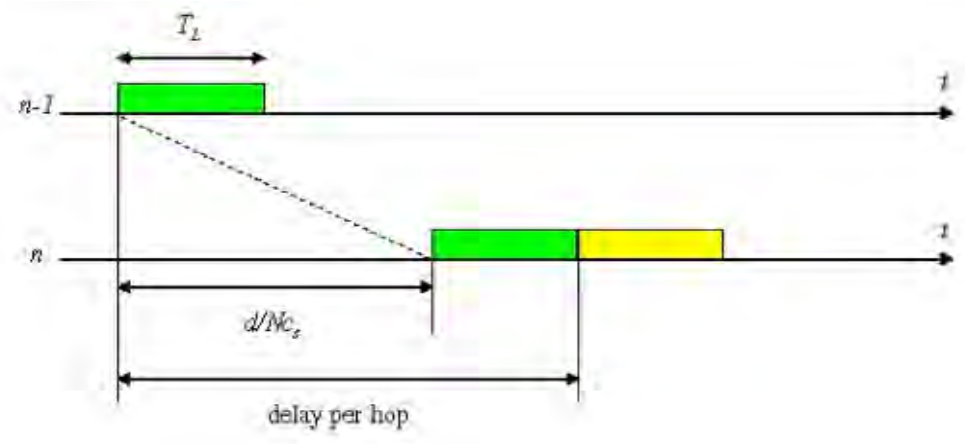


Figure 9. Delay between Relays

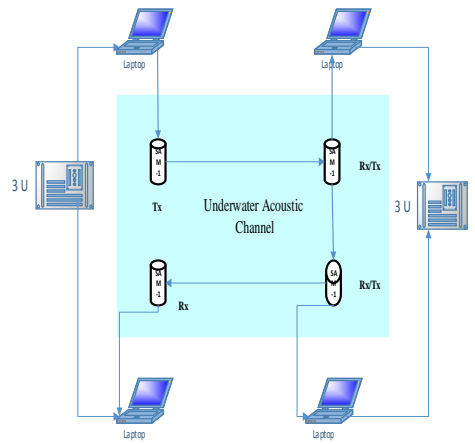


Figure 10. Acoustic Sensors by Vendor and Experimental set up in Underwater Communications

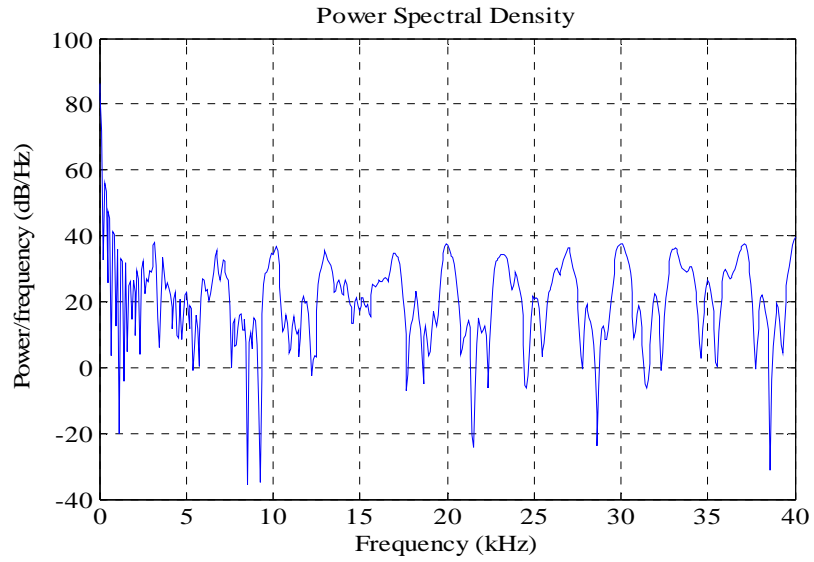


Figure 11. PSD of Noise ($N_o(f)$) experimentally measured in underwater

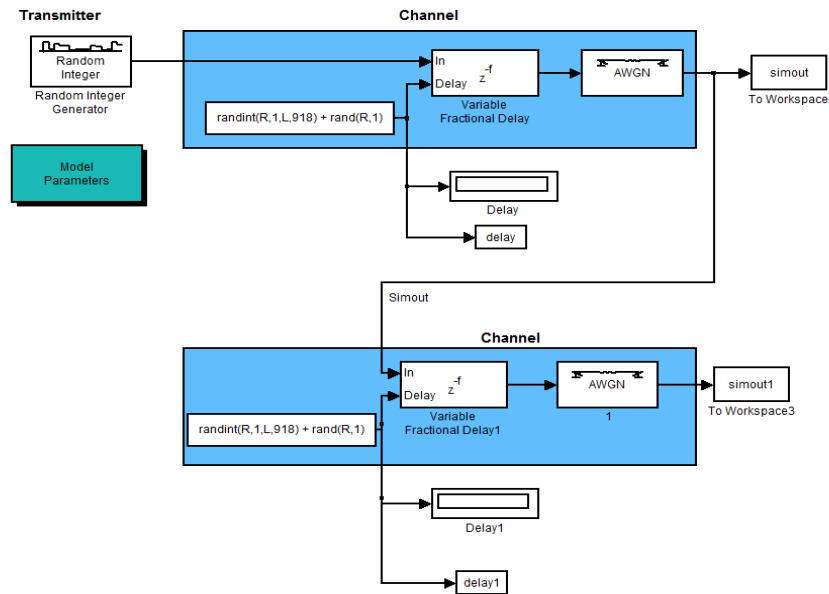


Figure 12. Matlab simulation Set Up for multi-hop network sensor model

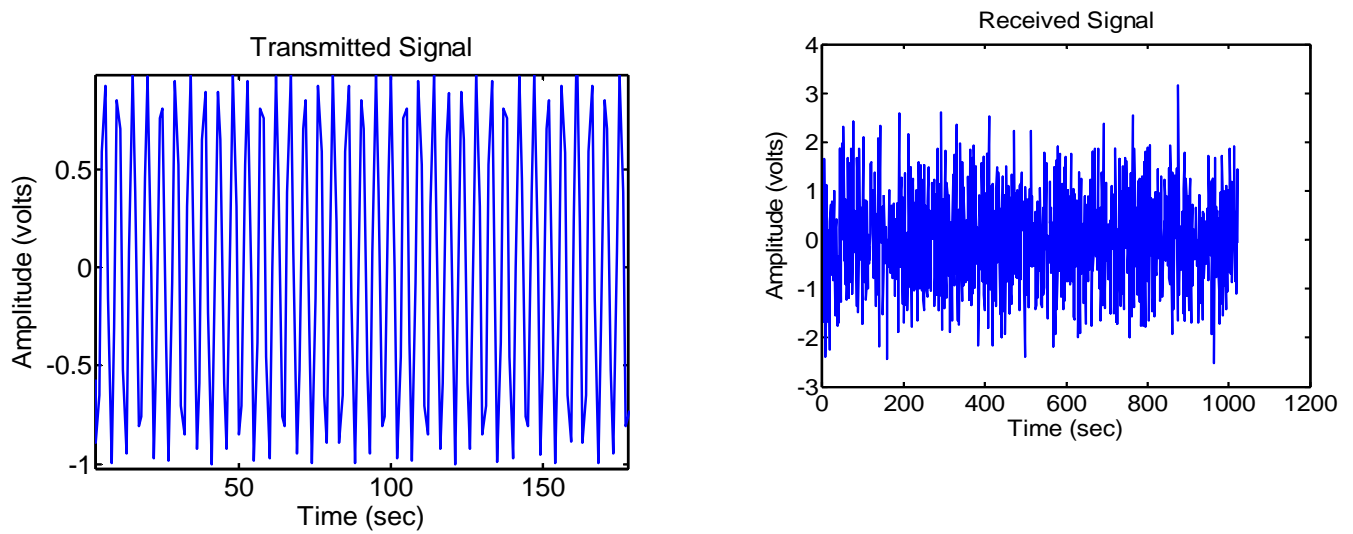


Figure 13. Transmitted and Received Modulated m-Sequence Signals (17 Kz)

Table 17. Modem Specifics and Operating Function

Type of command /specification	Operating function/condition of sensors
###	Sets to a command mode for configuration.
We used S5 for transmission @ 13bits /sec	Set acoustic transmit data speed
We used R5 for receiving @ 13bits/sec	Set acoustic receive data speed
Serial buffer	32 byte
Operating temperature	0-70 ⁰ C
Filter type	4 th order band pass filter
Operating frequency for single channel receiver	33.8khz
Operating frequency of modem	33khz-42khz Omnidirectional
Sonar Data format	16- bit data + 4 bit checksum per word
Modulation	Pulse Position Modulation

Table 18. Bit loss test for different distance of sensors

Distance between sensors	No. of bits transmitted	Received no. of bits	Bit loss	Bit error rate
5 m	1023	1015	8	0.007
7 m	1023	1011	12	0.011
10 m	1023	1011	12	0.011

Table 19. Result analysis for First Hop Tx₁ and Rx₁ (d=5 m)

Bits transmitted	Bits received	BER	$I(X;Y)$	Information loss $H(X/Y)$
1023	1023	0.0078	1.00	0.0
1023	1023	0.0087	1.00	0.00
1023	1023	0.0078	1.00	0.00

Table 20. Result analysis for Second Hop Tx₂ and Rx₂ (d=5 m)

Bits transmitted	Bits received	BER	$I(X;Y)$	Information loss $H(X/Y)$
1015	1015	0.0068	1	0
1014	1014	0.0078	1	0
1015	1015	0.0088	1	0

Table 21. Result analysis for third Hop Tx₃ and Rx₃ (d=5 m)

Bits transmitted	Bits received	BER	$I(X;Y)$	Information loss $H(X/Y)$
1008	1008	0.0079	1	0
1007	1007	0.0079	1	0
1006	1006	0.0089	1	0

Table 22. Result analysis for Tx₁ and Rx₄ (d=15 m)

Bits transmitted	Bits received	BER	$I(X;Y)$	Information loss $H(X/Y)$
1023	1012	0.0185	0.9156	0.0844
1023	1015	0.0156	0.9419	0.0581
1023	1009	0.0215	0.8952	0.1048

Table 23. Result analysis for Multihop relay link and direct link

S.N	Case study	$I(X;Y)$	BER	Information loss $H(X/Y)$
1	Tx ₁ and Rx ₁	1	0.0081	0
2	Tx ₂ and Rx ₂	1	0.0078	0
3	Tx ₃ and Rx ₃	1	0.0082	0
4	Tx ₁ and Rx ₄	0.9054	0.1853	0.0824

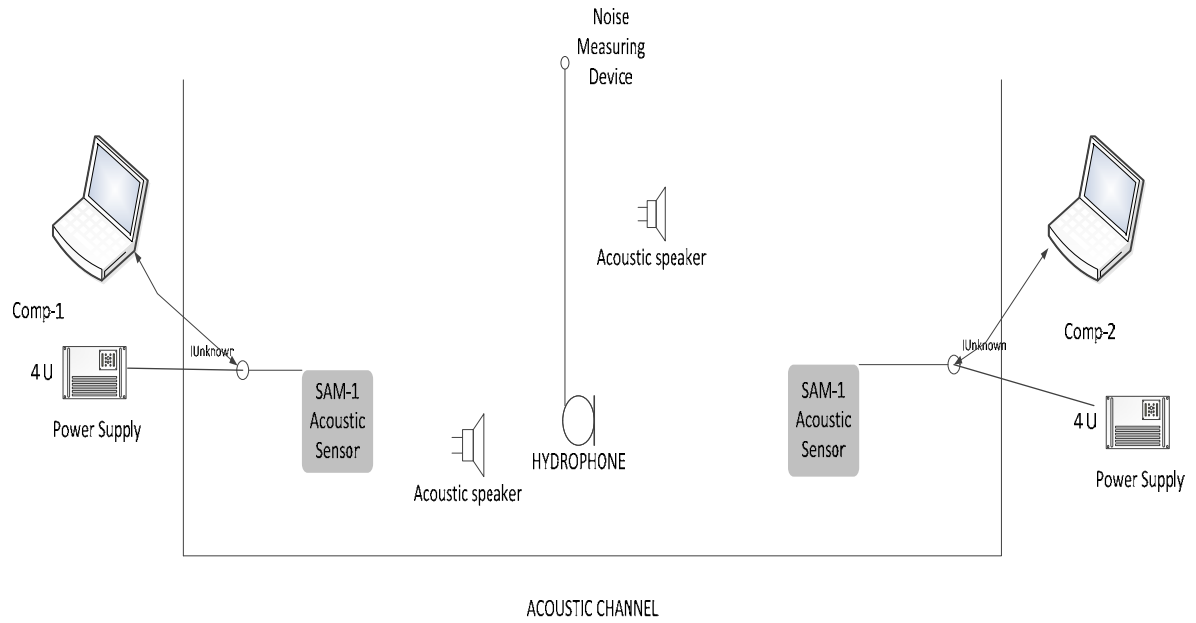


Figure 14 Experimental set up and its components

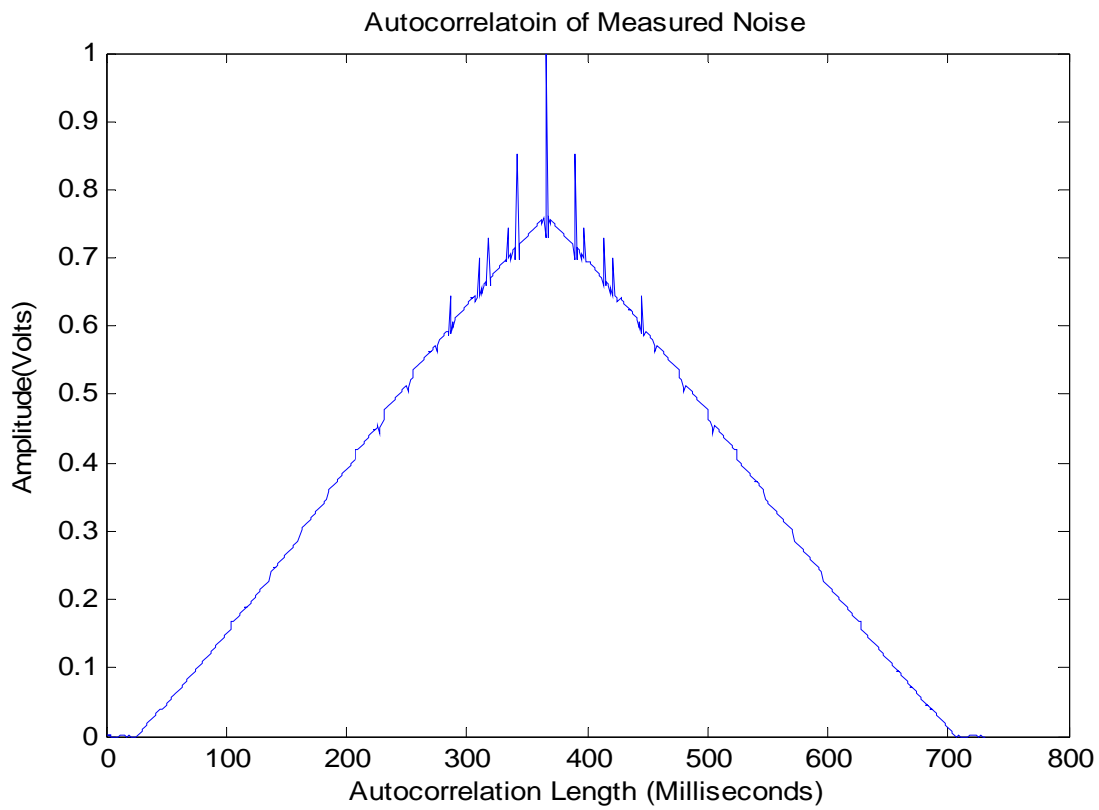


Figure 15 Autocorrelation of Noise Measured in Swimming Pool

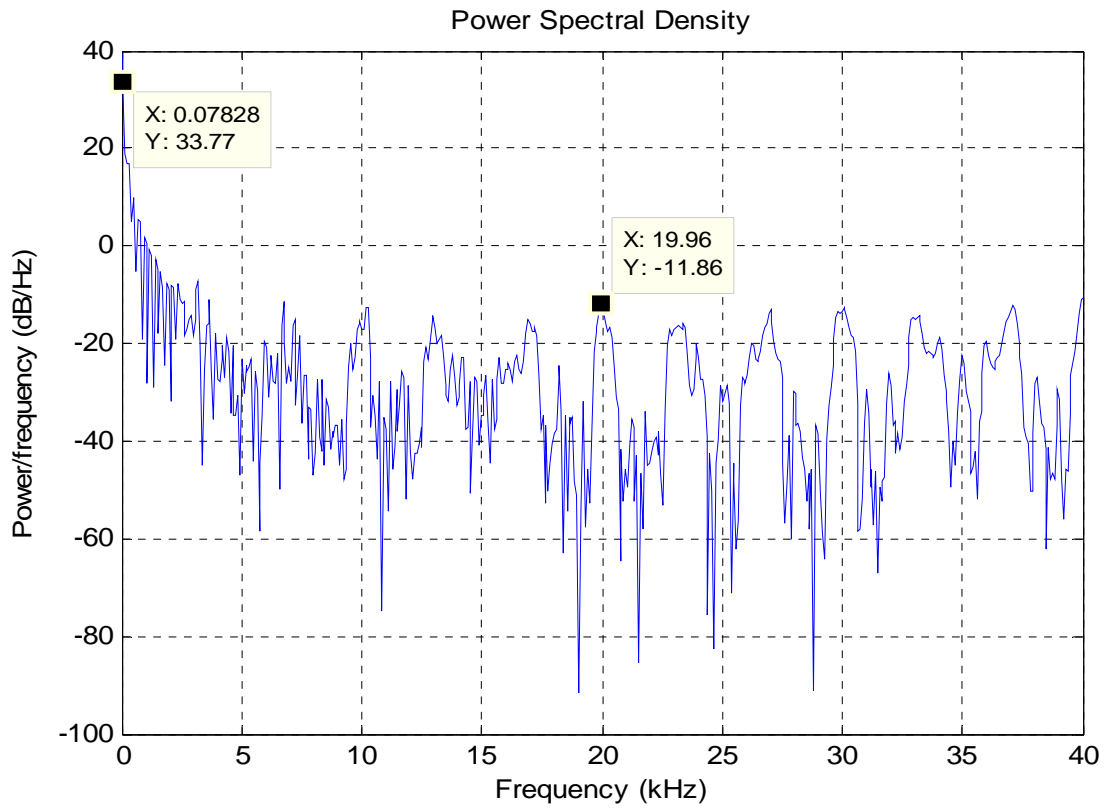
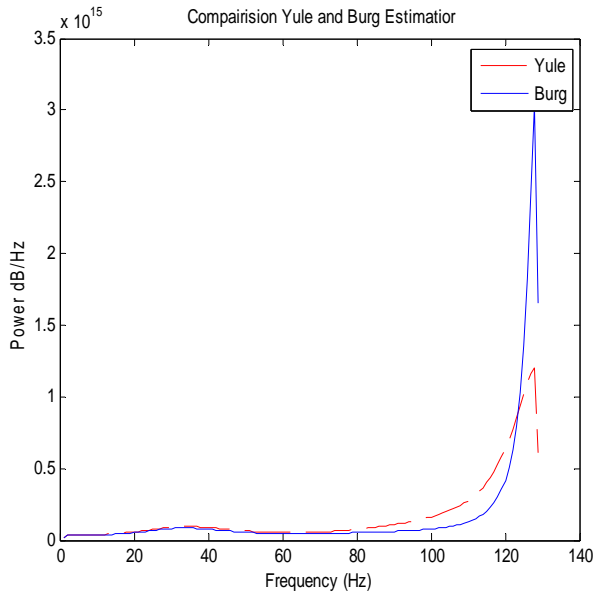
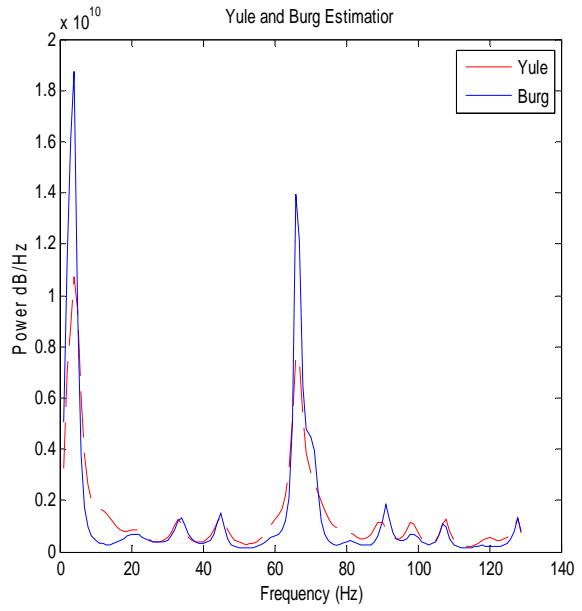


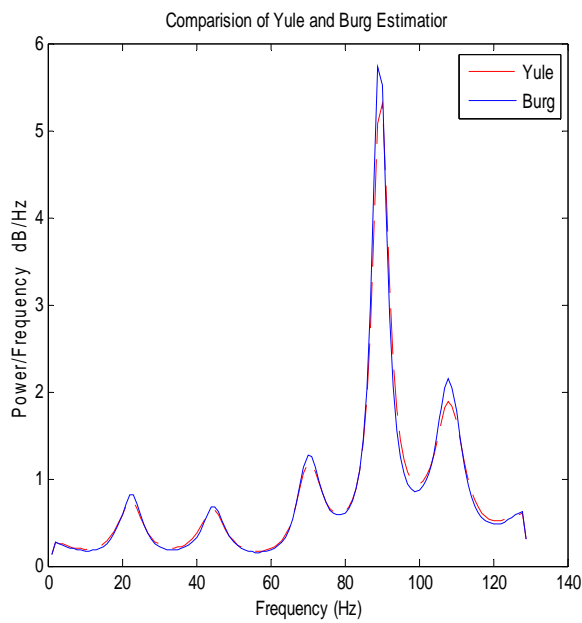
Figure 16. PSD of Measured Noise in Swimming Pool



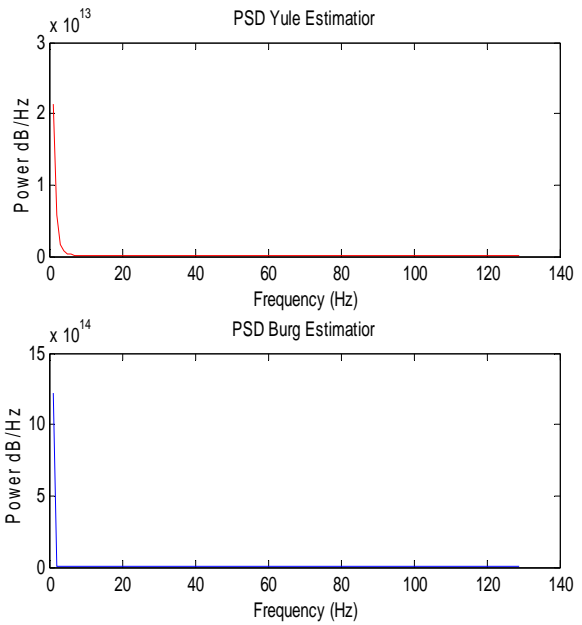
(a) PSD Estimation- AR Process



(b) PSD Estimation- ARMA Process

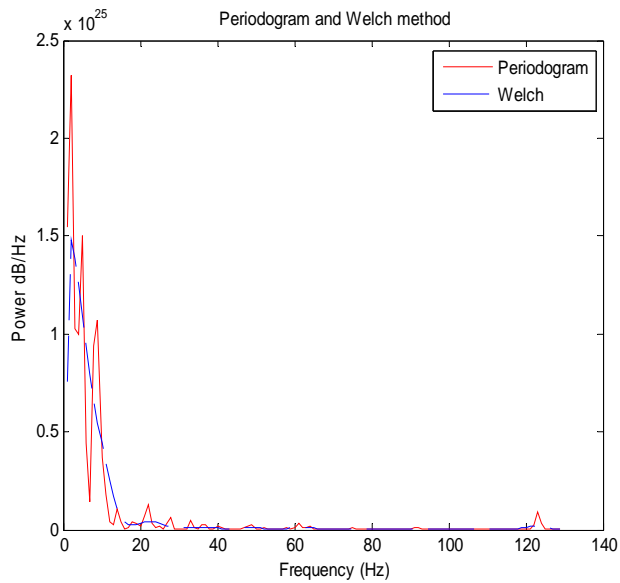


(c) PSD Estimation-MA Process

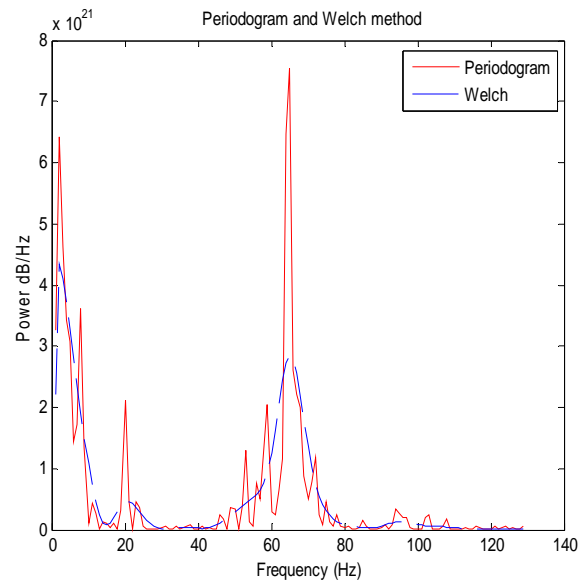


(d) PSD Estimation- AR Sinusoid Process

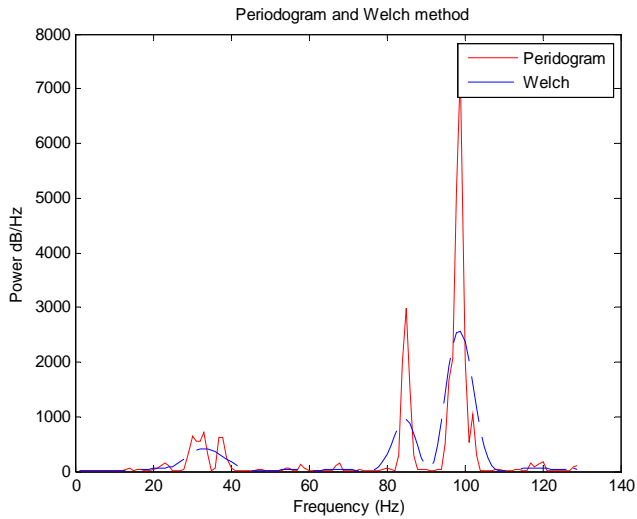
Figure 17. PSD Estimation by Parametric Methods



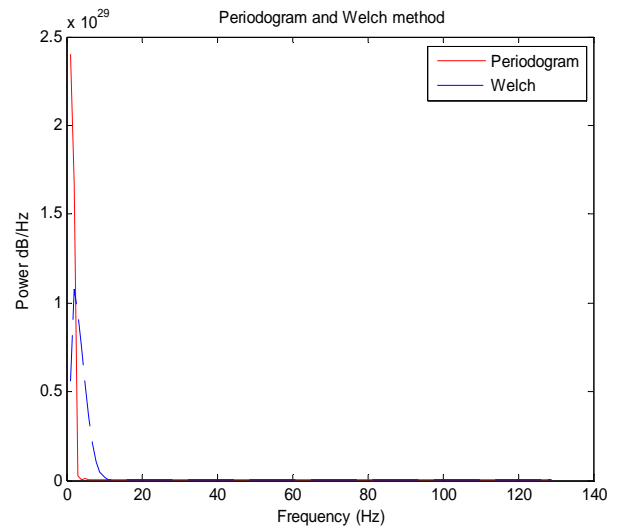
(a) PSD Estimation-AR Process



(b) PSD Estimation-ARMA Process

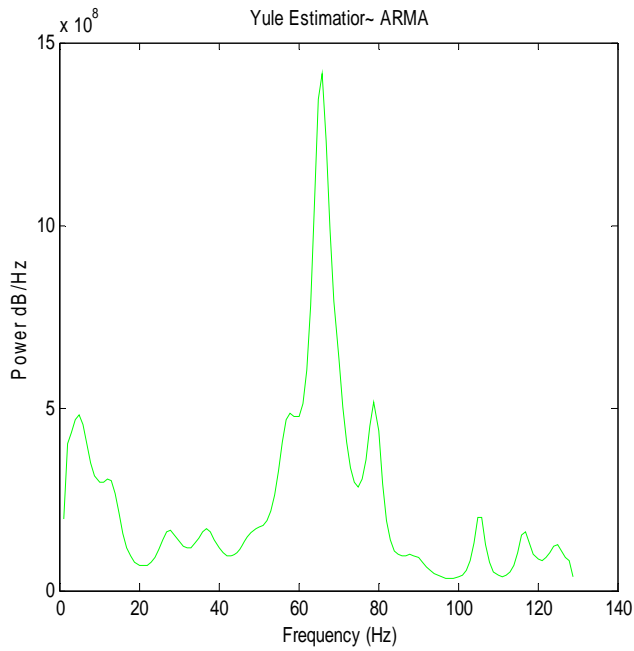


(c) PSD Estimation-MA Process
Sinusoid Process

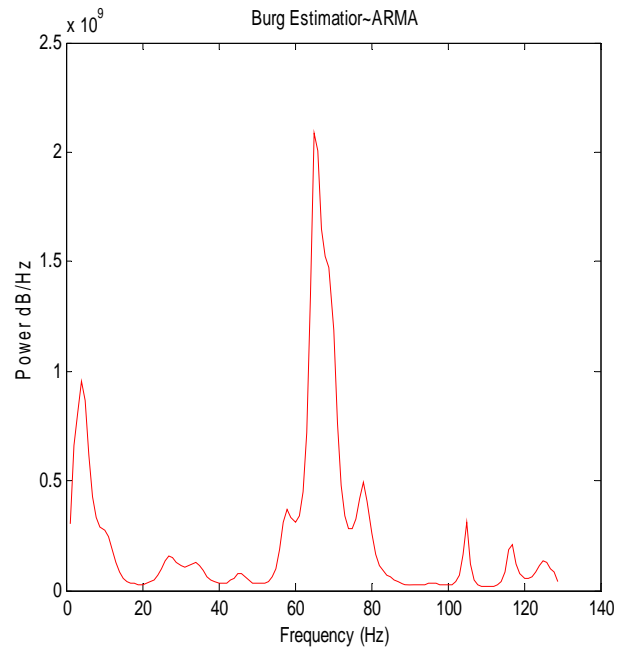


(d) PSD Estimation-AR

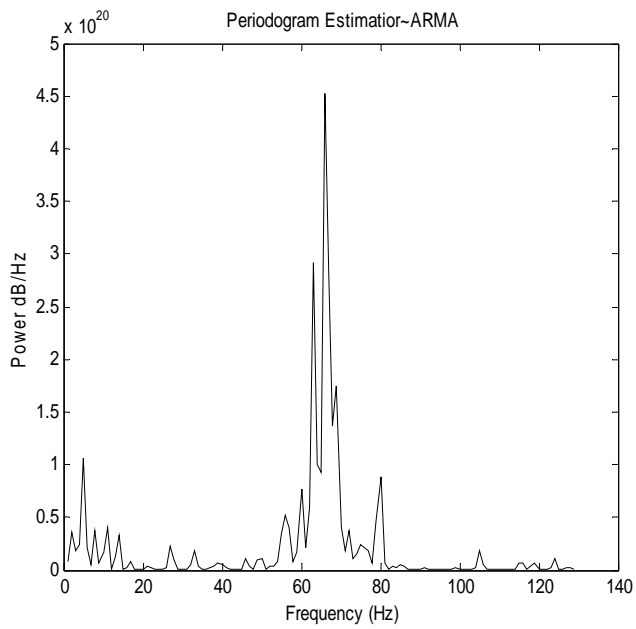
Figure 18. PSD Estimation by Blind Methods



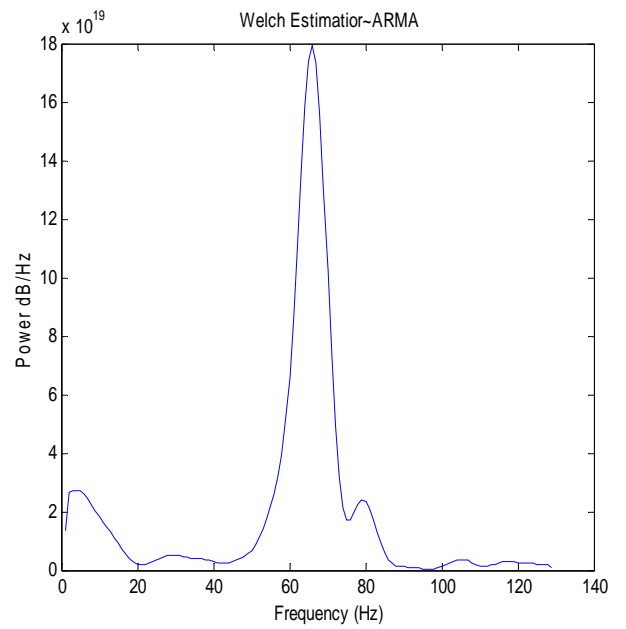
(a) PSD Yule



(c) PSD Burg

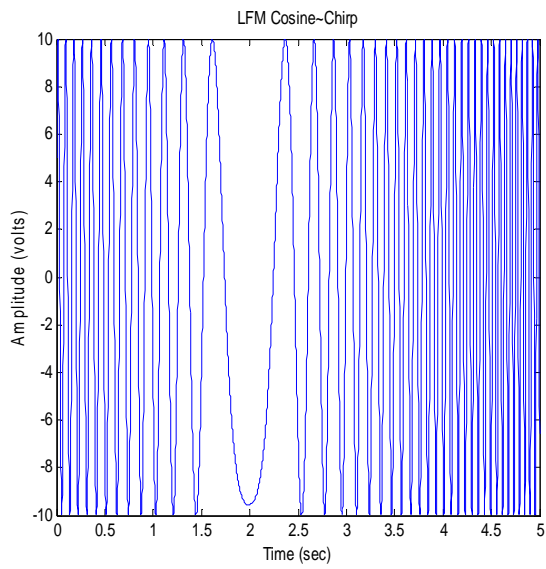


(b) PSD Periodogram

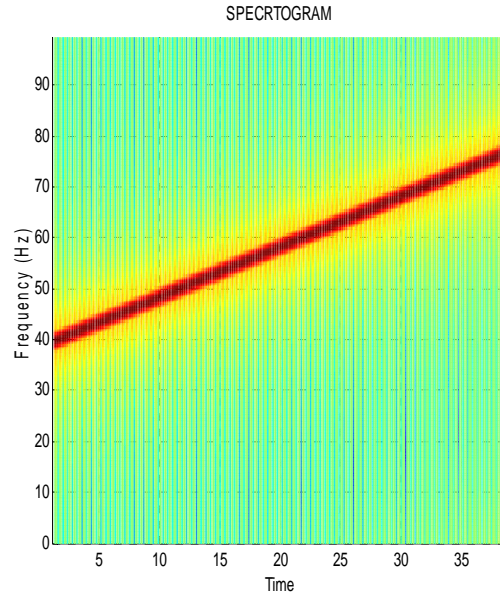


(d) PSD Welch

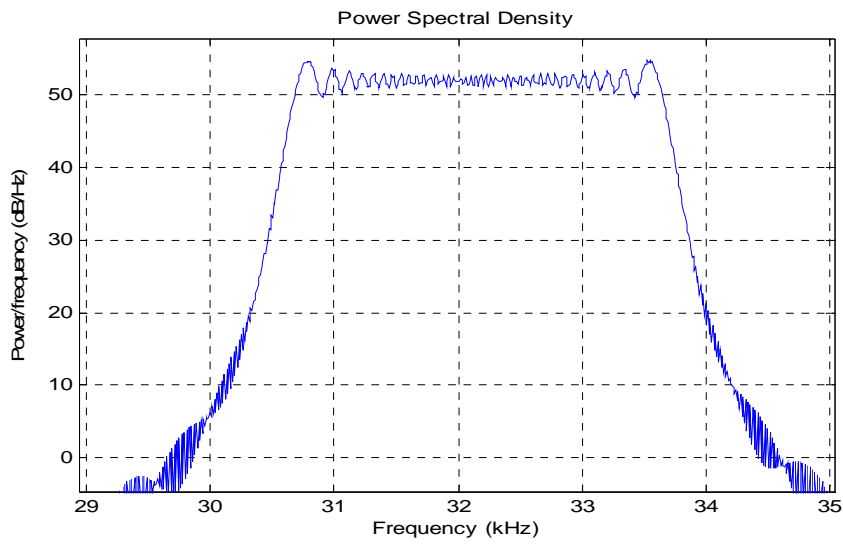
Figure 19. Comparisons of Parametric and Blind Spectral Estimation Methods



(a) LFM Chirp Cosine Signal



(b) Spectrogram of LFM signal



(c) PSD of LFM signal with 2kHz Swiping Frequency

Figure 20. Linear Frequency Modulation Cosine, and its PSD

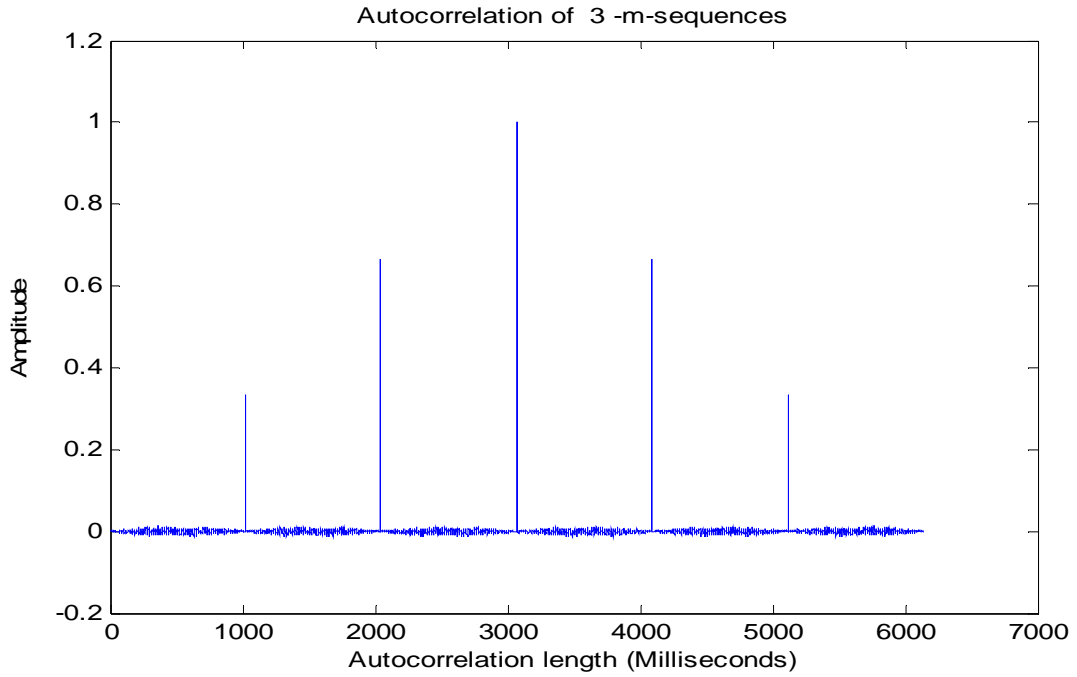
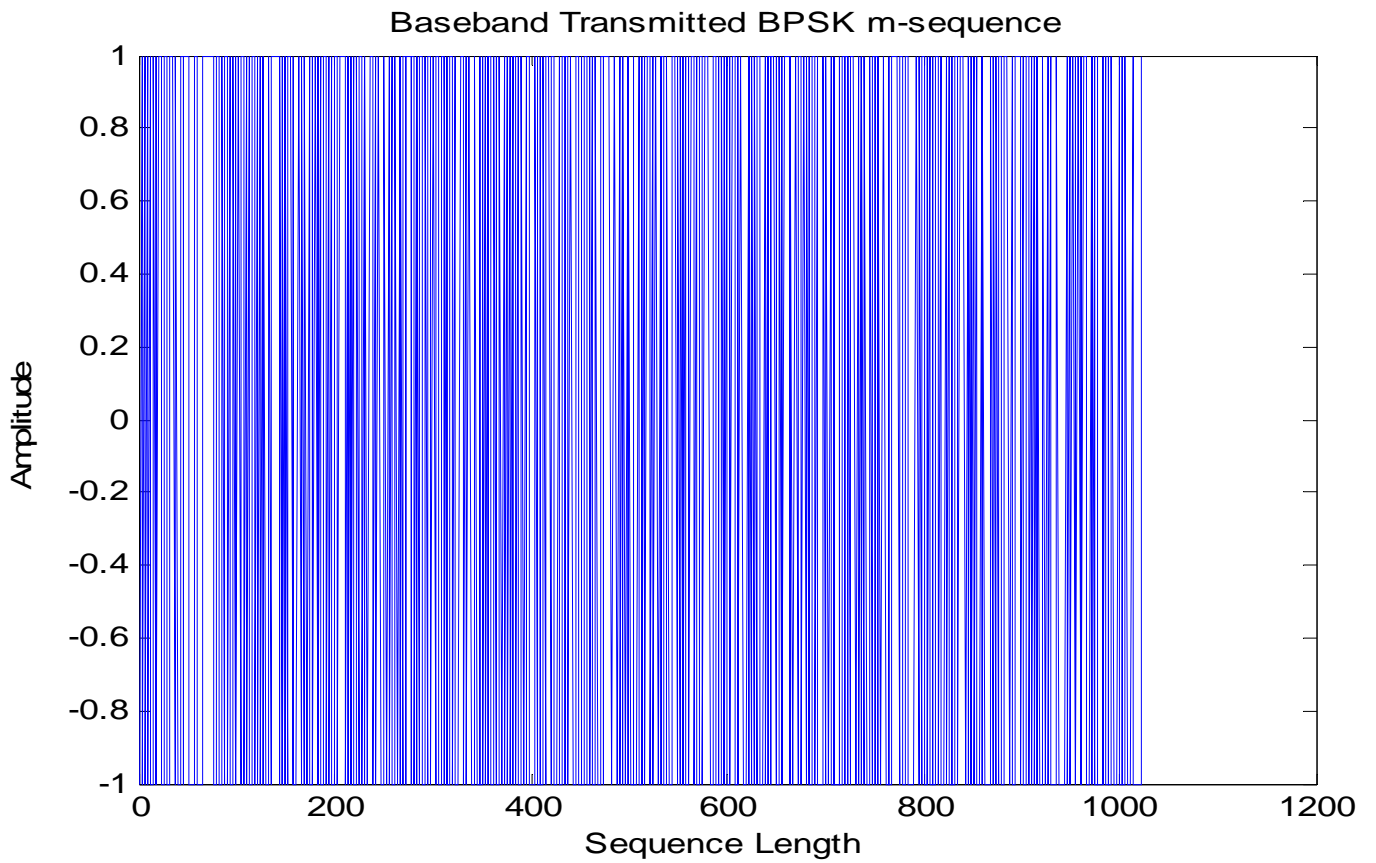
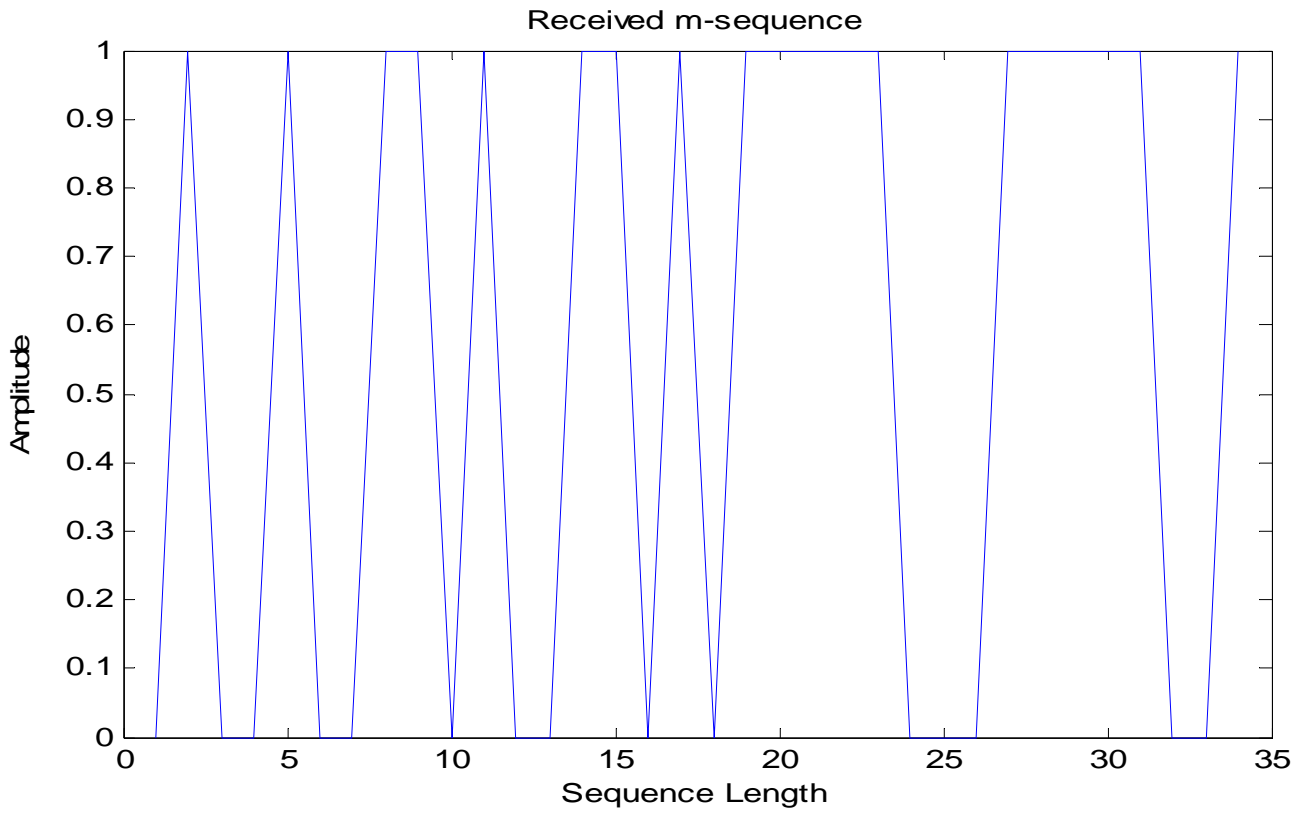


Figure 21. Periodic Autocorrelation of PN- Sequences



(a) Transmitted Binary Phase Shift keying (BPSK) signal



(a) Received m-sequences

Figure 22. Initial Transmitted (a) and Received (b) m-sequence signal

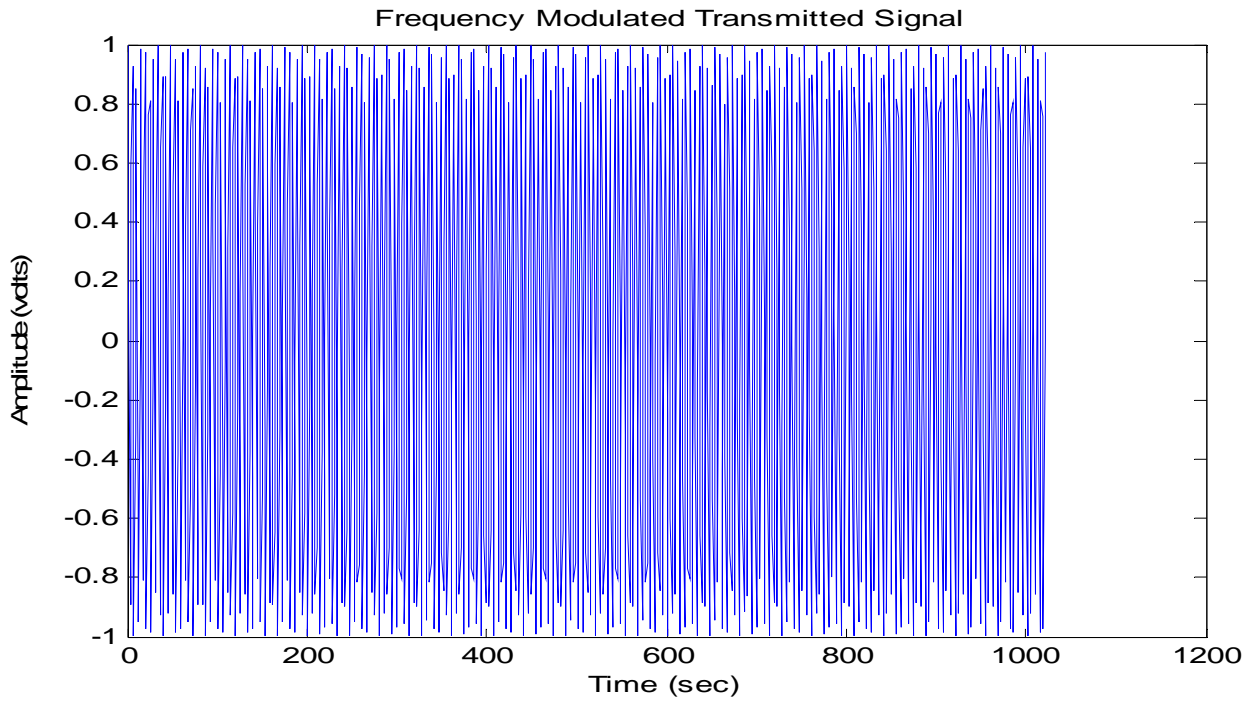


Figure 23 Frequency Modulated Transmitted Signal

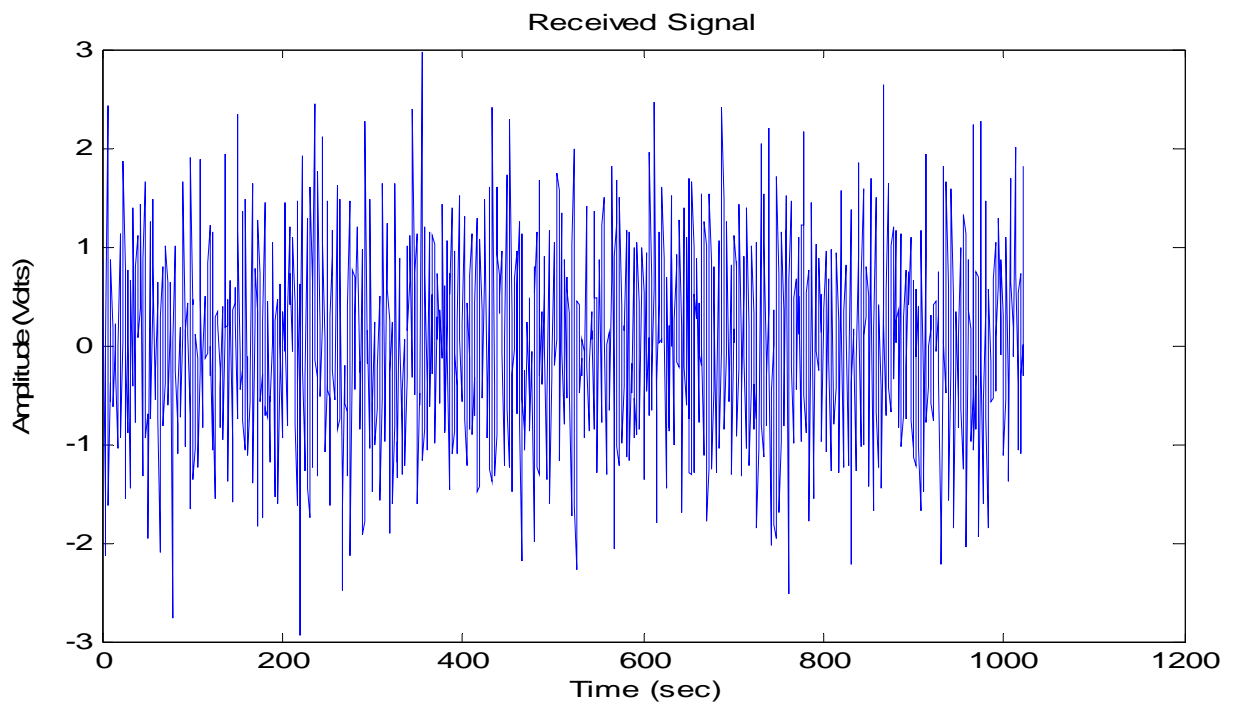
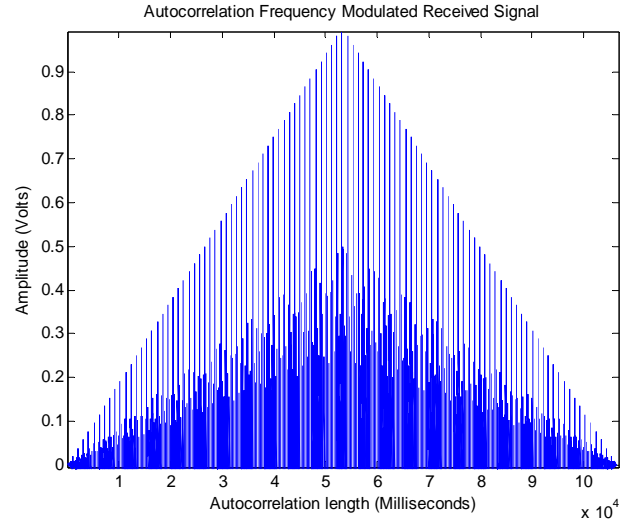
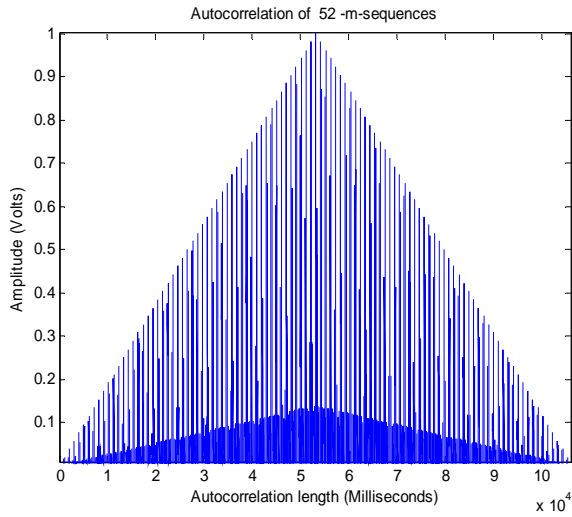


Figure 24 Frequency Modulated m-Sequence Received Signals (17 kHz)



(a) Autocorrelation of Transmitted signal

(b) Autocorrelation of Received Signal

Figure 25 Autocorrelation of Transmitted and Received 52-m -Sequences

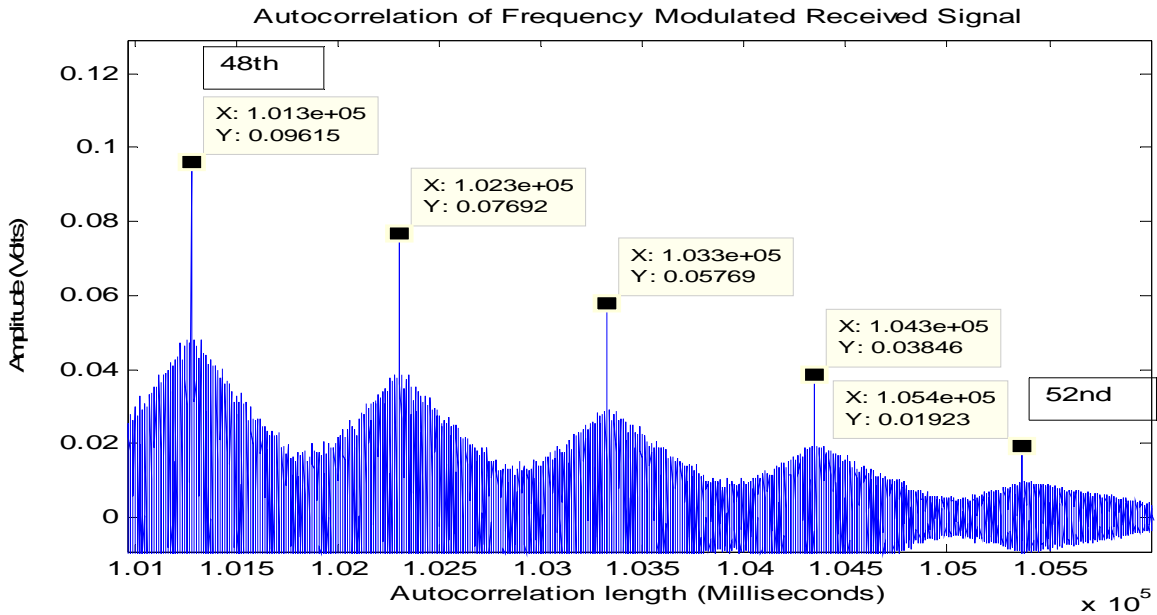
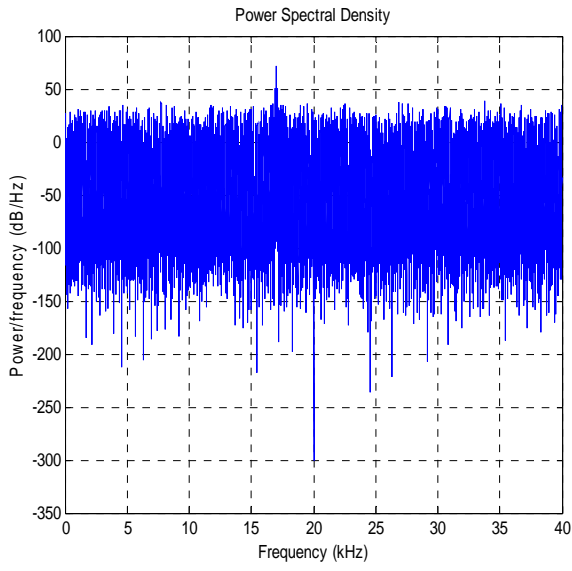
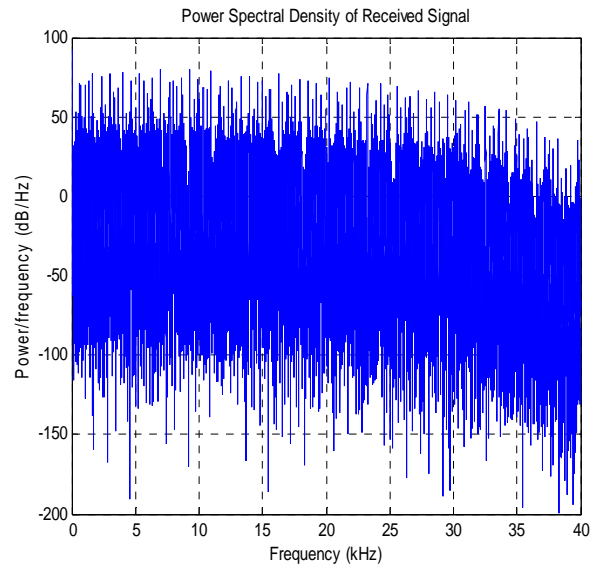


Figure 26 Partial Autocorrelation of Received Signals Showing 48th to 52nd m-Sequences

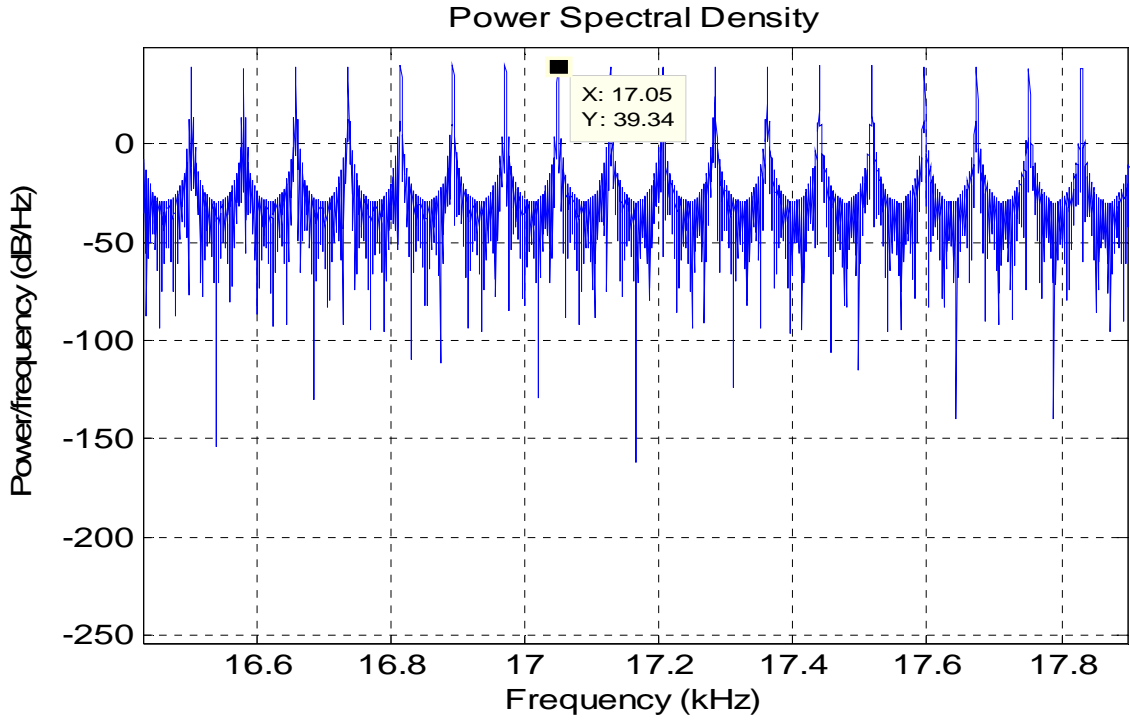


(a)

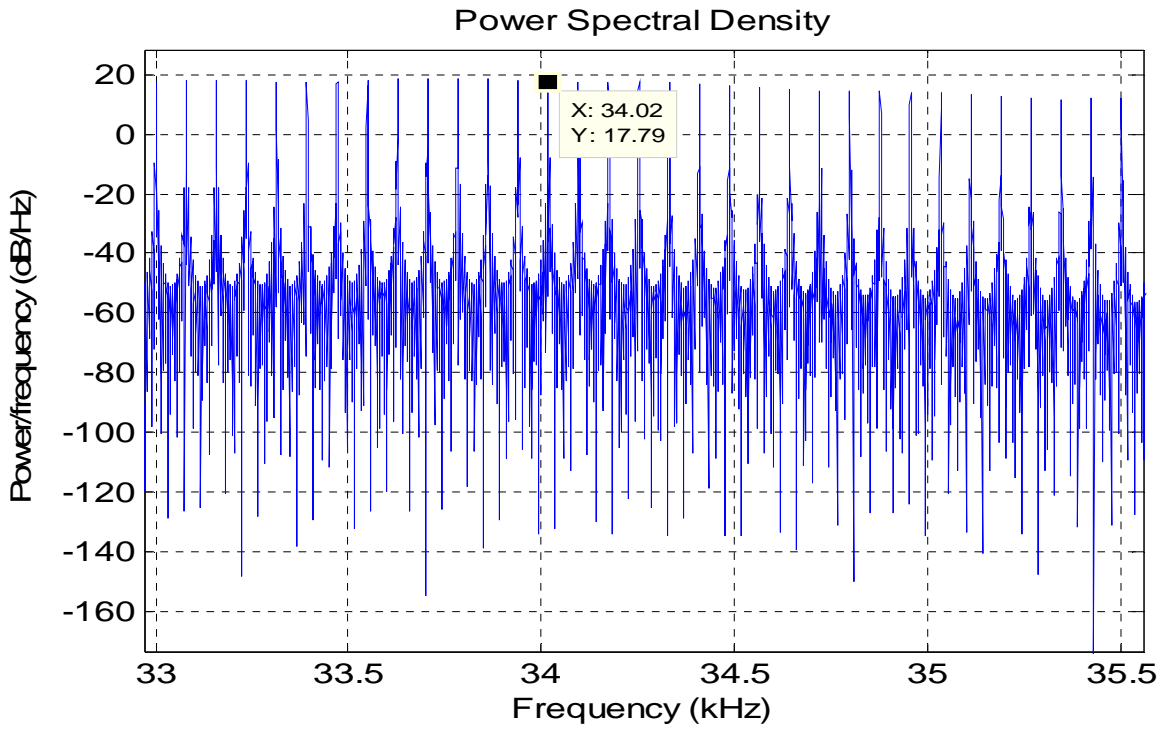


(b)

Figure 27 Power Spectral Density of Transmitted and Received Signal [Water Tank]



(a) Partial PSD around carrier frequency



(b) Partial PSD around twice the carrier frequency

Figure 28 Partial PSD of a Received Signal [Results for Water Tank]

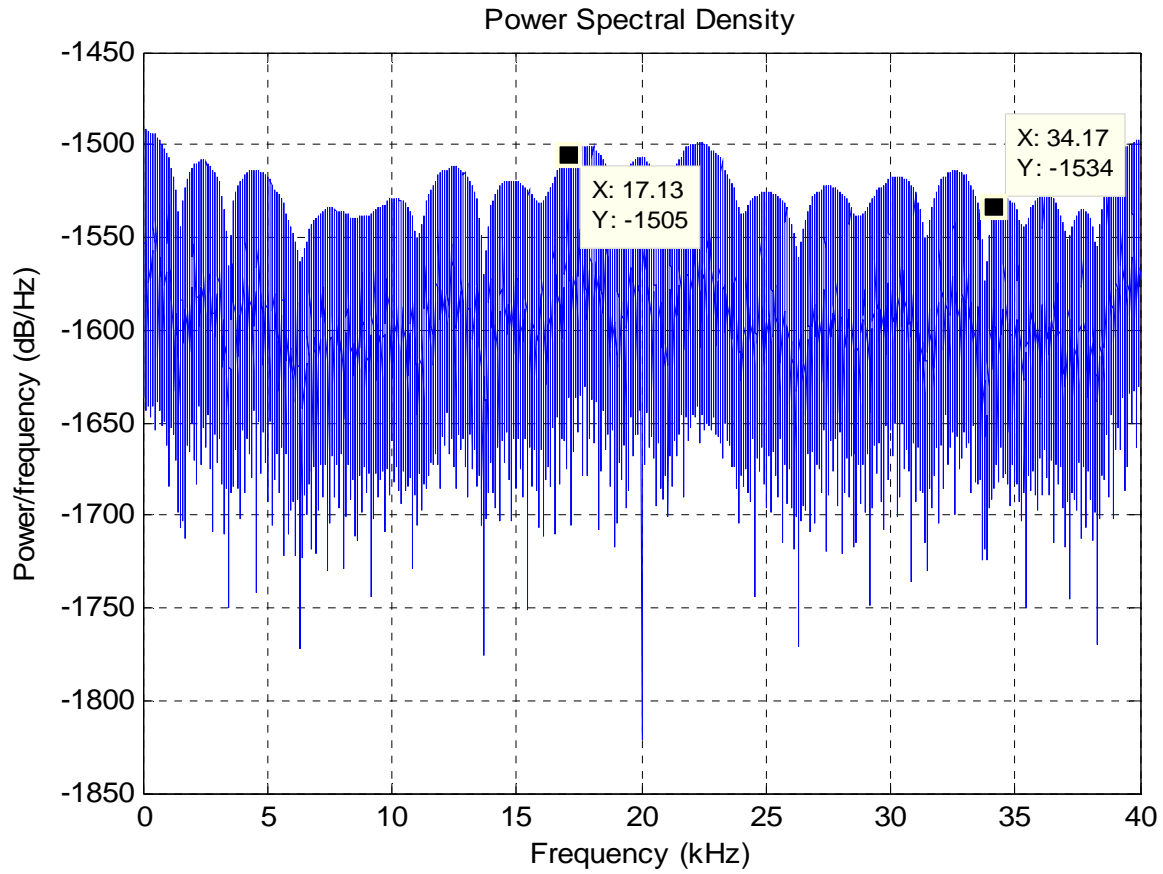
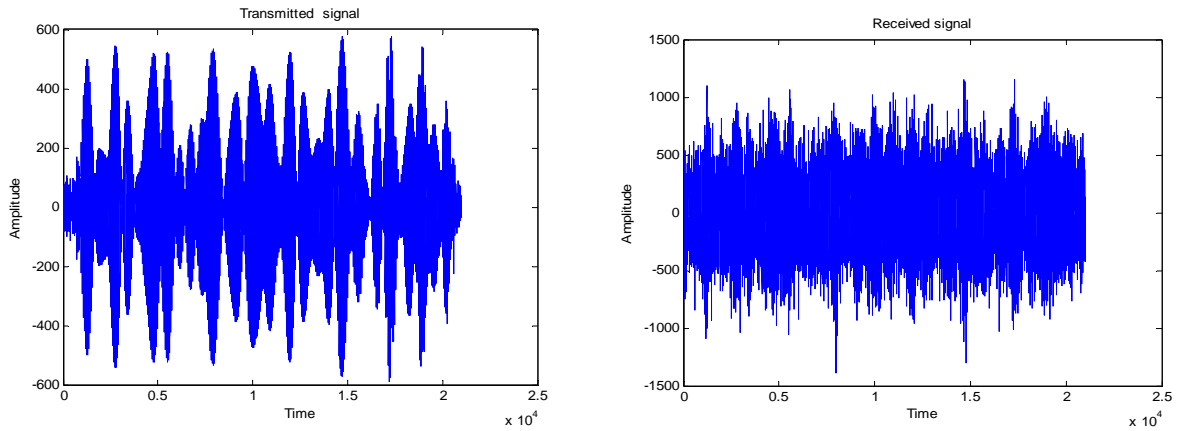


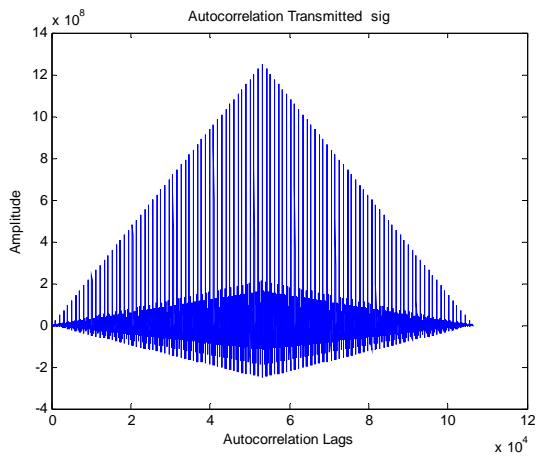
Figure 29 PSD of Received Signal [Results for Swimming pool]



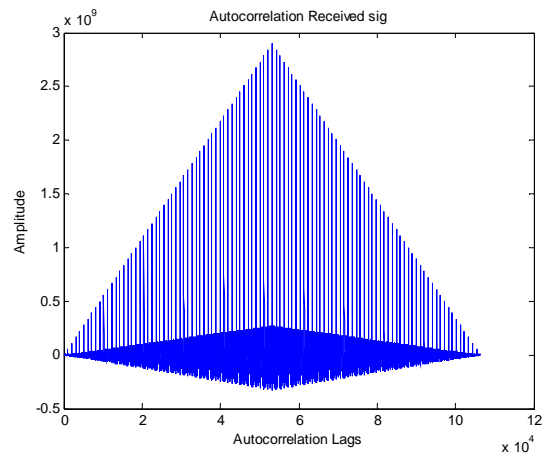
(a) Transmitted LFM modulated m-sequence

(b) Received LFM modulated m-sequence

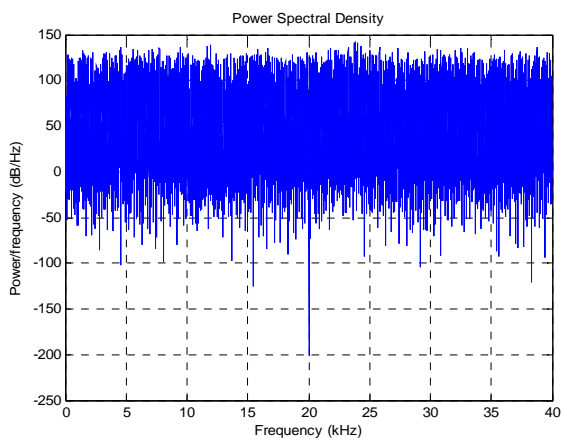
Figure 30 Transmitted and Received Signal for LFM m- Sequences [Pool]



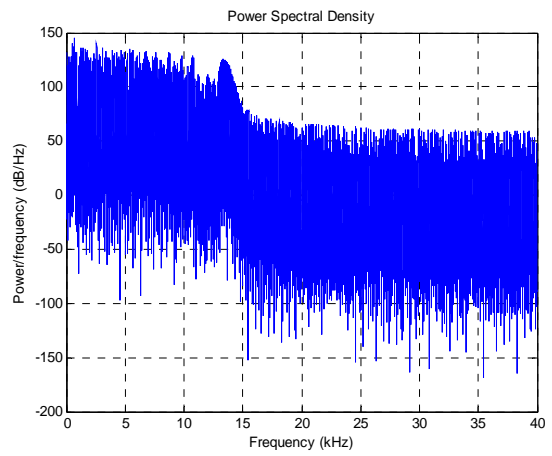
(a) Autocorrelation of transmitted signal



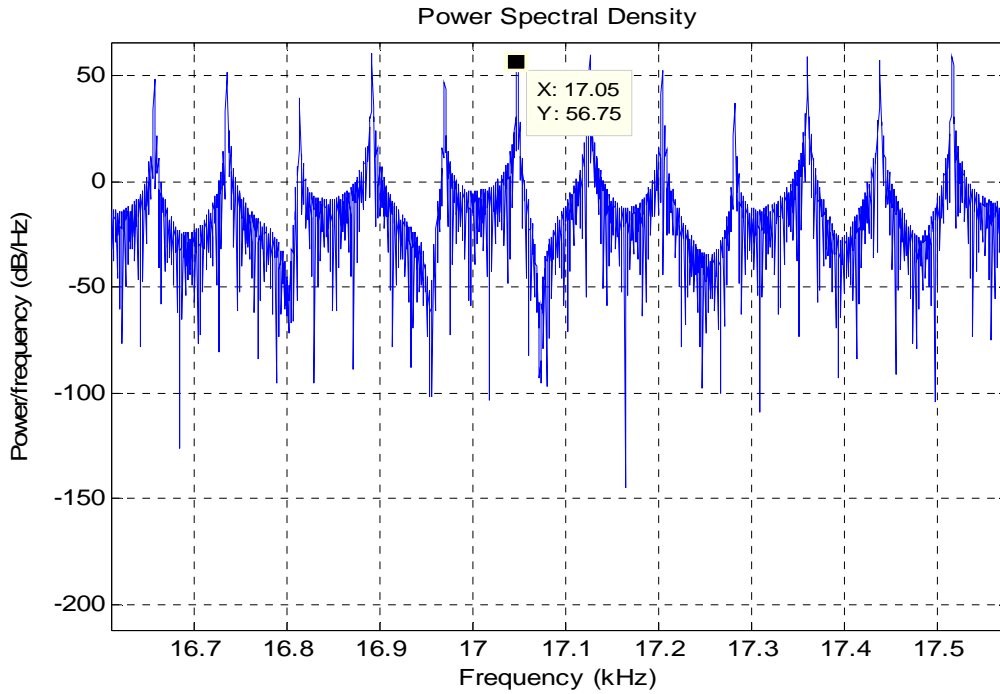
(c) Autocorrelation of received signal



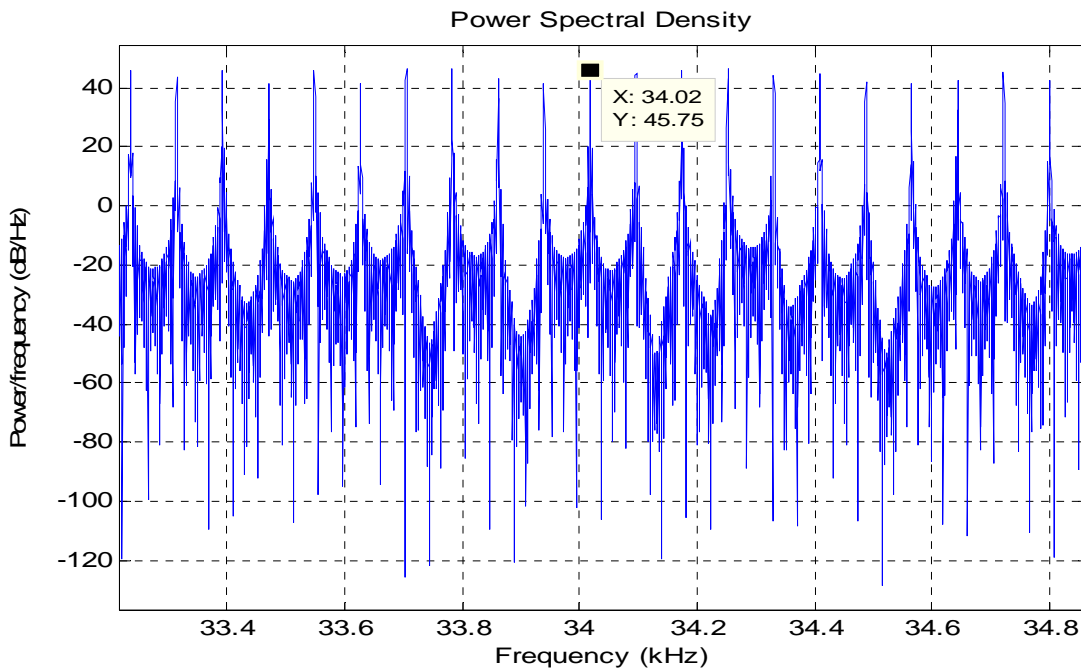
(b) PSD of transmitted signal



(d) PSD of received signal



(e) Partial PSD of received signal at 1st period (17 kHz)



(f) Partial Autocorrelation of received signal at 2nd period (34 kHz)

Figure 31 Autocorrelation, PSD and Partial Autocorrelation of LFM 52- m- Sequences

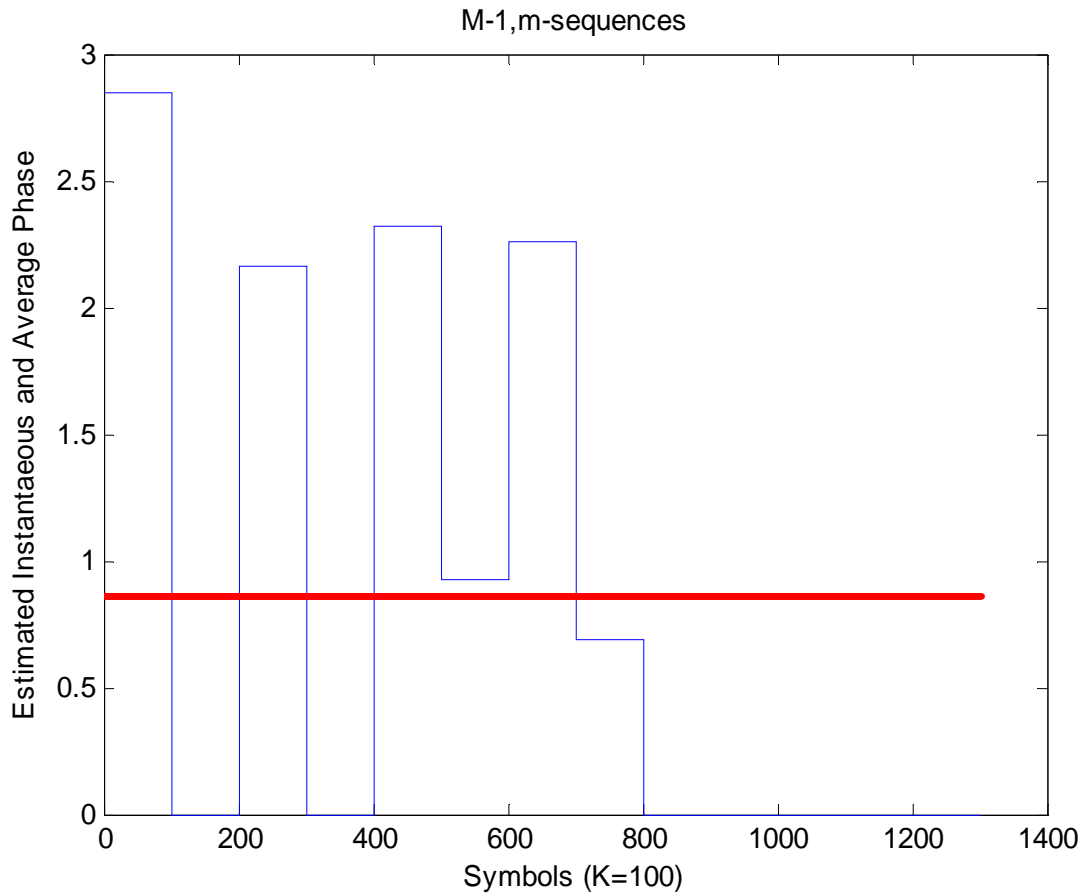


Figure 32. Estimation of Instantaneous and Average Doppler Shift Using Oerder & Meyr Algorithm

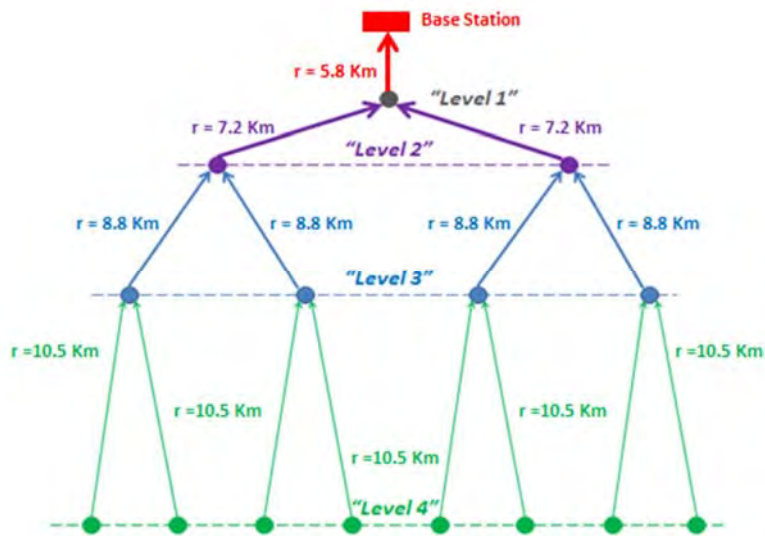


Figure 33. 4 level tree structured network with 2 children nodes

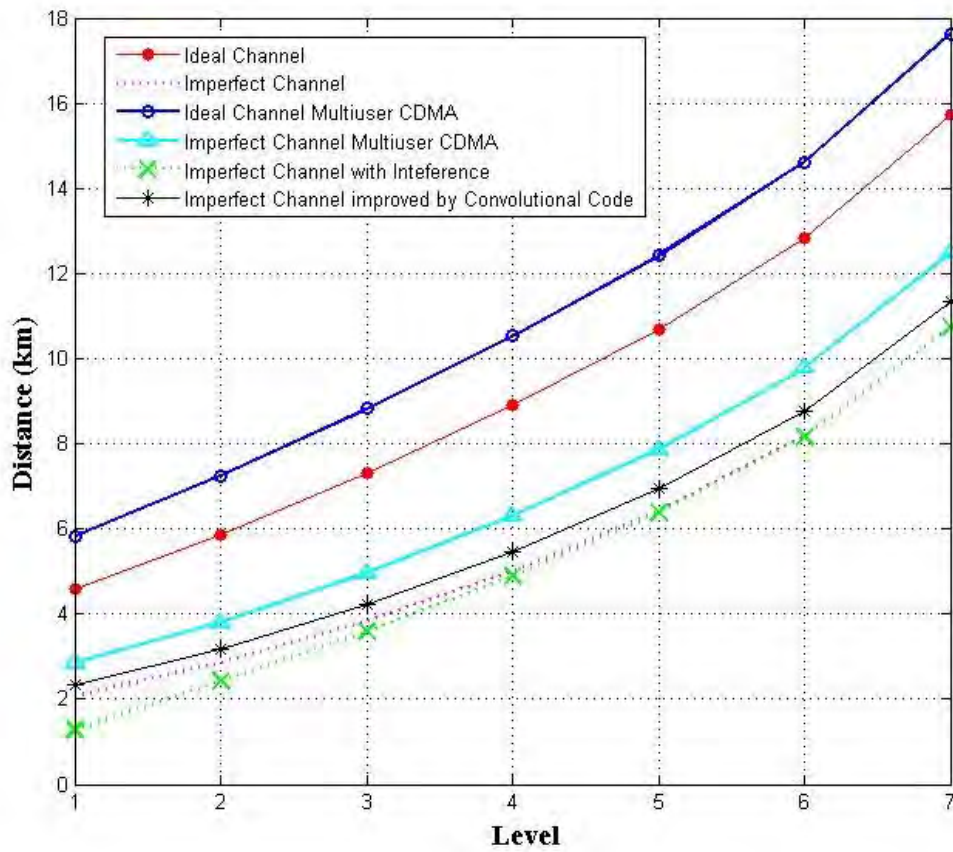


Figure 34. Optimal distance (on the top) for ideal and imperfect channels including BER and interference for a tree shaped topology with 7 levels

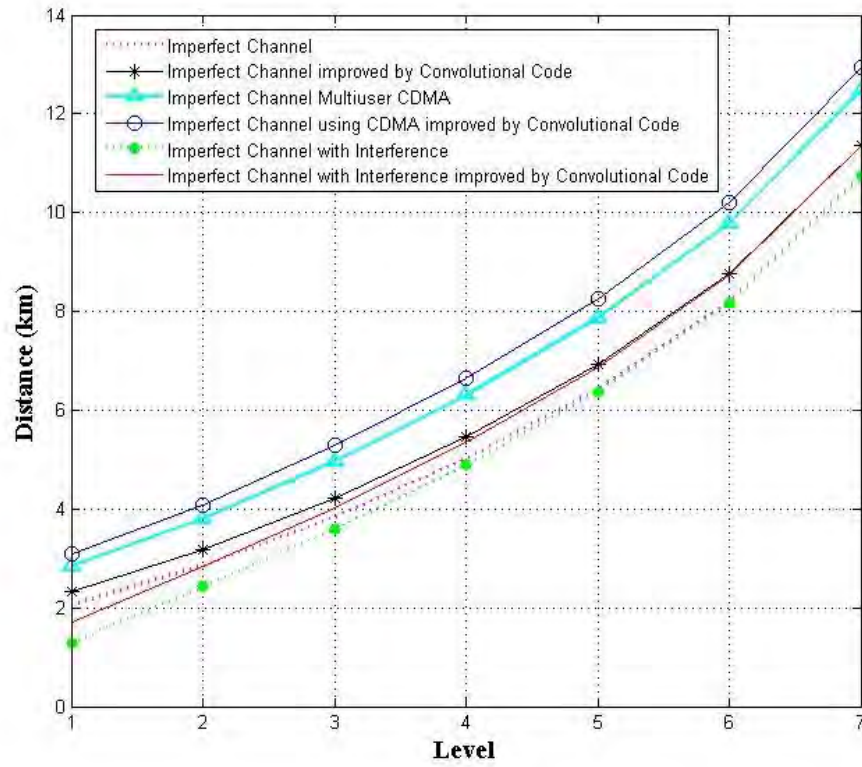


Figure. 35 The distances for different imperfect channel scenarios and their improved situations after applying CC

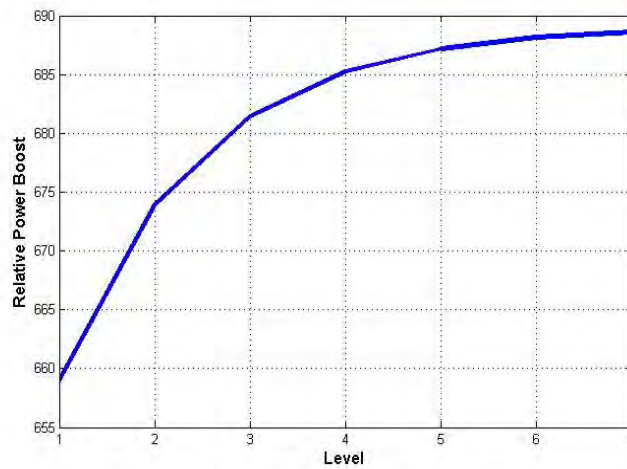


Figure 36. The ratio of the sensor power of the imperfect channel compared to the sensor power of the ideal channel

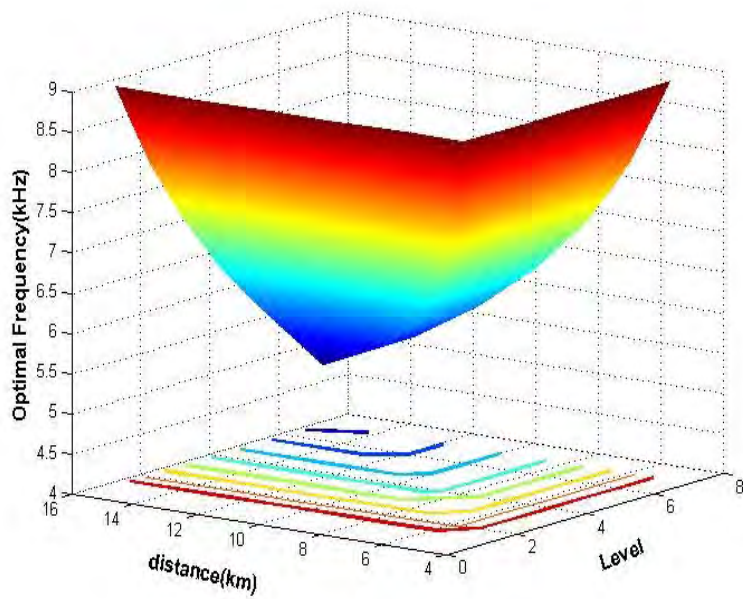


Figure 37. Optimal frequency at each distance associated with a specific level for an ideal channel in a 7-level tree structured network

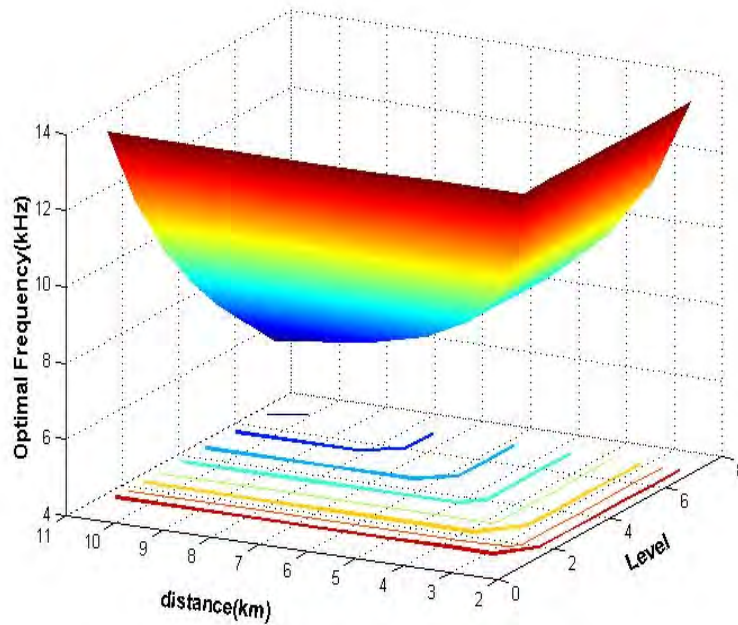


Figure 38. Optimal frequency at each distance associated with a specific level for an imperfect channel (BER = 0.001) in a 7-level tree structured UWS

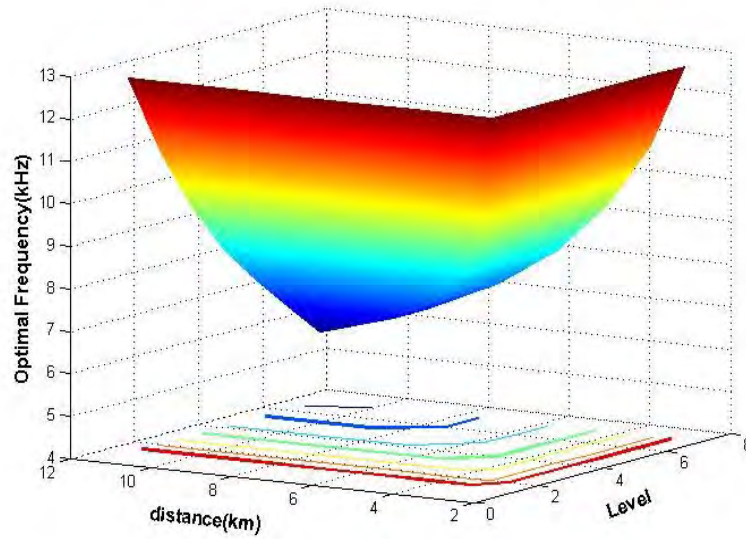


Figure 39. Optimal frequency at each distance associated with a specific level for an imperfect channel (BER = 0.001) improved with convolutional code in a 7-level tree structured network

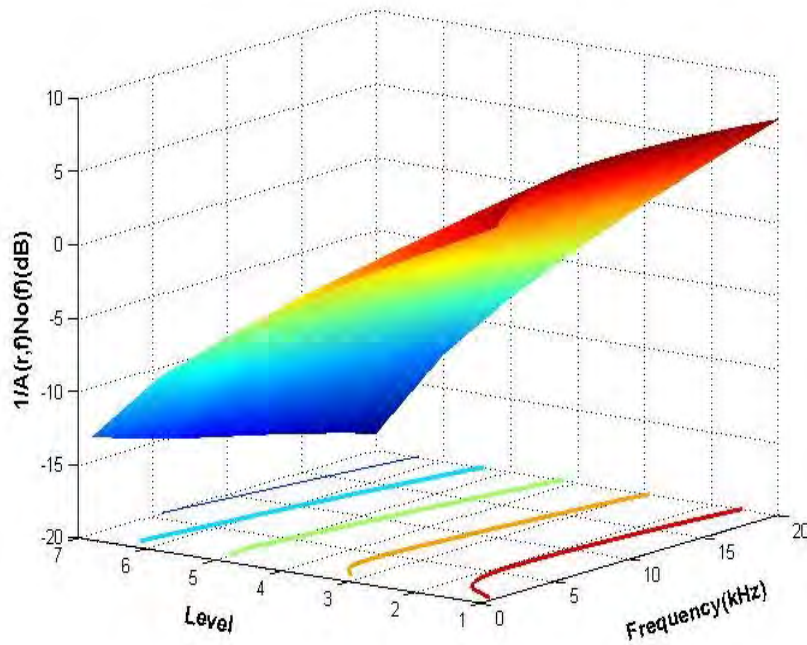


Figure 40. Frequency dependent portion of narrow-band SNR, $\frac{1}{A(r,f)N_o(f)}$

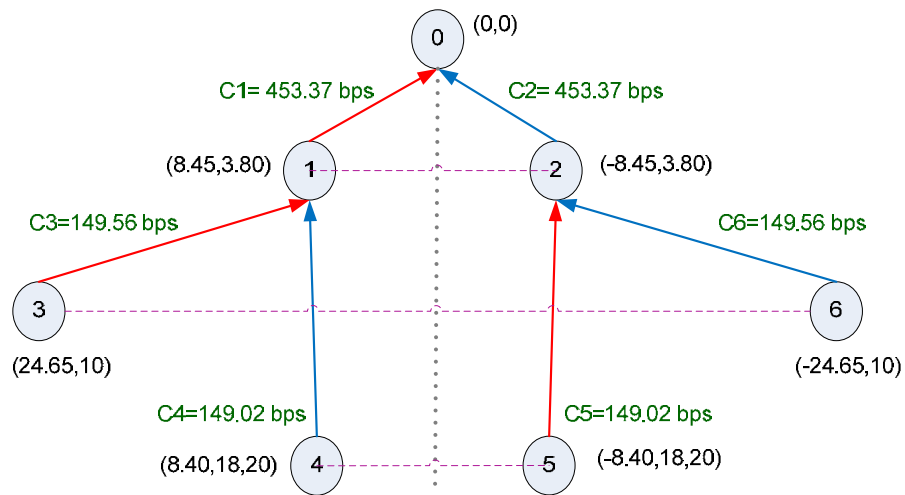


Figure 41. Optimal placement of the sensor nodes when the transmitting power is constant

Table 24. Optimized placements and other related parameters when the transmitting power of each node is constant and equal to 1 watt

Wireless Links (node to node)	Optimal Locations Km	Optim al SINR dB	Optimal links' Capacity bps
1 to 0 2 to 0	(8.45, 3.80) (-8.45, 3.80)	13.45	453.37
3 to 1 6 to 2	(24.65, 10.00) (-24.65, 10.00)	2.60	149.56
4 to 1 5 to 2	(8.40, 18.20) (-8.40, 18.20)	2.58	149.02

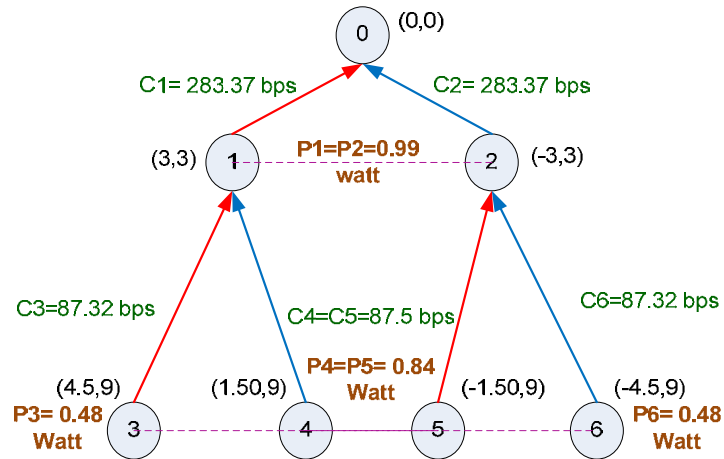


Figure 42. The optimal power allocations for the scenario 1 are shown near each sensor node (in Watts)

Table 25. Optimized energy allocation and other related parameters when the sensor nodes are fixed in their locations, first scenario

Wireless Links (node to node)	Nodes' Locations Km	Opt. Energy Watt	Opt. SINR dB	Opt. links' Capacity bps
1 to 0 2 to 0	(3.00, 3.00) (-3.00, 3.00)	0.99	7.8 7	283.37
3 to 1 6 to 2	(4.50, 9.00) (-4.50, 9.00)	0.48	- 0.8	87.32
4 to 1 5 to 2	(1.50, 9.00) (-1.50, 9.00)	1.00	- 0.79	87.5

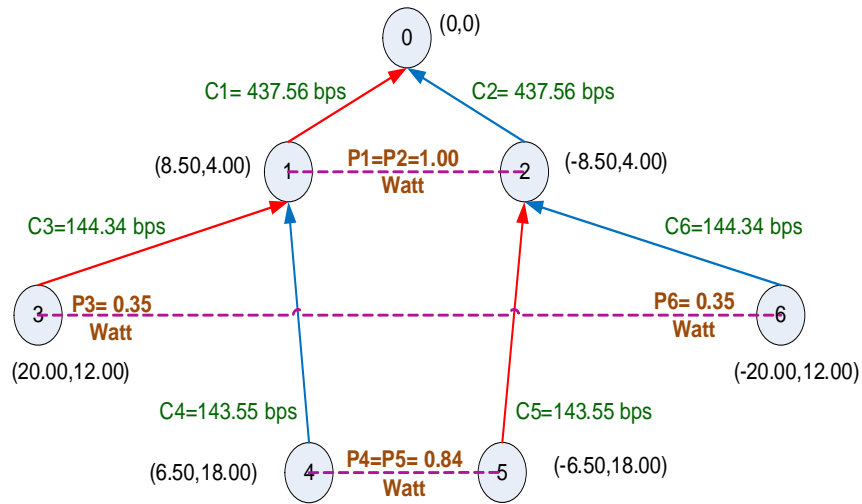


Figure 43. The optimal power allocations for the scenario 2 are shown near each sensor node (in Watts)

Table 26. Optimized energy allocation and other related parameters when the sensor nodes are fixed in their locations, second scenario

Wireless Links (node to node)	Nodes' Locations Km	Opt. Energy Watt	Opt. SINR dB	Opt. links' Capacity bps
1 to 0 2 to 0	(8.50 , 4.00) (-8.50 , 4.00)	1.00	12.9 6	437.56
3 to 1 6 to 2	(20.00, 12) (-20.00, 12)	0.35	2.35	144.34
4 to 1 5 to 2	(6.5, 18.00) (-6.5, 18.00),	0.84	2.32	143.55

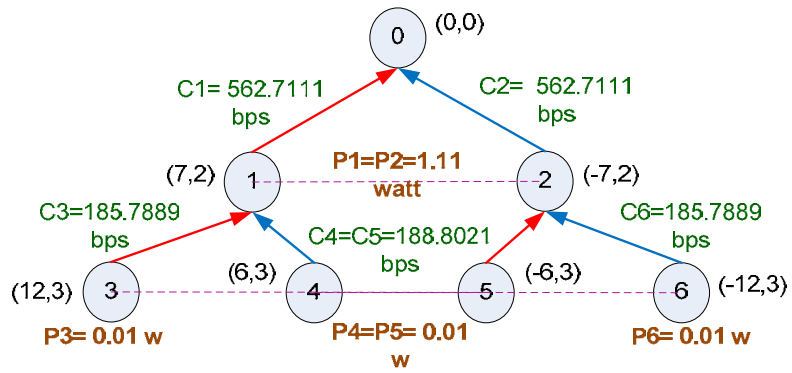


Figure 44. The optimal sensors' locations and power allocations (in Watts)

Table 27. Optimized placements, optimized power other related parameters

Wireless Links (node to node)	Optimal Locations Km	Optimal Power Watt	Optimal SINR dB	Optimal links' Capacity bps
1 to 0	(7,2)	1.11	48.42	562.71
2 to 0	(-7,2)		30	
3 to 1	(12,3)	0.01	2.650	186.79
6 to 2	(-12,3)		0	
4 to 1	(6,3)	0.01	2.701	188.80
5 to 2	(-6,3)		3	

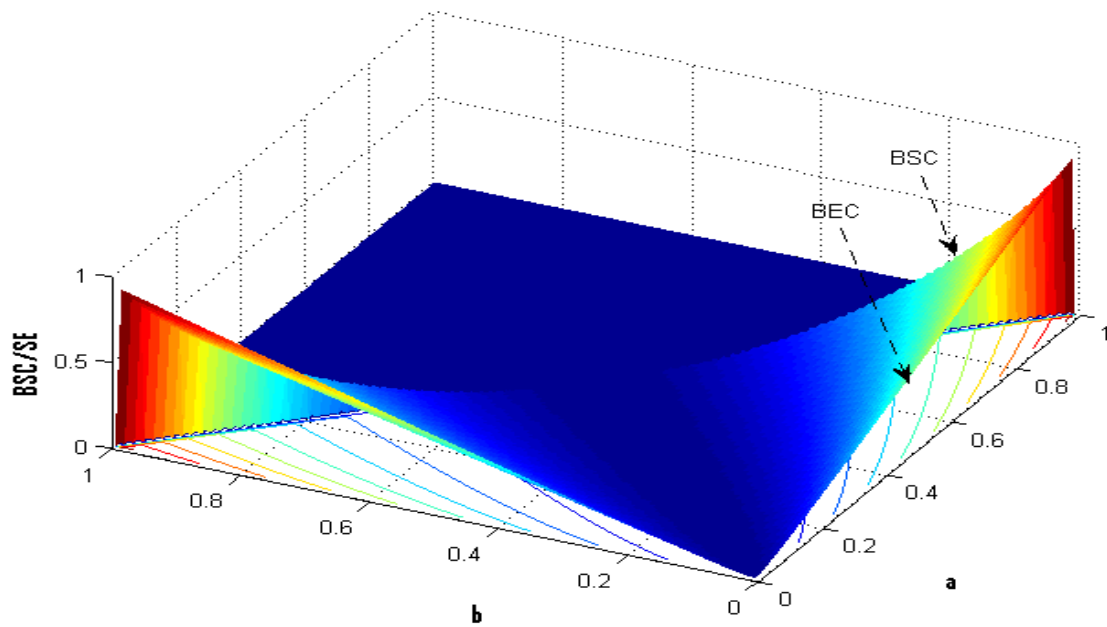


Figure 45. BSC/SE capacity

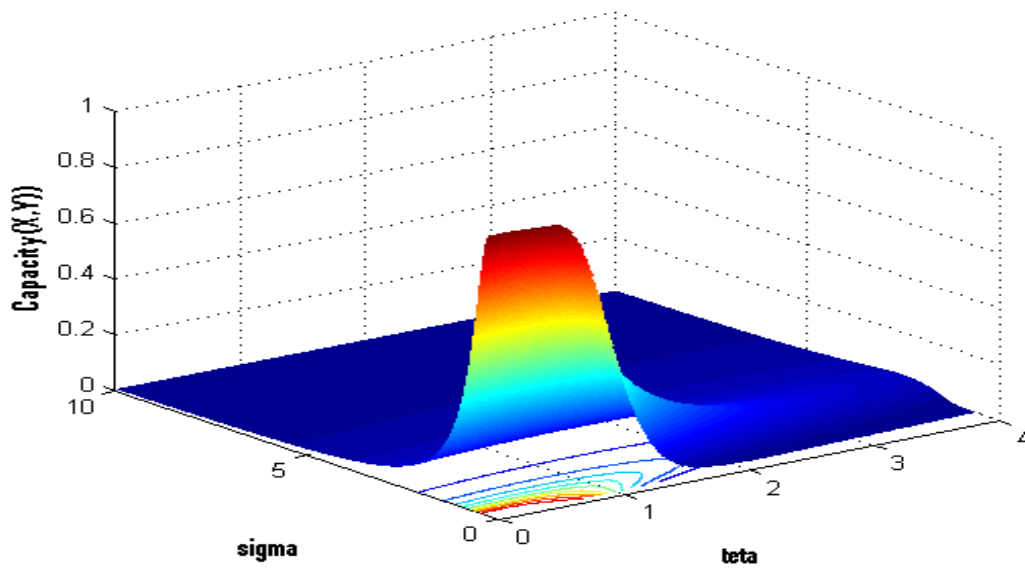


Figure 46. Capacity of BAC/SE

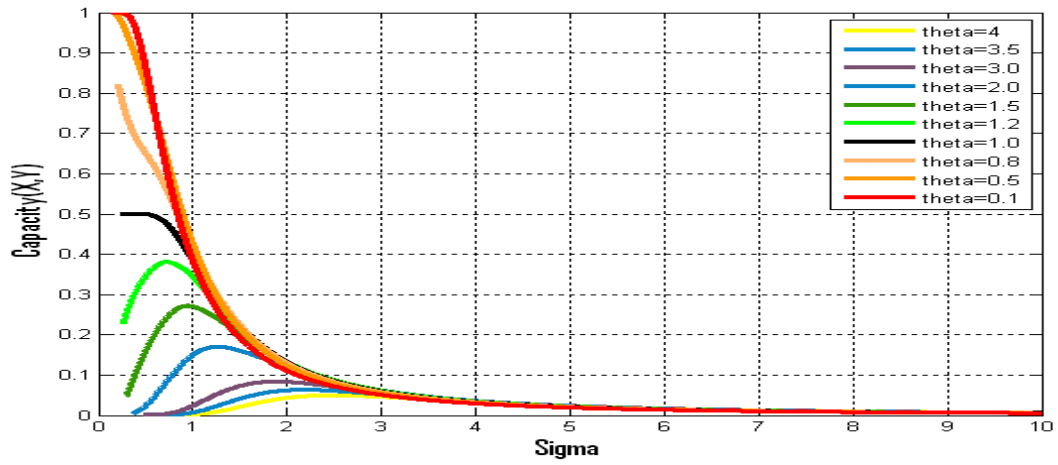


Figure 47. Capacity of BSC/SE for threshold values

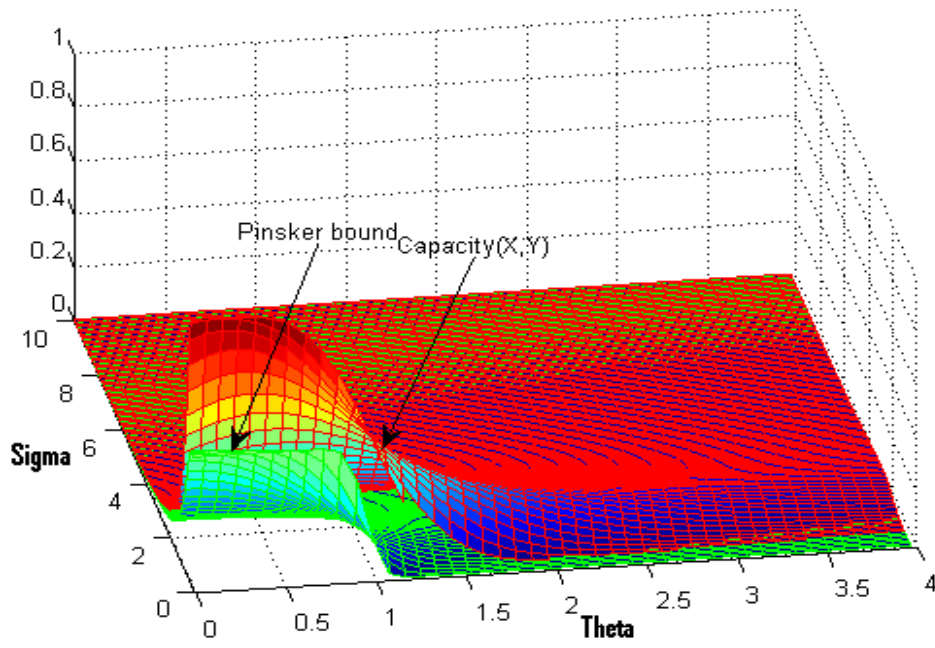


Figure 48. (2,3) DMC and Pinsker capacity Bound

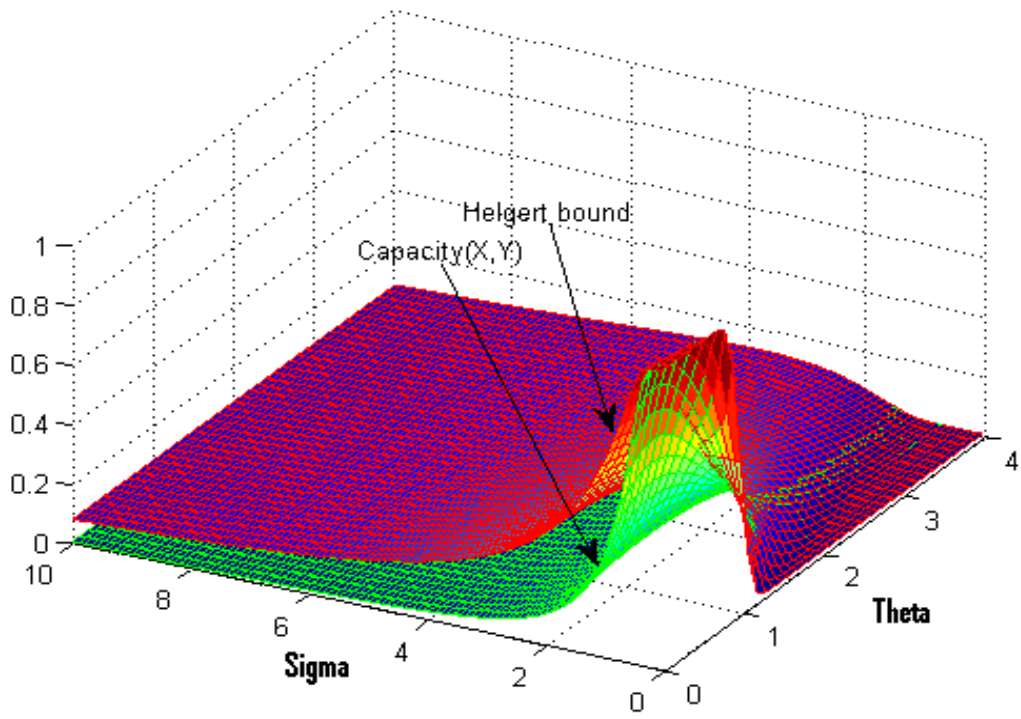


Figure 49. (2,3) DMC and Helgert capacity Bound

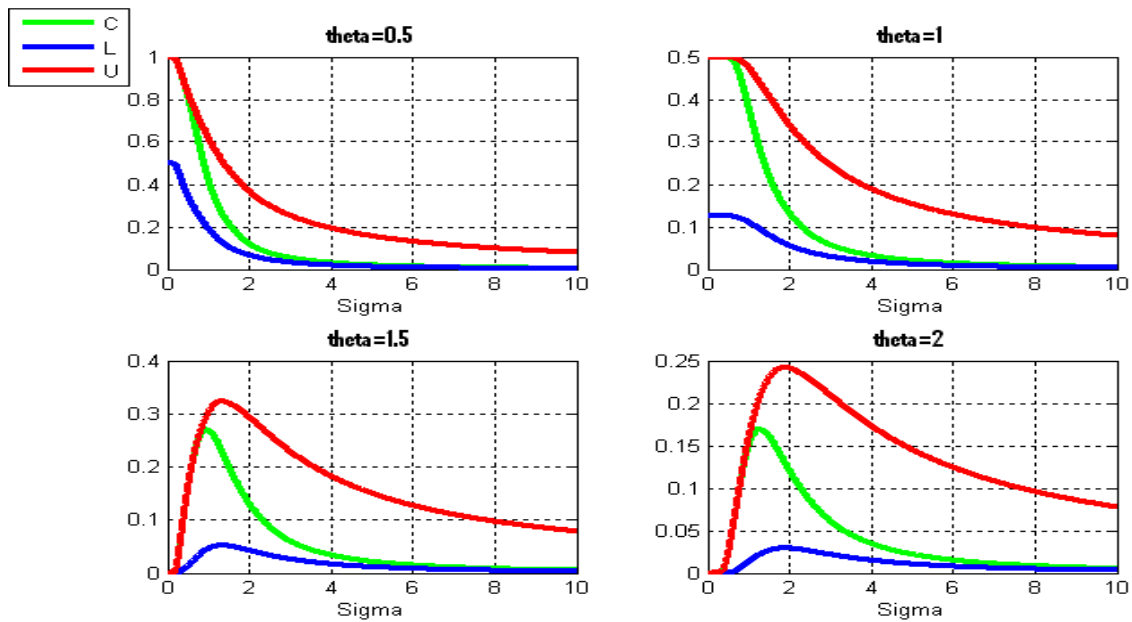


Figure 50. Capacity(C), Pinsker (L) and Helgert (U) bounds for different values of threshold

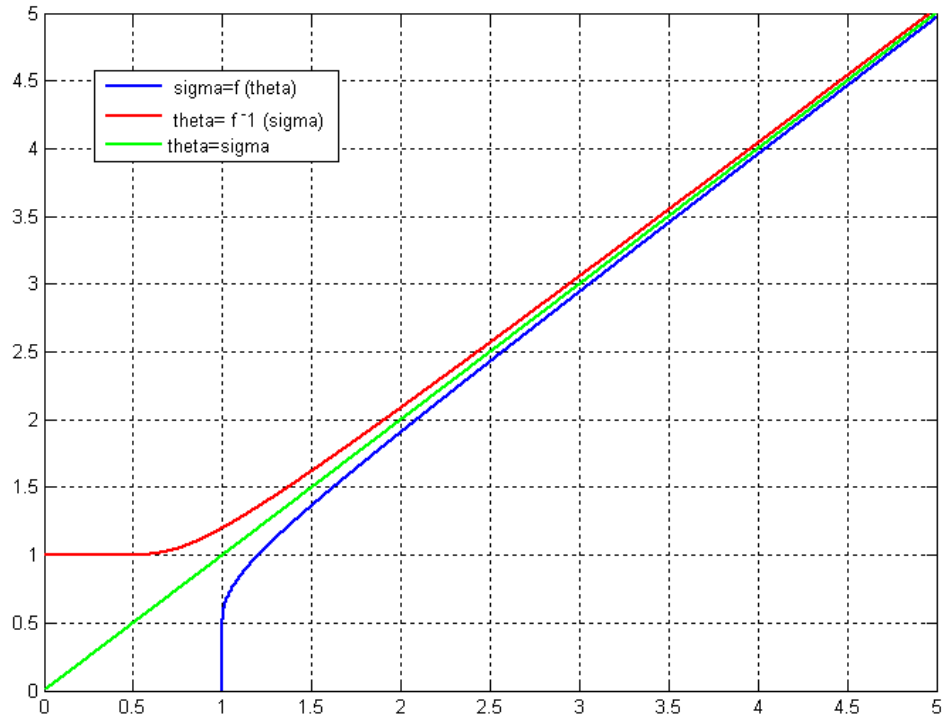


Figure 51. Optimal noise power and threshold for stochastic resonance, with a scalable factor

Table 28 : Summary of (2,3) DMCs

Channel	M	Constraints	Channel Capacity
(2,3) general DMC	$\begin{pmatrix} a & 1-a-b & b \\ c & 1-c-d & d \end{pmatrix}$		
BAC/SE	$\begin{pmatrix} a & 1-a-b & b \\ c & 1-c-d & d \end{pmatrix}$	$a > b$ $1-a-b = 1-c$ $-d$	$\sum_{j=1}^3 p(y_j x_j) \log_2 \left(\frac{p(y_j x_i)}{x(p(y_j x_1) - p(y_j x_2)) + p(y_j x_2)} \right)$
BSC/SE	$\begin{pmatrix} a & 1-a-b & b \\ c & 1-c-d & d \end{pmatrix}$	$a > b$ $a = d$ $b = c$	$a \log_2 \frac{2a}{a+b} + b \log_2 \frac{2b}{a+b}$
BSC	$\begin{pmatrix} a & 1-a-b & b \\ c & 1-c-d & d \end{pmatrix}$ $\equiv \begin{pmatrix} a & 1-a \\ 1-a & a \end{pmatrix}$	$a + b = 1$ $a = d$ $b = c$	$1 - h(a)$
BEC	$\begin{pmatrix} a & 1-a & 0 \\ 0 & 1-a & 0 \end{pmatrix}$	$b = c$ $= 0$ $a = d$	a